A NUMERICAL INVESTIGATION OF NEW AUSTRIAN TUNNELING METHOD AND TUNNEL BORING METHOD FOR TUNNEL CONSTRUCTION

Thesis Submitted by

Johana Sharmin

Student ID: 0417042206

A thesis submitted to the Department of Civil Engineering, Bangladesh University of Engineering and Technology, Dhaka, in the Partial Fulfillment of the Requirement for the Degree of Masters of Science in Civil Engineering (Geotechnical)

DEPARTMENT OF CIVIL ENGINEERING

BANGLADESH UNIVERSITY OF ENGINEERING AND TECHNOLOGY

April, 2022

The thesis title "A NUMERICAL INVESTIGATION OF NEW AUSTRIAN TUNNELING METHOD AND TUNNEL BORING METHOD FOR TUNNEL CONSTRUCTION", submitted by Student – Johana Sharmin, Roll No.: 0417042206, Session: April 2017, has been accepted as satisfactory in partial fulfillment of the requirement for the degree of Master of Science in Civil Engineering (Geotechnical) on 16th April, 2022.

BOARD OF EXAMINERS

Dr. Mehedi Ahmed Ansary
Professor
Dept. of Civil Engineering BUET,
Dhaka-1000.

Chairman
(Supervisor)

Dr. Md. Delwar Hossain
Professor and Head
Dept. of Civil Engineering
BUET, Dhaka-1000.

Member
(Ex-Officio)

Dr. Abu Siddique
Professor Dept. of Civil Engineering
BUET, Dhaka-1000.

Member

Dr Khondaker Sakil Ahmed
Associate Professor
Dept. of Civil Engineering
MIST, Dhaka-1206

Member
(External)

DECLARATION

I hereby declare that this research is my original work and this has been written by me entirely. I have duly acknowledged all the sources of information which have been used in the thesis. This thesis has also not been submitted for any degree in any university or publish any online medium previously.

Johana Sharmin

Johana Sharmin

ACKNOWLEDGEMENT

First and foremost, praises and thanks to the Almighty, for His showers of blessings and ability throughout the research work to complete the research successfully.

The author would like to express her deep and sincere gratitude to her research supervisor, Dr. Mehedi Ahmed Ansary, Professor, Department of Civil Engineering, Bangladesh University of Engineering and Technology, Dhaka for giving the opportunity and encouragement to do the research and providing invaluable guidance throughout the research work. His dynamism, sincerity and motivation were inspiring to present this research work as clearly as possible.

The author is grateful to Dr. Md. Delwar Hossain, Professor and Head, Department of Civil Engineering, Bangladesh University of Engineering and Technology, for the valuable time he provided as a member of my advisory committee. The author would also like to take the opportunity of expressing sincere appreciation to Dr. Abu Siddique, Professor, Department of Civil Engineering, Bangladesh University of Engineering and Technology and Dr Khondaker Sakil Ahmed, Associate Professor, Military Institute of Science and Technology, Dhaka, for his kind consent to be the member of my advisory committee. Their co-operation and essential suggestions helped me to understand the importance of research.

The author likes to express gratitude to both of the families, especially her parents and husband, and friends, especially Antora and Sharbani, for their constant love, uncountable support and encouragement to complete this research.

ABSTRACT

To alleviate traffic congestion and curtail environmental deterioration GoB and JICA in cooperation with the World Bank formulated the 'Strategic Transport Plan for Dhaka' which includes establishment of Mass Rapid Transit system (MRT). Among all lines of MRTs, Line 1 (Standard gauge, 28.8km route length) will be the part of the integrated transportation network including the underground (12 stations: Shield tunnel by Tunnel Boring Machine with outer diameter 7m) and elevated (7 stations: PC Box girder and RC pier) rail line systems.

Scope of this research is to identify the differences between New Austrian Tunneling Method (NATM) and Tunnel Boring Machine (TBM) methods considering proposed underground tunnel alignment of MRT Line 1 based on 3D numerical analysis. To validate the effectivity of PLAXIS 3D in tunnel modeling, two metro lines, Mashhad Metro Line 2 and Delhi Metro Phase 3 have been chosen and comparison between FLAC 3D and Optum G2 with PLAXIS 3D have been focused as well as with empirical formulas. From the comparative analysis of Mashhad Metro Line 2, it can be seen that O' Reily & New empirical relation shows closest values (3.91%, 1.66% and 4.81% deviation with FLAC 3D, MC model in PLAXIS 3D and MCC model in PLAXIS 3D respectively). From the comparative analysis of Delhi Metro Phase 3, it can be seen that the vertical surface settlement found from Peck's formula, Optum G2 abd PLAXIS 3D are 34.10, 29.70 and 31.20mm respectively.

In this research, the tunnel depth of MRT Line -1 has been considered not below than 30m considering the deep foundations of surrounding structures. The tunnel depth and diameter of NATM method are kept constant (depth 35m and diameter 7m) as NATM method is not as flexible as TBM method. For TBM method, three types of depths (30m, 32m, and 35m) and three types of diameters (5m, 6m, and 7m) are considered to take account the effect of parameters in settlement values. Both of the methods are modelled in three different types of systems (MC, MCC and HS) to evaluate the appropriate numerical analysis method by comparing the results with established empirical solutions provided by different researchers.

As the variation in meshing is found considerable (4% for TBM and 10% for NATM), for saving the computation time and finding the close results, medium mesh is considered. It can be concluded after analyzing the results that the total settlement decreases with an increase in depth of the tunnel (almost 11% decrement for every 5m increment of depth) and increases with an increase in diameter (almost 20% increment for every 1m increment of diameter). MCC model shows relatively precise value to the empirical solutions and best fit shape to Gaussian curve. The average deviated values between the numerical result and empirical result shows that, the O'Reily & New equation is better to be used to predict the transverse surface settlement and the deviated percentages from this equation are 5.38%, 3.84% and 6.39% for MC, MCC, and HS models respectively. Increasing the TBM depth results to increase around 4% in distance of inflexion point from center whereas increasing in radius results to decrease around 5% in inflexion point distance from center of the tunnel. Jacobsz formula for predicting longitudinal shows approximately close value to numerical value (around 2 to 16% for NATM and 3 to 10% for TBM). From comparison of longitudinal and lateral settlement, it can be shown that NATM method shows more settlement (10 to 30% more) than TBM method as it includes blast technique which induce more ground surface variation than TBM machine advancement, especially in soft soil. Therefore, Preferring TBM to NATM for constructing the Dhaka MRT Line-1 is the accurate answer.

TABLE OF CONTENTS

LIST OF FIGURES

LIST OF TABLES

ABBREVIATIONS AND NOTATIONS

Symbol	Description
c’	cohesion
φ	Friction angle
ψ	Dilatancy angle
E	Young’s modulus
E_{50}	Secant elastic modulus at 50% peak strength
E_{oed}	Oedometer modulus
E_{ur}	Unloading/reloading modulus
p^{ref}	Reference pressure
λ	Cam-Clay compression index
κ	Cam-Clay swelling index
q	Deviatoric stress
q_a	Asymptotic value of deviatoric stress
q_f	Deviatoric stress at failure
p’	Mean effective stress
e	Void ratio
V_s	Volume of settlement trough
S_v	Vertical displacement
S_h	Horizontal displacement
S	Settlement
S_{max}	Maximum settlement
i	Distance of inflexion point from tunnel center line
Z_0	Depth of neutral axis from the surface
δ_z	Vertical displacement at the surface
υ’	Poisson’s ratio
γ_d	Dry density (kN/m^3)
ω_d	Moisture content (%)
m	Stress dependent stiffness
Cc	Compression index
Cs	Swelling index
M	Material stiffness matrix
G	Shear modulus

K	Bulk modulus
MC	Mohr Coulomb
MCC	Modified Cam Clay
HS	Hardening Soil
SPT	Standard Penetration Test
FEM	Finite Element Method
NATM	New Austrian Tunneling Method
TBM	Tunnel Boring Machine
EPB	Earth Pressure Balancing
SCL	Sprayed Concrete Lining
SEM	Sequential Excavation Method

Chapter 1

INTRODUCTION

1.1 General

Tunnels can be defined as an important section of subterranean structures and underground passages constructed to mitigate the traffic hassle by ensuring the direct transportation of passengers or goods between two certain points through certain obstacles. Tunnels are analyzed according to their shapes, prevailing ground conditions, construction techniques, ground response, changes in pore pressure, plasticity, lining deformations, effects of existing structures, etc. Numerical procedures, such as finite element technique, can simulate construction sequence, model realistic soil behavior, handle complex ground and hydraulic conditions, deal with ground treatment, account for adjacent services and structures, deal with multiple tunnels, simulate intermediate and long-term conditions, etc. and produce realistic results.

When underground space or a large span tunnel is excavated, there is an inevitable chance of disturbing the in-situ stress field causing ground movements leading to surface settlement and potential damage to adjacent structures. Selection of an appropriate excavation method (depends on tunnel depth, tunnel shape, tunnel length, tunnel diameter, conditions of ground water present, use of tunnel, supporting logistics, and appropriate management of risks) for large span urban tunnel projects in soft ground is a key factor for successful completion of the project.

NATM (New Austrian Tunneling Method) is based on the concept that the ground around the tunnel acts as a load as well as a load-bearing element and the tunnel can stabilize itself by using the surrounding rock mass geological stress. It was developed soon after World War II and since then consistent improvements have been made by Mueller, Rabcewiz, Brunner and Pacher. It is now established as a well-recognized flexible technique due to its success in diverse conditions ranging from hard rock to soft rock, soft stable ground to weak, friable and unstable ground. Depending on the project conditions (e.g., shallow soft ground tunnel, deep rock tunnel) and the result of the geotechnical parameters, the requirements of the specific support are determined. The excavation cross section is divided into crown, bench and invert (for soft ground, invert arch is generally required to ensure stability) depending on environmental factors, surface settlements, ground conditions and logistical requirements and

the tunnel is typically advanced by drill and blast following the sequential excavation method. The performance of this method is not found satisfactory in weak formations and shallow tunnels in the urban areas because (1) deformation to some extent is the requirement of the system to relieve or minimize he amount of stress, (2) the ratios of the horizontal to the vertical stress is not the requirement to keep the tunnel face stable, (3) vibration may cause damage to the existing buildings, and (4) need of installation of structural support around the tunnel excavation to re-establish the equilibrium.

TBM (Tunnel Boring Machine) is used for the excavation of tunnels with a cross section of circular or rectangular shape through the different types of rock and soil strata. Diameters of the excavated tunnel can be varied from 1m to almost 16m. TBMs have limitations of predetermined tunnel diameter and shape along the length of TBM drive. During the excavation process of tunnel, TBMs limit the surrounding ground disturbance and produce a smooth wall of tunnel. EPB (Earth Pressure Balance) tunneling machine is used to provide the support to the tunnel face by the excavated soil itself during the excavation process. EPB consists of several devices like cutting wheel for excavating soil, screw conveyor for removing soil from working compartment, pressure cells for monitoring the pressure in the working chamber, excavation chamber closed from tunnel face by pressure bulkhead, mixing vane for assisting to remould the soil. EPB machine is mostly used in the variable and poor ground conditions with low cohesion ground, high permeable ground, high water pressure ground, and clay with gravel, boulder and sand interfaces.

The construction of a tunnel usually leads to surface disturbance, particularly settlement (not important in greenfield sites). The available analytical and empirical solutions are not sufficient to include complex ground conditions and hence a comprehensive analytical solution couple with numerical modelling is necessary to model the effect of surface settlement due to soft ground tunneling. This research discusses different approaches in predicting the settlement and comparison with numerical analysis is also done to validate the solutions.

The objective of the MRT Line – 1 project is to mitigate the traffic congestion, improve environmental pollution, and contribute to economic and social development in Dhaka city by constructing mass rapid system. MRT Line 1 consists of two lines: one route connects Kamlapur in central Dhaka with the Dhaka International Airport (hereafter the Airport Line), and the other route branches off from the Airport line at Notun bazar station to the Purbachal area (hereafter the Purbachal Line) where large scale urban development is currently under

way. The airport line will run entirely through an underground tunnel (14.765km) and the Purbachal line will become an elevated structure to its destination at depot in Rupganj (15.426km). This research presents a framework for selecting the appropriate tunneling method (NATM and TBM) with respect to induced ground surface settlements considering proposed underground tunnel alignment of MRT Line 1 based on PLAXIS 3D numerical analysis.

For simulating tunnel construction methods interaction with soil, PLAXIS 3D finite element software is used in this thesis. Different consecutive models are incorporated in PLAXIS such as simple linear elastic-perfect plastic Mohr-Coulomb (MC) model, the elastic-plastic non-linear stress-dependent stiffness Hardening Soil (HS) model, and isotropic work-hardening plasticity cap Modified Cam-Clay (MCC) model. The real behavior of the excavation process, 3D arching of soil, distribution of settlement, etc. can be precisely simulated in this software. In addition to evaluating the effects of the consecutive model on the soil behavior, empirical methods are used and all results are compared with each other eventually.

1.2 Background of the Study

The Strategic transport Plan (STP) (20-year long plan) has been addressed by Bangladesh Government with JICA (Japan International Corporation Agency) to fix the road congestion caused by crippled transportation system coupled with sluggish traffic conditions. Since 2009 till date, a plan for Mass rapid Transit (MRT) was conceptualized forming the implementing agency DMTCL (Dhaka Mass Transit Company Ltd.). According to the plan, there will be six MRT lines comprising of 61.172km long underground and 68.729km long elevated network system featured with 105 stations across Dhaka city to ease the traffic situation. MRT Line-1 is comprised of 31.241km long and is divided into two sections: Airport Route (19.872km long, total 14 stations) and Purbachal Route (11.369km, total 7 stations). In this thesis, underground portion is focused, where the route alignment is: Airport – Airport Terminal 3 – Khilkhet – Nadda – Natunbazar – North Badda – Badda – Hatirjheel East – Rampura – Malibagh – Rajarbagh – Kamlapur. (NKDOS Consortium Proposal, 2019)

1.2.1 General Topography and Geology of the Study Area: Dhaka is situated between latitudes 23º42’N and 23º54’N and longitudes 90º20’E and 90º28’E. The city is bounded by the Buriganga River to the south, Turag to the west, Balu to the east, and Tongi Khal to the north. The Dhaka city area does not show any surface folding, however a large number of faults and lineaments have N-S, E-W, NE-SW, NW-SE trends recognized from air photo interpretation and the nature of the stream courses. Dhaka city and its surroundings are shown

to be situated in the seismic zone 2 (medium risk zone). The studied area falls into Madhupur Tripura Tract physiographic division of Bengal basin. The soil carried out up to maximum to the Holocene and Pleistocene age sediments in geological time scale in this area. The study area is mostly consisted of clayey soil than the sandy soils. The upper soil layer comprises of grayish to brownish stiff to medium stiff clayey soil and brownish medium dense soil of Basabo Silty Clay formation and hard clayey soil or brownish very dense sand below this, can be of from Madhupur Clay and Sand formation. (ProSoil Survey, 2019)

1.2.2 Parameters Affecting Settlements in Tunnel: To have knowledge about the effects of the parameters of influence zone of ground settlement, it may be helpful to carry out the measurement and give a better solution in the form of numerical modeling. Ground surface settlement behind a reinforced wall takes place due to the unbalanced pressures resulting removal of soil mass inside tunnel excavation. Based upon several case history reviews, the factors that effecting the settlement in tunneling can be grouped into three major categories, such as, geometric parameters (tunnel diameter, tunnel depth, depth of tunnel axis from ground level, the distance from tunnel face excavation and face stability of shield-driven tunnels), geological conditions (geology at tunnel invert and crown, groundwater level, etc.), and shield operation parameters (penetration rate, face pressure, pitching angle, percent of tail void grouting and amount of excavated material per ring). In this thesis, we emphasized the effects of tunnel geometry parameters (tunnel depth, tunnel diameter, influence zone) to the settlements. (Loganathan and Poulos, 1998)

1.2.3 Importance of The Research: In comparison, NATM and TBM are essentially equivalent from the viewpoint of construction operation. The final choice is determined by the local geological conditions for the project and the length of the tunnel. Though International Consultants team has already proposed the Shield tunnel by TBM-EPB as the tunnel construction method for Line 1 project, I want to shed light on some factors of NATM in urban areas. Also, I want to compare the displacement effects between both techniques and from this perception I want to establish the fact if NATM is also viable like TBM for our Dhaka city or not.

1.2.4 Reliability of FEM as Method for Numerical Analysis: In a real tunnel, the different facets are clearly coupled and the problem is complex, involving pore pressure changes, plasticity, lining deformations and existing structures. Numerical procedures, such as the finite

element technique, lend themselves to the analysis of such complex problems (Potts, 2001). The finite element method can:

i. Simulate construction sequence.

ii. Deal with complex ground conditions.

iii. Model realistic soil behavior.

iv. Handle complex hydraulic conditions.

v. Deal with ground treatment (e.g., compensation grouting).

vi. Account for adjacent services and structures.

vii. Simulate intermediate and long-term conditions.

viii. Deal with multiple tunnels.

1.2.5 Choosing 3D Numerical Analysis over 2D Analysis: The complex interrelation between the interconnected elements makes for a highly complex mathematical problem. The analysis is performed by solving the equation matrix that models, the mesh made up of the limited number of elements. That is, a system of equations is set up which relates unknown quantities to known quantities via a global stiffness matrix. For instance, the relationship of nodal forces to displacements is analyzed this way throughout the finite element mesh. Highly complex underground conditions and tunnel characteristics can be analyzed in 3D. The capability of the 3D analysis includes the simulation of complex constitutive laws, non-homogeneities, and the impact of advance and time dependent characteristics of the construction methods. As tunnel excavation is clearly a three-dimensional problem, considering the third dimension should intuitively lead to more accurate predictions (Tatiya, 2005).

1.3 Objectives of the Study

The main goals of the research:

i. To conduct numerical analysis of proposed tunnel in NATM method to obtain ground movement and deformation.

ii. To conduct numerical analysis of proposed tunnel in TBM method to obtain ground movement and deformation.

iii. Comparison between two methods based on the results (comparative parameter: displacements for three types of models) of numerical analysis and establish a portfolio for the suitable method.

1.4 Methodology and Flow Chart of the Study

The field data collection are prior arrangements for determining site conditions (ground water level, soil type, visual soil parameters, etc.) mobilizing the soil samples to laboratory for further testing. Through conducting laboratory tests according to the codes, soil properties (geotechnical) can be determined which can be used as parameters for FEM analysis. FEM analysis needs to follow some definite steps to acquire approximately accurate results which are described later in this section. Literatures of previous researchers are needed to be verified and numerical analysis with PLAXIS 3D have been used for the establishment of the papers. Also, PLAXIS 3D is used to develop models varying different types and different parameters for the NATM and TBM methods. The methodology of the study can be described in the Figure 1.1:

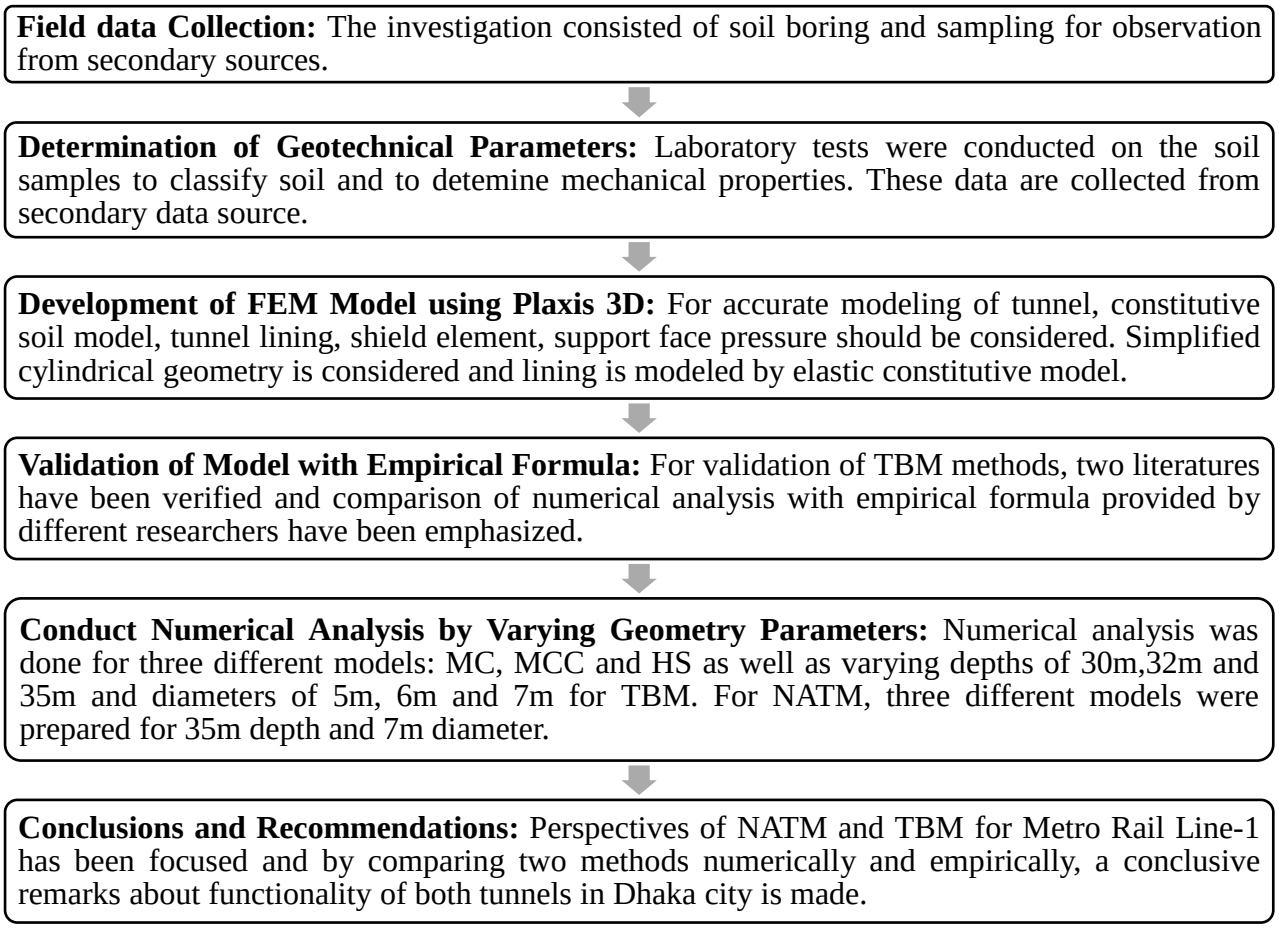

Figure 1.1: Overall Methodology Flow Chart of the Research

Development of FEM model analysis consists of following steps:

Step 1: Define the Objectives for Model Analysis: If the objective is to decide which is proposed to explain the behavior of a system, then a crude model may be constructed, provided that it allows the mechanisms to occur. Complicating features should be omitted if they are likely to have little influence on the response of the model.

Step 2: Create a Conceptual Picture of the Physical System: It is important to have a conceptual picture of the problem to provide an initial estimate of the expected behavior under the imposed conditions. The considerations which will dictate the gross characteristics of the numerical model are: anticipation of stability or instability of the system, linear or non-linear response, large or small expected movements, effect of well-defined discontinuities, influence of groundwater interaction, geometric symmetry of the structure, etc.

Step 3: Construct and Run Simple Idealized Models: When idealizing a physical system for numerical analysis, it is more effective to construct and run simple test models first before creating the detailed model. The results from the simple models help to guide the plan for data collection by identifying which parameters have the most influence on the analysis.

Step 4: Assemble Problem-Specified Data: The types of data required for analysis of a model include: details of the geometry, locations of geologic structure, material behavior, initial conditions, and external loadings. Since typically, there are large uncertainties associated with specific conditions, a reasonable range of parameters must be selected for this investigation.

Step 5: Prepare a Series of Detailed Model Runs: The numerical analysis involves a series of computer simulations that include the different mechanisms under investigation. It can be difficult to obtain information to arrive at a useful conclusion if model run times are excessive. The state of the models is saved at several intermediate stages so that the entire run does not have to be repeated for each parameter variation.

Step 6: Perform the Model Calculations: At any time during a sequence of runs, it is possible to interrupt or pause the calculation, view the results, and then continue the model.

Step 7: Present Results for Interpretation: The final stage of problem solving is the presentation of the results for a clear interpretation of the analysis.

1.5 Organization of the Thesis

The thesis is divided into several chapters to achieve the stated objectives. The chapters are structured as follows:

Chapter one discusses an introduction of the relevant research background, statement of problems as well as the objectives of this research.

Chapter two presents the tunneling construction methods, principles and differences between NATM and TBM methods, effects of different parameters in ground settlement for NATM and TBM methods, and properties of different soil consecutive tunnel modelling procedures in PLAXIS 3D with the applicability verification.

Chapter three represents the validation of models of two projects, Mashhad Metro Line 2 and Delhi Metro Phase 3, considering the actual soil and geotechnical properties in PLAXIS 3D. The calculated results are then compared with the proposed empirical relations and real time data of the projects to validate the FEM.

Chapter four emphasizes the field data collection and investigation to know the subsoil condition of MRT Line 1 Project area. Also, geology and soil sources or patterns are described on the basis of the findings in geotechnical and historical investigation. Methods of site investigation includes different types of soil related tests (SPT, sieve analysis test, Atterberg limits test, natural moisture content test, specific gravity test, consolidation test, and triaxial test) to determine the properties of soil layers to ease the numerical modeling. In this chapter, the numerical modeling procedures need to be followed to acquire definite objective are also portrayed. Both NATM and TBM methods are picturized in the MC, MCC and HS models. Also, effect of depth, diameter and meshing are focused on the models. Also, this chapter presents the findings of the research program with different graphical and tabular representation.

Chapter five states the conclusive remarks and recommendations for the future research scope.

Chapter 2

LITERATURE REVIEW

2.1 Introduction

Urbanization has increased with the rapid rate in the recent past, with excess people drifting towards Dhaka increasing the population density. Hence, the developers and country leaders are trying to utilize both underground and above surface spaces judiciously. Due to the unavailability of ground space and current transportation system, it is proposed to use underground space for rapid transport which may reduce transit time and more habitual environment. In recent past years, the advances in rock mechanics to evaluate ground conditions along with the developments in ground consolidation and support techniques have enabled us to create large underground excavations. As tunnels move through different geological and hydrological conditions as well as different overburden pressures, the proper construction of the tunnels is vital for its long-term stability. While driving through soft ground, the main concern is to avoid collapse and subsidence of the overlying strata as ground, when dug, is not self-supporting and cannot stand without support beyond a very short period (Naqvi et al., 2021). Also, it is necessary to understand the interaction and effect of a newly constructed building overlying the pre-existing underground tunnel for stability purposes.

When unground space or a large span tunnel us excavated, it inevitably disturbs the in-situ stress field causing ground movements leading to surface settlement and causing serious damage to adjacent structures. The ground needs to be excavated sequentially and setting up of temporary supports goes side by side up to disposal of muck and replacement of temporary support to permanent ones. Appropriate ground improvement or advance timbering using piles or use of shields may overcome the problem of decompression or ground fall. Generally, several methods – such as numerical analyses, empirical approaches, physical modelling and closed form solutions – can be used to predict the settlements. By considering the capability of numerical methods, such as the finite element (FEM) and finite difference (FDM) could be the best approaches for studying the complex situation of soil, soil-structure interaction, and time-dependent problems. One of the common approaches to evaluate surface settlements is the empirical formulas proposed by Peck. For a precise simulation of tunneling, it is better to simulate using 3D model as FEM software are developed to evaluate the effects of the constitutive model on the soil behavior (Peck, 1969).

2.2 Philosophy of Tunneling

Ground, with all its uncertainty, and general inability to influence its properties (notwithstanding ground improvement techniques), is the construction material of tunneling. Although a tunnel structure often needs steel and concrete support systems, it is the ground that acts as the major part of the structure (both a supporting and a leading role). A tunnel construction in a ground mass which is previously in equilibrium, can be interpreted as the removal of the ground stresses in the contour of the excavation. The removal of the soil volume induces a new stress state in the vicinity of the excavation that searches for a new state of equilibrium. This equilibrium can be reached without any support, when the ground is classified as self-supporting, or with the application of a specific support system, as for example a sprayed concrete layer in the contour of the excavation in order to control the soil deformation (Franca, 2006).

The key to successful tunnel construction is, therefore, to understand the strength and stability characteristics of the soil. It is up to the Engineer to determine the relevant ground conditions and its associated properties as only a small fraction of the total ground to be affected by tunnel construction can be tested and also knowledge of effects of layering, fissures and discontinuities is still limited. Often the assumption is that ground acts as continuum and allows three-dimensional stress redistribution around tunnel void, thus taking some of the load, so that full overburden does not act as tunnel load. The deformations allowed to the ground mass due to an excavation lead to a stress redistribution, in which the soil in the vicinity of the excavation is mobilized. In addition, the strength/stiffness of the lining, already applied in the contour of the excavation behind, is also mobilized due to stress redistribution as well, which then contributes to the generation of a new state of equilibrium. The mechanism that leads to this stress redistribution is called the arching effect.

In general, in an intact soil mass, the direction of the principal stresses before a tunnel excavation is undertaken, coincides with the vertical and horizontal directions. The direction of the principal stresses indicates the planes in which no shear stress occurs, thus it is possible to identify that before an excavation, in an ideal situation, and there is no shear stress in the vertical and horizontal planes of the soil mass. However, as it was already introduced, a tunnel excavation necessarily mobilizes shear stresses in the vicinity of the tunnel contour, hence the planes in which no shear stress is identified change, inducing a rotation of the principal stresses' direction. The stress redistribution above mentioned, occurs not only in a plane perpendicular

to the tunnel axis but also longitudinally, both in vertical and horizontal planes (Barbosa, 2016b).

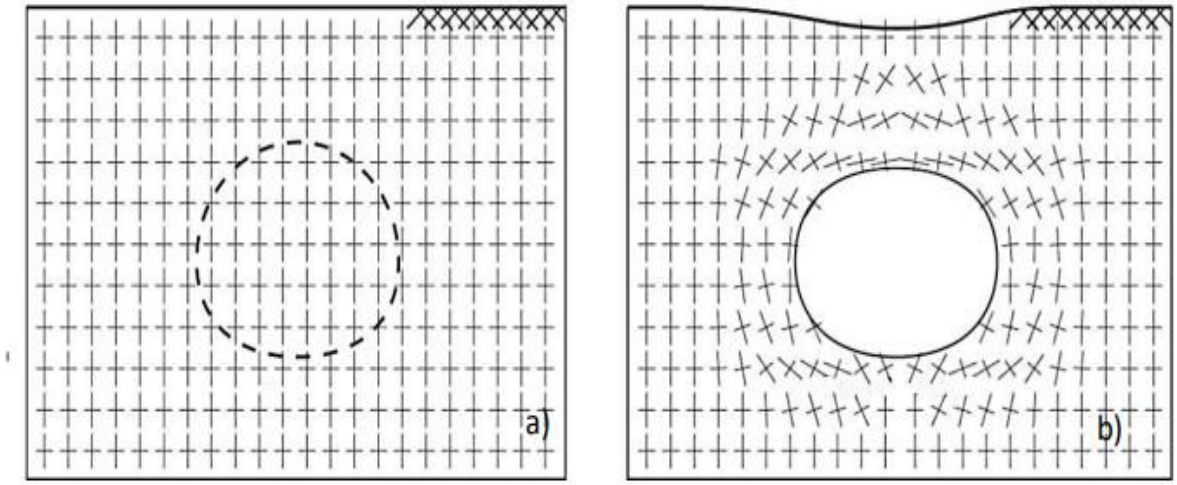

Figure 2.1: Direction of the Principal Stresses: a) in an intact soil mass, b) after tunnel excavation (Franca, 2006)

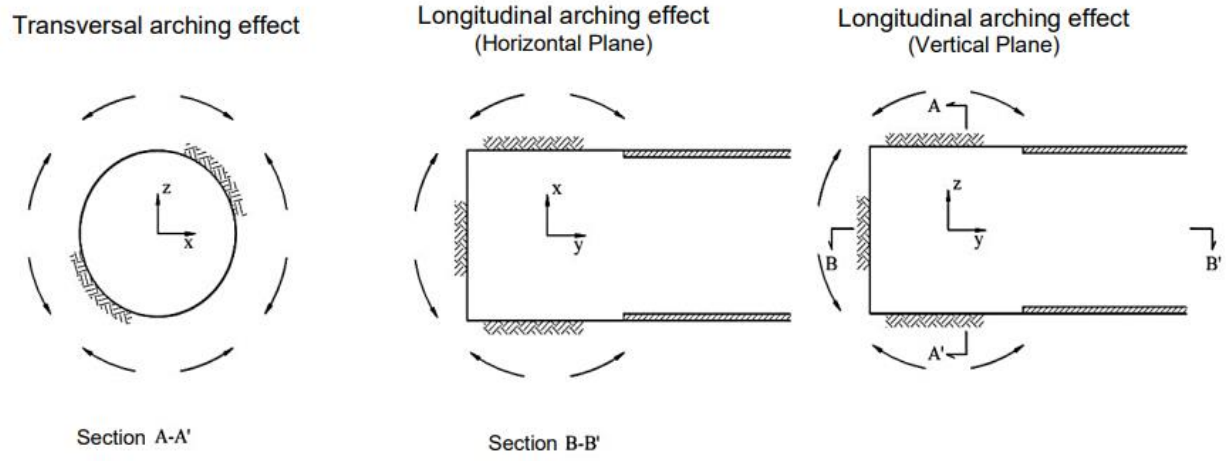

Figure 2.2: Three-dimensional arching effect (Zhao et al., 2007)

A tunnel excavation leads inevitably to convergence of the ground in vicinity of the excavation. The longitudinal displacements reach a maximum value when the excavation face is crossing a reference section. After the reference section is left behind, the longitudinal displacements start to record an opposite movement, disappearing at a certain distance. On the contrary, the importance of the radial displacements is greater for a certain distance from the excavation face, which is reached after the passage of the excavation face. For the majority of the cases, the effect of the excavation is registered within two diameters, both ahead and behind the excavation face. Thereafter, a plane strain analysis can be carried out for a section of the tunnel

where the excavation face has no more influence since the equilibrium has been reached. However, a plane strain analysis must only be applied when both geotechnical and geometrical properties remain constant along the tunnel axis.

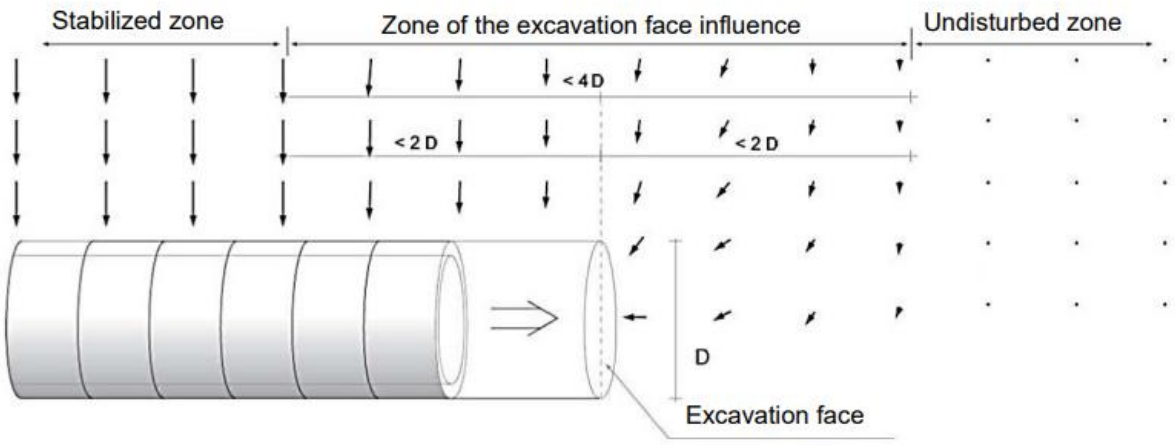

Figure 2.3: Influence of the Excavation Face: Ground Mass Displacements (Franca, 2006)

2.3 Tunnel Construction Methods

The selection of appropriate method for the excavation of the tunnel is mostly based on the field experience embracing the theoretical knowledge and calculative approaches, because of the variable ground condition. Nowadays, tunnels are excavated through different underground formations ranging from clay to high strength igneous rock (Garry, 2012). The most effective factors to decide the proper excavation method are tunnel shape, tunnel size, underground hydrology, structural geology, regional geology, properties and geotechnical characteristics of surrounding materials, weak zone characteristics, induced and in situ stresses (Yu and Chern, 2007). It is quite common in the engineering literature to find a distinction between tunneling techniques to be applied in soft ground or in rock, however, tunneling techniques are now being used in a wider range of ground conditions and this boundary is becoming increasingly blurred. The major difference between both types of ground conditions relies on the stand-up time of the ground, which for soft soils is very short or almost non-existent. Therefore, the adoption of the construction method is driven by the need to support the ground immediately after the creation of the void, ensuring the stability of the created void, and controlling the deformations within acceptable limits (Barbosa, 2016a).

The different methods of tunnel construction are indicated in Figure 2.4 and the details of NATM method and TBM-EPB method are described in Section 2.3.1.

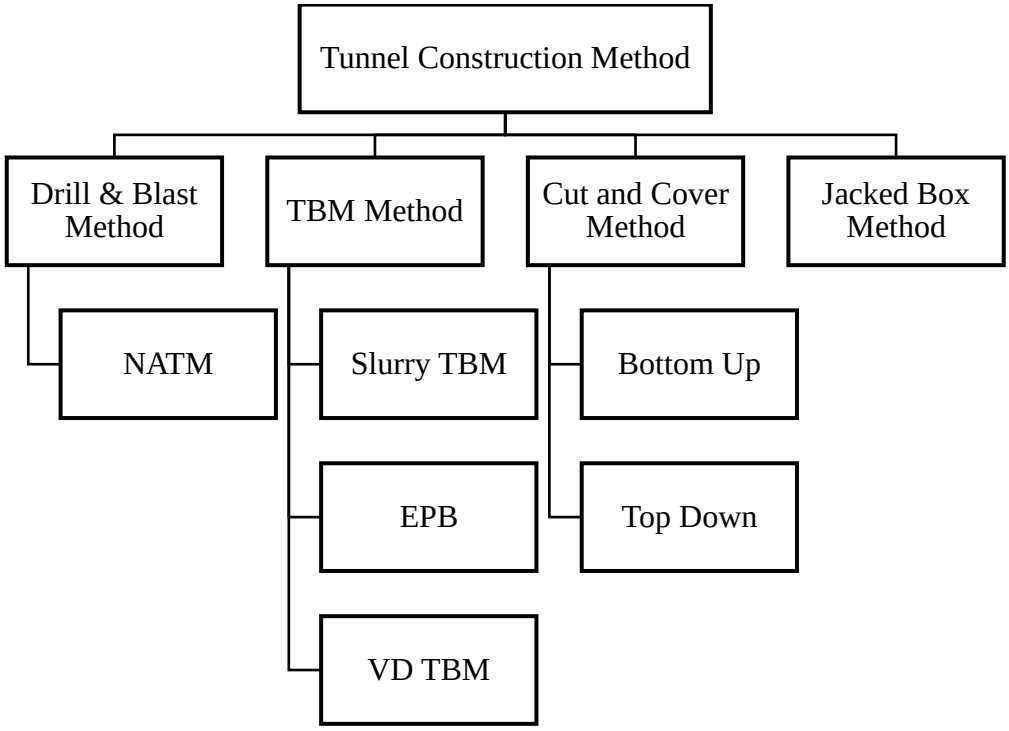

Figure 2.4: Classifications of Tunnel Construction Methods (Tatiya, 2005)

2.3.1 Drill And Blast Method – NATM

Drill and blast method is appropriately applicable for varying properties of rock mass and for non-circular cross sections with tunnels of shorter length. NATM (New Austrian Tunneling Method) assimilates the principle of rock mass behavior and monitors the underground construction performance during construction. The New Austrian Tunnelling Method, NATM, is one of the most adaptable and responsive tunnelling excavation and support methods available. ICE (1996) identifies four main principles to define this excavation method:

i. The strength of the ground around a tunnel should be deliberately mobilized to the maximum extent possible;

ii. Mobilization of ground strength is achieved by allowing deformation of the ground;

iii. Initial or primary support, which has load-deformation characteristics appropriate to the ground conditions, is installed. Permanent support works are normally carried out at a later stage;

iv. Instrumentation is installed to monitor the deformations of the initial support system and the build-up load upon it. When appropriate, the results of this monitoring, form the basis for varying the primary (and permanent support), and the excavation sequence.

A main feature of the construction technique of the New Austrian Tunnelling Method (NATM) is that the proposed tunnel is sequentially excavated and supported, and the excavation sequences and face areas to be excavated can be varied (ICE, 1996). The typical excavation sequence and support conditions are visually showed in the Figure 2.5 and Figure 2.6. The key to minimize surface and subsurface deformations is to maintain the stability of the exposed excavation face, consequently, since the stability of the excavation face is in inverse proportion to its size, subdividing the cross-section into multiple drifts is advantageous.

Typical configurations for NATM tunnels subdivide the excavation face into crown, bench and invert excavations, more complex configurations may include a sidewall drift or even twin sidewall drift. The primary lining, applied sequentially alongside the excavation of each drift, is provided by sprayed concrete in combination with a wire mesh, and when necessary, steel arches and ground reinforcements, such as rock bolts (Leca and Clough, 1992). Ongoing excavation induces stresses redistribution, in which the stresses decrease due to the removal of the soil in the zone of active excavation, and increase ahead and behind the tunnel face. As introduced in the previous section, the final equilibrium occurs within a distance of about two times the tunnel diameter, hence at this point the structural tunnel lining must be effective, which is achieved by closing the tunnel lining in the invert within this distance behind the face. It is then clear that prompt ring closure is essential to minimize ground movements. The interpretation of the geotechnical monitoring allows changes to be applied in the excavation and support system during the excavation process, to improve the overall tunnelling performance. Lastly, the permanent support is usually provided by a cast in-situ concrete lining, which is normally considered separately for design purposes.

The basic concept of the NATM method is to form the ground arch using the support function of ground surrounding the tunnel and to keep the space stable. NATM is also referred as to Sequential Excavation Method (SEM) because while excavating a tunnel, the face of the tunnel is divided into a number of temporary drifts reducing the surface settlements, and ensuring face stability (Galler et al., 2009). During the excavation process of a tunnels, a flexible thin and closed shell concrete is applied on to the walls after excavating a tunnel cross section. The excavated area is kept small and timely installation of initial support is ensured. This method claims that immediate sequential support prevents micro and macro movements. Strong interaction between viscous rock/soil mass and hardening shell of shotcrete, soil creep characteristic, time span between excavations, and shotcrete mixture stiffening characteristics are the characteristics features of this method (Hellmich et al., 1999). The schematic views of

sequential construction methods of NATM are presented in different figures (Figure 2.7, Figure 2.8, and Figure 2.9). The performance of this method is not satisfactory in weak formations and shallow tunnels in the urban area because of the deformation of the system, vibration induced by the method and ratios of the horizontal to the vertical stress. Sprayed concrete, anchors, rock bolts/dowels, wire mesh, lattice girder, etc. are used to stabilize the tunnel perimeter in NATM method. NATM applications in soft soil differ from the applications in rock both in the excavation sequence and in the completion of the primary support. The application of these measures is even more important for tunnels constructed in urban areas, where settlements must be limited in order to avoid damaging overlying structures. The principal measures as presented in ICE (1996) are listed below:

i. Excavation stages must be sufficiently short, both in terms of dimensions and duration;

ii. Completion of primary support, in particular the closure of the sprayed concrete "ring" must not be delayed. The staged excavation should be limited to an extent in terms of dimensions and duration in order to reduce the settlement which is one of the most important problems encountered in soft soil tunneling.

Additionally, artificial measures, such as freezing or grout injection, may be used to improve the capacity of self-supporting of the soil, when the stand-up time is almost inexistent. This is when the limit of this construction technique is reached (Chapman et al., 2017). Overall, this sequential excavation method is relatively slow, nevertheless it is considered to be very useful in areas where existing structures found in the vicinity, such as a sewer, that could not be relocated. NATM offers a flexible construction technique that can cost-effectively adapt to irregular geometries and unforeseen conditions.

Following are some situations where NATM is suitable:

i. For projects with highly varying ground conditions, as methodology can be altered according to the changes in the geology.

ii. As this is a flexible technology it can be used for different geometry of the tunnels. By changing the blasting patterns required geometry of the tunneling sections can be achieved.

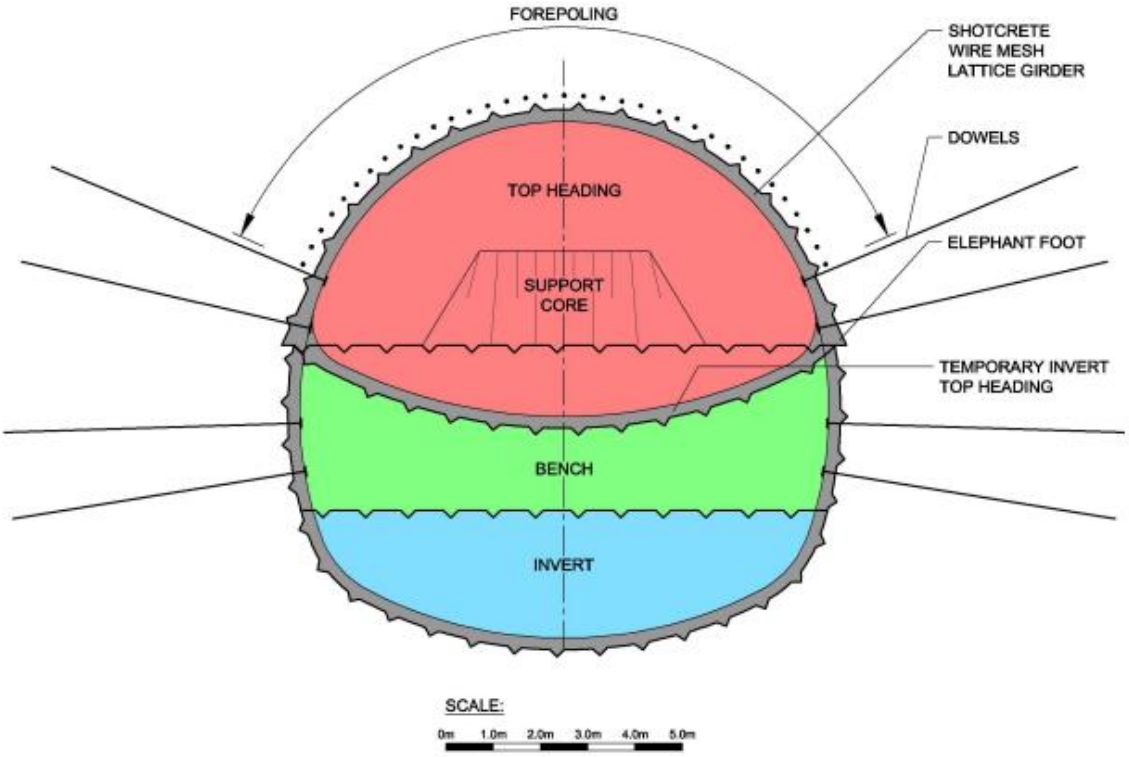

Figure 2.5: Typical Excavation and Support in Soft Ground Conditions (ICE, 1996)

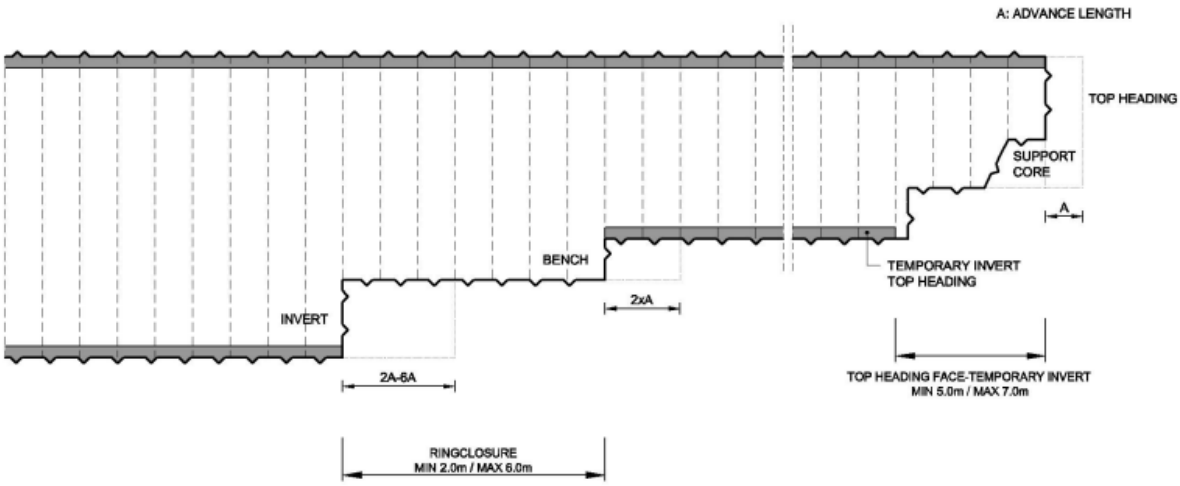

Figure 2.6: Typical Excavation Sequence in Soft Ground Conditions (ICE, 1996)

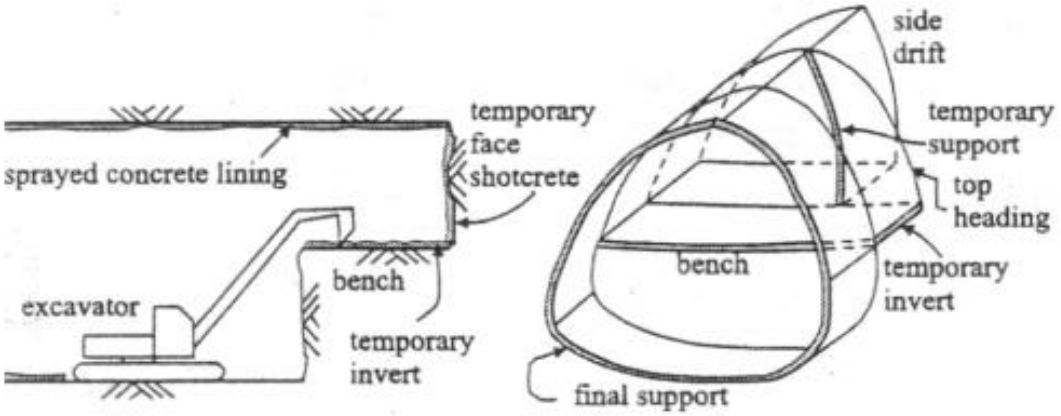

Figure 2.7: Schematic View of SCL Method (Potts, 2001)

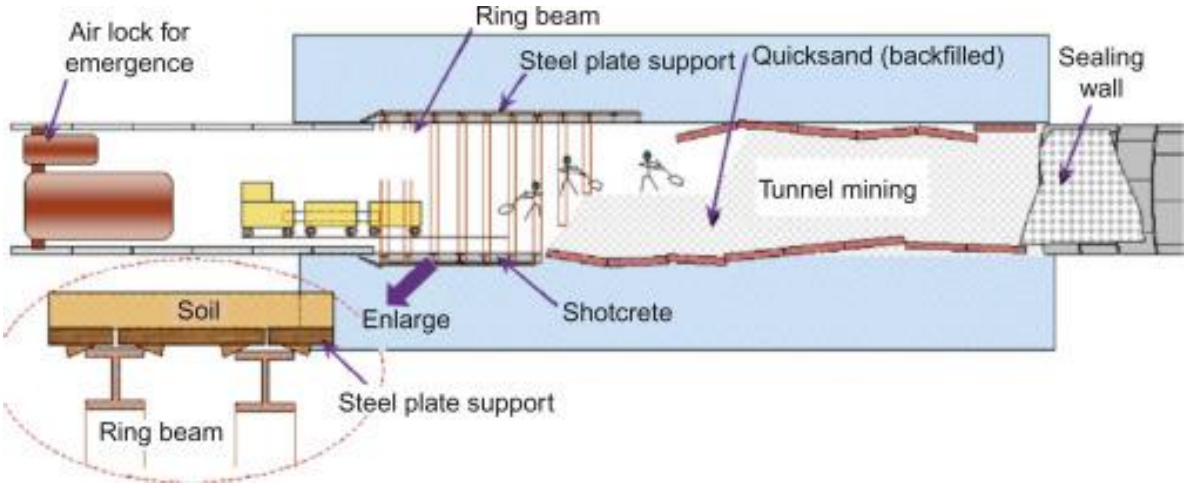

Figure 2.8: Construction Procedure of NATM Method (Schubert, 2001)

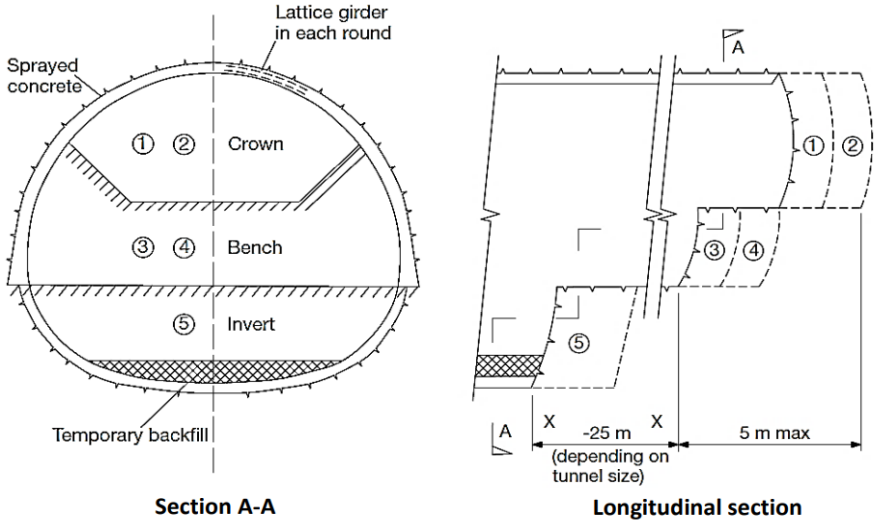

Figure 2.9: Sample Construction Sequence of Crown, Bench and Invert (ICE, 1996)

The SCL (Sprayed Concrete Lining) construction method, as it is used in soft ground in urban areas throughout the UK, uses an incremental excavation sequence, where a sprayed concrete layer is applied to form a primary lining with, or without, wire mesh, steel fibers, lattice girders, dowels, anchors or bolts. This is then followed by the installation of a permanent lining later on. The primary support particularities are determined in advance of the construction by the designer and are validated during construction by instrumentation and monitoring. A number of methods have been used for subdividing the face. This subdivision is applied in order to provide a better control of face stability, convergence and settlement, by ensuring earlier support.

For large openings using SCL it is always the case that the tunnel is created by the method of advanced headings. This can involve excavation of the crown first, leaving a temporary invert, or the use of left and right-side drifts, or a combination depending on the ground quality and the size of opening. In stiff competent strata, such as London Clay, full face excavation is possible up to 30 m^2 in cross section (ICE, 1996), however when advancing full face, a stepped profile of heading and invert is commonly adopted.

2.3.2 TBM Method – EPB

A tunneling method that maintains the face stability (the stability of the tunnel face) against earth and water pressure by mud or slurry in the excavation chamber, drives the shield machine, and erects the lining to maintain stability of the ground. TBM (Tunnel Boring Machine) method, also known as a ‘mole’, is a machine used to excavate tunnels with a circular cross section through a variety of soil and rock strata (Chappell and Parkin, 2004). TBMs have the advantages of limiting the disturbance to the surrounding ground and producing a smooth tunnel wall. Modern TBMs typically consist of the rotating cutting wheel (cutter head), a main bearing, a thrust system and trailing support mechanisms. In soft ground, Earth Pressure Balance Machines (EPB), Slurry Shield (SS) and open face type TBMs are mainly used. An earth pressure balanced shield machine should be designed to ensure that the excavation and drive units, cutting face stabilization unit, additive injection unit, mixing unit and excavated material transport unit function reliably under the prevailing ground conditions.

An EPB machine should be selected according to the ground conditions and all elements of the mechanical components should be highly durable and watertight. EPB machines are used in soft ground with less than 7 bar pressure and it uses the excavated material that is kept under pressure inside excavation chamber and thrust jacks on the shield to balance the pressure at the

tunnel face. TBMs with positive face controls (EPB) are used in urban tunneling to reduce the risks of surface subsidence and voids. Soil enters the excavation chamber through openings, where mixing arms on cutting wheel and bulkhead mix the soil paste. Bulkhead transfers the pressure of thrust cylinders to pliable soil paste and when pressure of soil paste in excavation chamber equals the pressure of surrounding soil and groundwater, necessary balance has been achieved. The cuttings are removed by the cutter head buckets or scoop that transfers them to a screw conveyor. After completing a boring stroke, the tunneling machine is advanced by hydraulically pulling the gripping mechanism in from the tunnel's walls, and then stroking forward and resetting the gripper to a new forward position on the walls (Phadke, 2017). The components of a TBM-EPB machine are shown in the Figure 2.10 for the reference.

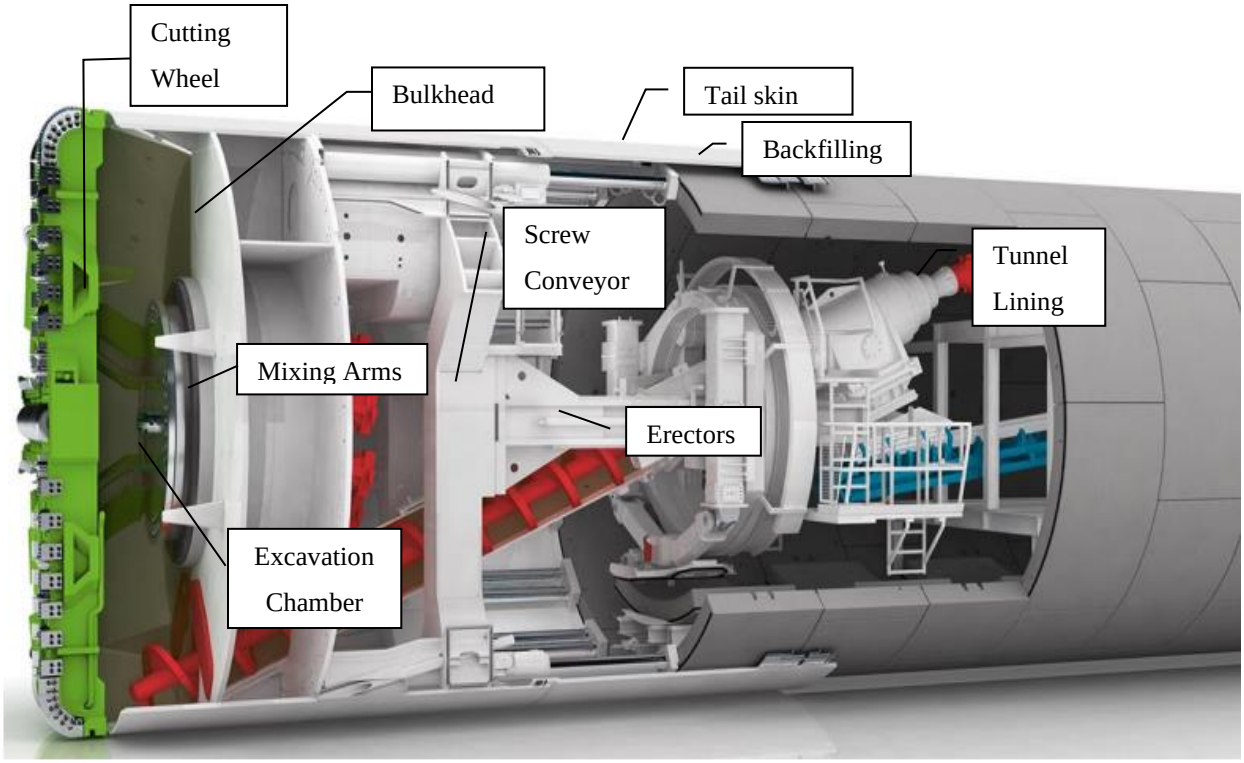

Figure 2.10: Components of a TBM-EPB Machine (Source: Internet)

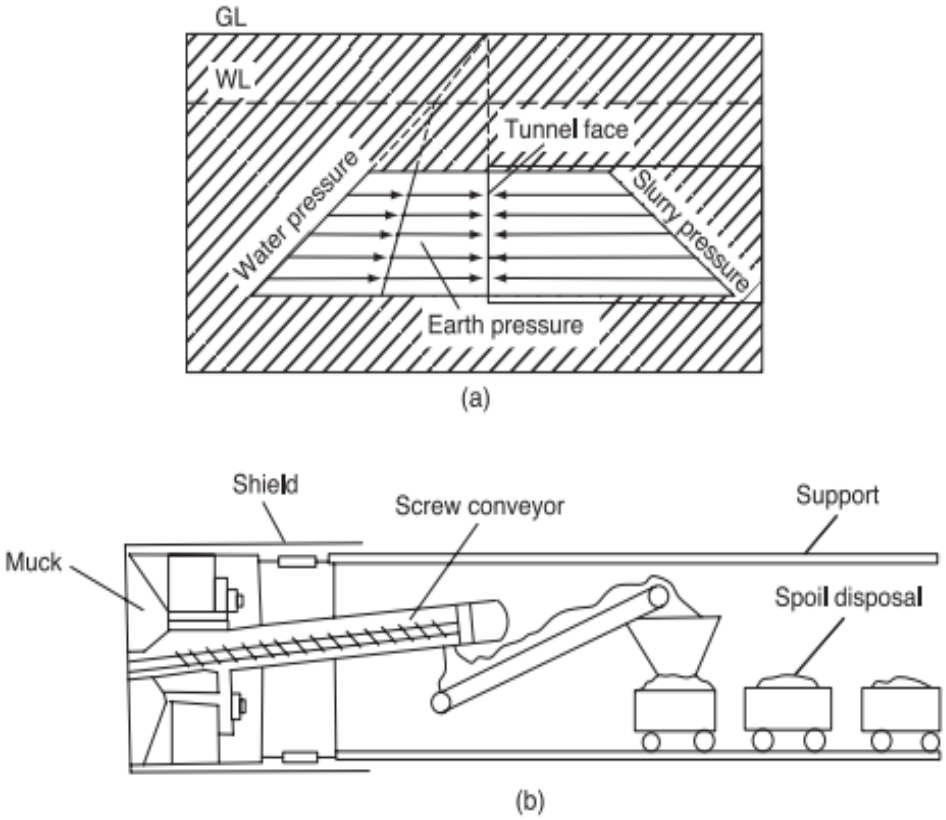

Figure 2.11: Conceptual Diagrams for EPB shields: (a) method to counter water and earth pressures; (b) mechanical components and arrangements in the EPB concept (Tatiya, 2005)

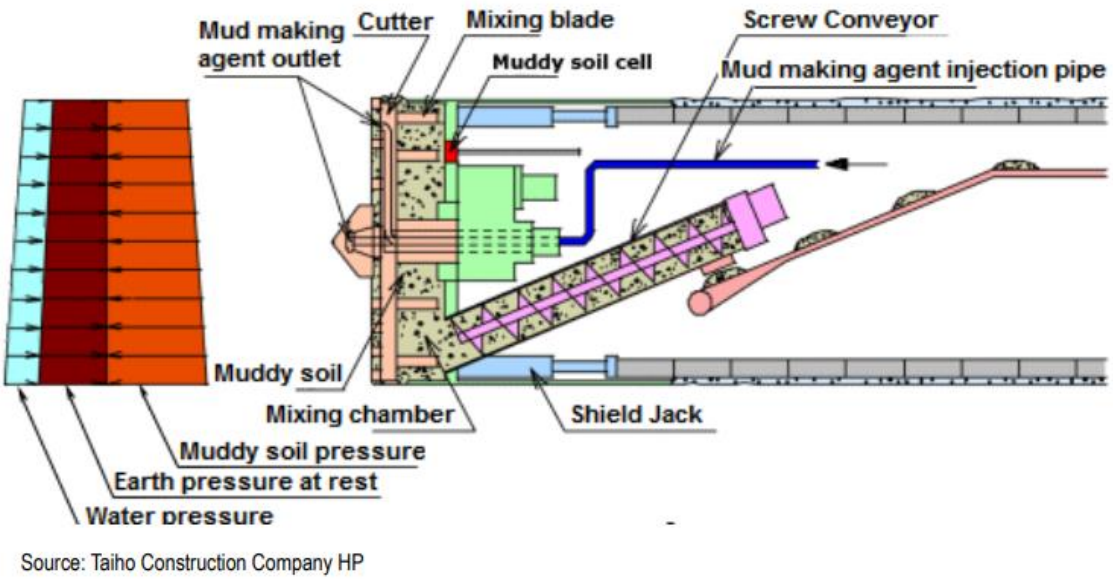

Source: Taiho Construction Company HP

Figure 2.12: Overview of Earth Pressure Shield Machine (Source: Taiho Construction Company Website)

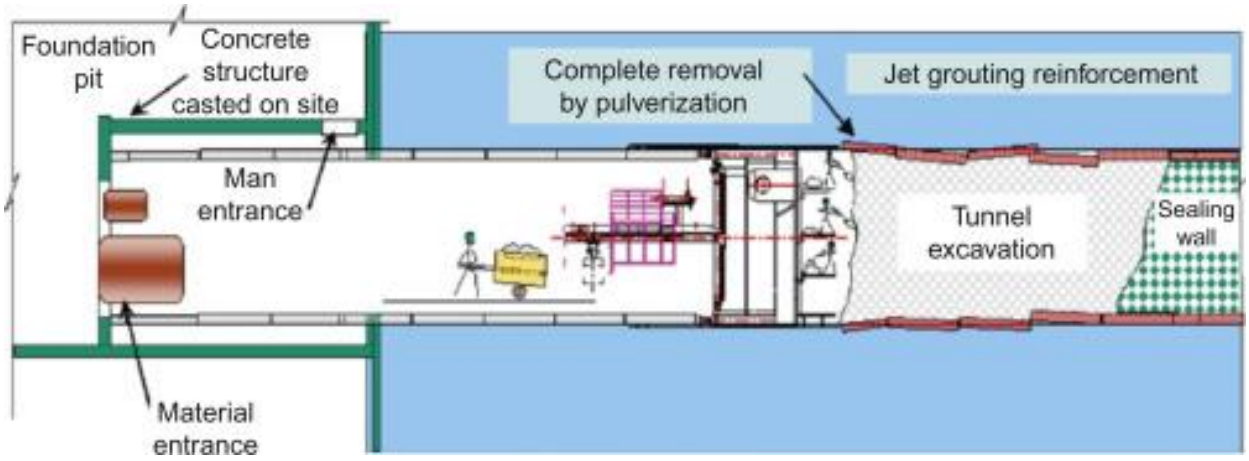

Figure 2.13: Construction Procedure of TBM-EPB Method (Source: Internet)

In the EPB machine method, creating a supporting pressure prevents loss of stability at the working face. In this method, the soil loosened by the cutting wheel serves to support the working face. The shield area in which the cutting wheel rotates is designated as the extraction chamber and is separated from the shield section, which is under atmospheric pressure, by the pressure wall. The soil is loosened by the tools of the cutting wheel, drops through the openings in the cutting wheel into the extraction chamber and mixes with the plastic pulpy soil which is already there. Transferring the power of the tunneling jacks from the pressure wall to the pulpy soil prevents uncontrolled penetration of the soil from the working face into the extraction chamber (Khan, 2016). At the point when the pulpy soil mixture is in the extraction chamber, the pressure of the earth and water, which lies ahead, causes a state of equilibrium to be reached, and the jacks to no longer compress the chamber. The tunnel is usually lined with steel-reinforced concrete lining segments, which are positioned and fastened by the erector in the shield area behind the pressure wall under atmospheric pressure conditions. The method to counter the water and earth pressures along with mechanical components and arrangements, and construction procedure are visualized in Figure 2.11, Figure 2.12, and Figure 2.13. This system has the following features (Tatiya, 2005):

i. Could be used in ground with a high percentage of silt/clay.

ii. No separation plant is needed.

iii. With little cover, there is no danger of blowouts through pulpy support slurry.

iv. Mechanical excavation ensures better performance and accessing the tunnel face (under pneumatic air pressure) is possible; this sometimes needs to be done to remove obstacles.

v. It does not require secondary support in the form of compressed air, suspension media or breast plates. Rather the material is cut mechanically by the cutting wheel; serves as a support medium.

vi. In this technique the material that is yielded by the rotating cutting head is not allowed to fall into the excavation chamber but is diverted to mix with the plastic earth slurry.

2.3.3 Difference between NATM and TBM

Table 2.1: Descriptive Mentionable Differences between NATM and TBM Methods

	NATM	TBM
Outline of the method	Makes use of ground supporting function of the area surrounding the excavation. It requires ground arch effect to be in effect and a self-standing face. When these two conditions are not satisfied, it may still be applied using auxiliary measures.	TBM is driven coping with earth and water pressure at the cutting face by filling chamber with slurry or excavated muddy soil, etc. Tunnel walls are prevented from ground collapsing by a segmental lining which is assembled in the shield machine.
Applicable geological conditions	Generally, it is applicable to hard rock and Neocene soft rock, and it can be used in diluvial formations depending on ground condition of the project. In this case, it can be executed in unconsolidated ground that have an unconfined compressive strength higher than $100kN/m^2$ and a modulus of deformation higher than $10000kN/m^2$.	Generally, it is applicable in alluvial, diluvial and very soft and weak Neocene ground. It has flexibility to accommodate variations in ground conditions.
Countermeasure for groundwater	If there is a large amount of water inflow, it is necessary to adopt auxiliary measures, such as grouting, deep wells, well points, drainage tunnels and others.	No auxiliary measure is required.

Tunnel depth	When tunneling through unconsolidated ground with a small ratio of overburden (<2) and diameter (H/D), and effective auxiliary measure is necessary to keep the crown from collapsing or settling.	According to the common practice, the minimum overburden is between 1.0D and 1.5D. Tunneling is carried out at a depth of less than 100m in sandy soil and other types of unconsolidated ground.
Cross Section	The crown of the cross section should be arched.	Circular, elliptical and rectangular shaped tunnels can be constructed. It is difficult to change the cross section after starting of tunneling operations.
Size of cross section	No limitation	Ratio of the radius of curvature to the outer diameter of the tunnel is usually in the range of 3 to 5.
Influence of surroundings	In case of construction near existing structures, auxiliary measures are needed. In urban areas, attention should be paid to the surface settlement caused by boring and reduced level of the groundwater. Noise and vibration damage is confined within the vicinity of the tunnel portal.	In some cases of construction near existing structures, auxiliary measures of bolstering up of existing structures is needed depending on the amount of separation. The influence on road traffic is extremely small except in the vicinity of vertical shafts. Noise and vibration damage is confined within the vicinity of vertical shafts.

2.4 **Shape and Size of Tunnel Inner Section**

The inner cross section of NATM tunnel is decided by adding ventilation facilities, lighting facilities, emergency facilities, and road signs to the construction gauge, and by allowing for tolerable construction errors. A mountain tunnel can be designed with a high freedom in its sectional geometry and dimensions. The stress distribution of around the NATM tunnel is affected by excavation cross section and initial stress distribution in the ground. The standard

cross section and commonly provided facilities and structure of a single track and a double track railroad tunnel for NATM and TBM methods are shown in Figure 2.14 and Figure 2.15.

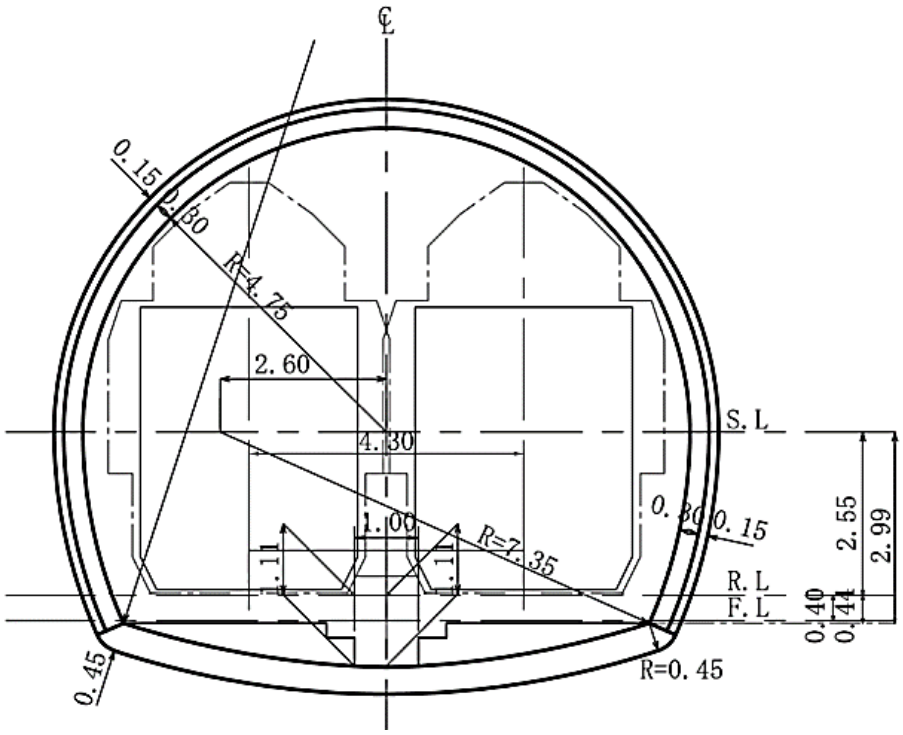

Figure 2.14: Example of standard cross section of railway tunnel (NATM) (Daraei and Zare, 2019)

The main reason that a circular section is generally selected for TBM is as follows:

i. A dynamically stable structure with a slightly thinner lining than the other sectional types.

ii. Simple excavation mechanisms can be used.

iii. Normally strong against external pressure.

iv. Advantageous for driving a shield machine, for excavation, for manufacturing, and for assembly of segments.

v. Easy to cope with rolling movement of the TBM or segments.

The inner section of a railroad tunnel needs to be selected considering: construction gauges, track center clearances, the presence of a secondary lining, rooms for maintenance and management, track structures, the requirement of spaces for maintenance, and construction errors in the TBM method due to vertical and horizontal meandering, deformation and uneven

settlement. The allowable construction errors are generally in the range of 50 to 150mm from center in the vertical and horizontal directions.

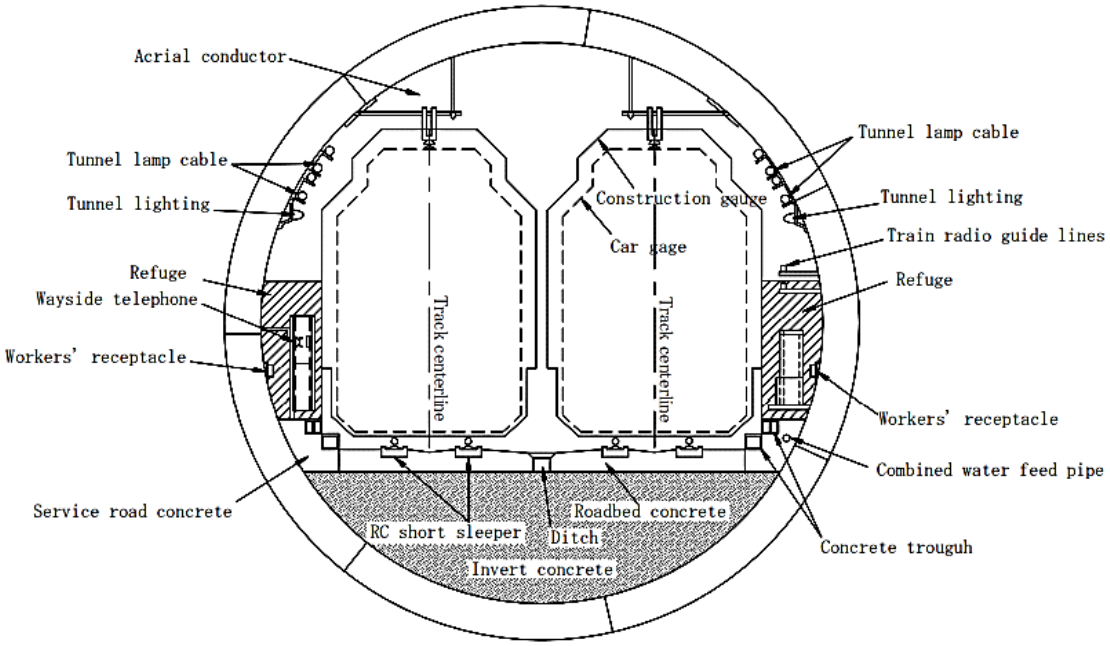

Figure 2.15: Example of facilities and structure of a double-track railroad tunnel (TBM) (Harer et al., 2008)

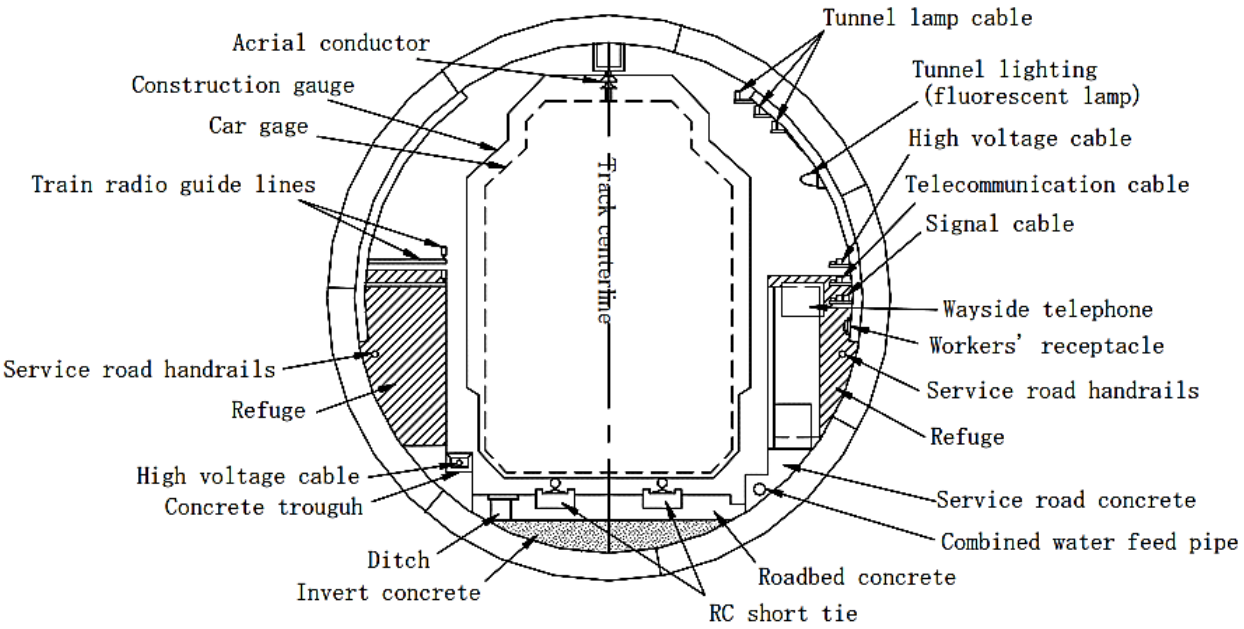

Figure 2.16: Example of facilities and structure of a single-track railroad tunnel (TBM) (Harer et al., 2008)

2.5 Tunnel Alignment

The tunnel alignment refers to both the plan alignment and the vertical alignment. These alignments should be determined considering the purpose and conditions of use, site characteristics, underground obstacles, and construction conditions including ground conditions.

For NATM,

i. The alignment of tunnels shall be as straight as possible for ease of construction. If curved alignment is used, the radius shall be as large as possible.

ii. A gradient of at least 0.2% is sufficient to allow natural drainage of water inflow with good longitudinal drainage after completion of tunnel.

For TBM,

i. The plan and alignment should be planned as a straight line or gradual curve with as large a radius as possible in construction of site condition.

ii. The vertical alignment should be provided with an adequate gradient considering the purpose of use, maintenance, positional relation with existing and planned structure.

iii. When parallel tunnels are constructed, or a tunnel is constructed close to other structures, the alignment should be planned with particular attention to the mutual interactions between the vicinity structures.

2.6 Shafts and Lining

Shafts should be positioned according to the basic plan for both ends of a shield tunnel, access points leading to the ground surface, and transitions of inner sections while taking into account the location, traffic, and acquisition of necessary sites, tunnel length, and other construction conditions. The different kinds of shafts are depicted in Figure 2.17 for better view. A launching shaft is used for carrying in and assembling a shield machine, delivering materials such as segments and several kinds of equipment, taking excavated soil out of a tunnel, and providing workers with access of a tunnel. An intermediate shaft is used mainly for inspecting a TBM and also used for delivering and removing materials and equipment to facilitate arrival and departure of the machine to strategic places along a route. An arrival shaft is used for dismantling and removing a TBM at the terminal of a tunnel. Shafts are installed at the places

where Underground Railroad stations or access ramps for tunnels are constructed, the open-cut areas for constructing merging/diverging tunnels, and the ends of shield tunnel sections.

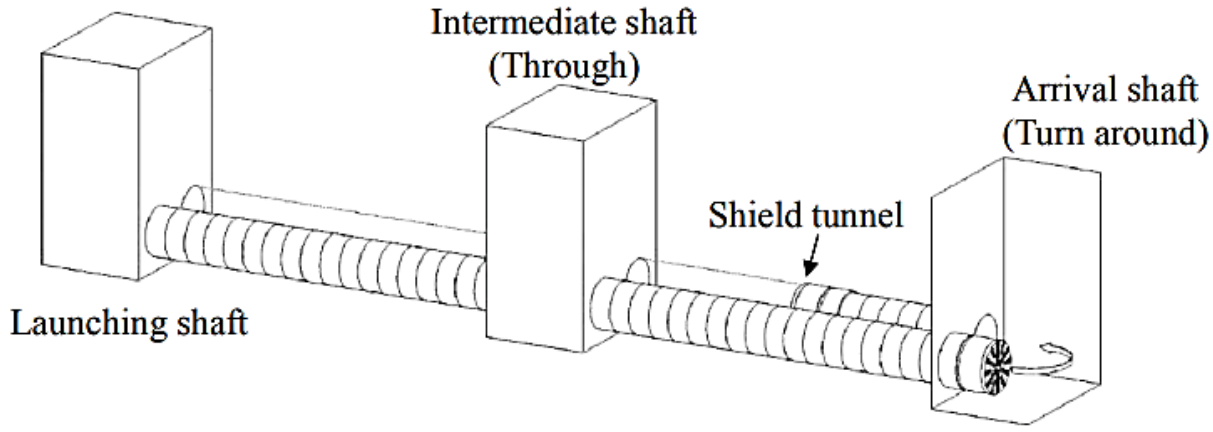

Figure 2.17: Kinds of Shafts (Source: Internet)

The tunnel lining should be guaranteed to be a safe and sound structure able to withstand earth and water pressures and other loads from the surrounding ground so as to maintain inner cross-section dimensions and to retain functions that are suitable for the purpose of tunnel use, maintenance and construction conditions. The placement of primary and secondary lining is shown in Figure 2.18. The allowable stress design method or limit state design method should be applied to the lining design. The allowable design method is a simple design method dealing with structural members within elastic stress ranges has been used in the construction of many tunnels. The limit design method is capable of incorporating variations in the quality of the materials used, fluctuations in the loads acting on structures, and uncertainties in structural calculation methods into the structural design as safety coefficients. Segmental rings that form the primary lining and are formed from A, B and K segments. There are two types of segmental ring with respect to the direction of insertion of the segments. One method is to insert the segments from the inside of the tunnel, in which the longitudinal side faces of the K segment are tapered in the direction of the tunnel radius. The other is to insert the segments from the cut face side in the longitudinal direction of the tunnel, in which the longitudinal side faces of the K segment are tapered in the longitudinal direction of the tunnel. The components of a segmental ring and types of K segment with the position and angle of joints are showed in Figure 2.19.

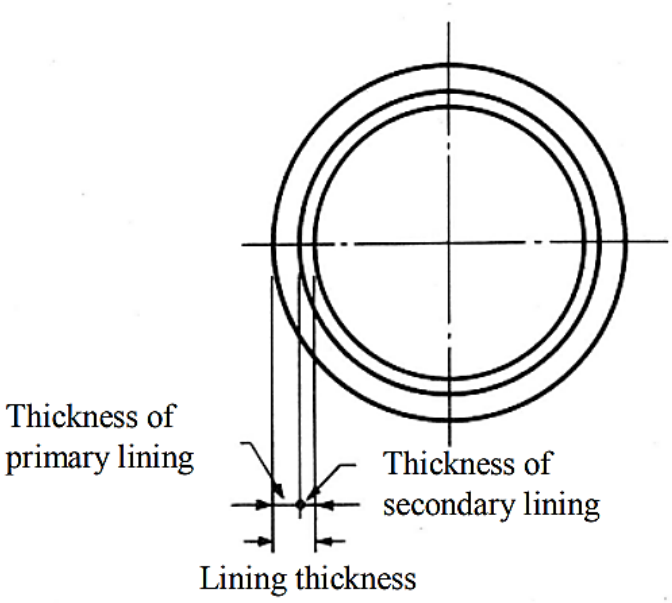

Figure 2.18: Position of Primary and Secondary Linings (Source: Internet)

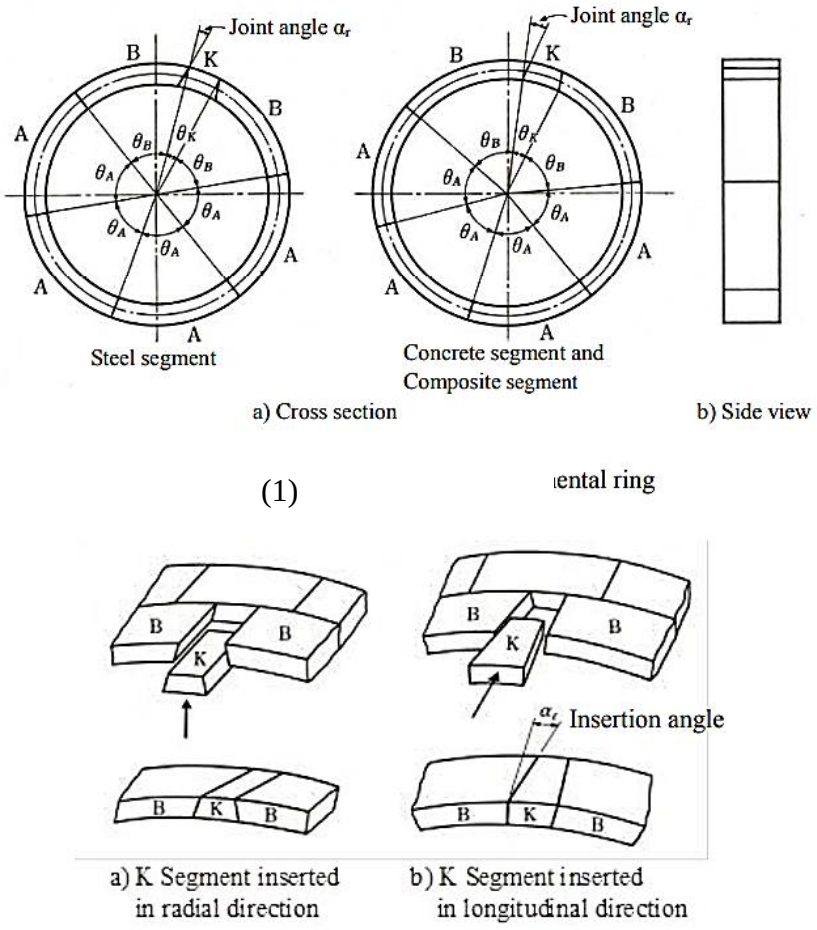

Figure 2.19: (1) Components of a Segmental Ring, (2) Types of K segment (Source: Internet)

2.7 Design of Inverts

Construction joints, excavation surfaces and shotcrete surfaces shall be cleaned and drained sufficiently prior to placement of invert concrete. The construction joints with the lining concrete should be perpendicular to the axis of the invert in order to effectively transmit the axial force. The desired performance of invert is classified into serviceability and mechanical performance. The placements of construction joints with lining concrete, invert concrete and in the vertical direction of tunnel is shown in Figure 2.20. For serviceability,

i. To hold necessary inner section together with lining (maintenance of inner section)

ii. To decrease water leaks and improve water tightness (maintenance of water leakage)

iii. To maintain the facilities, such as drainage facilities in the tunnel (maintenance of facilities)

iv. To ensure the flatness of road surface and the safe driving of vehicles on roads and in railroad tunnels (maintenance to flatness)

v. To provide smooth flow path together with lining (maintenance of water permeability)

For mechanical performance,

i. To prevent settlement of the footing due to lack of bearing capacity in case of poor ground or displacement of side wall of tunnel induced by plastic earth pressure.

ii. To improve stability against structural deformation of the tunnel by early formation of a ring-like structure which combines with tunnel supports to control convergence of the tunnel.

iii. To enhance the structural stability by forming a ring-shaped structure integrated with tunnel supports and lining to achieve sufficient load carrying capacity against the long-term acting loads.

iv. To improve durability of tunnels against deformation due to ground heaving.

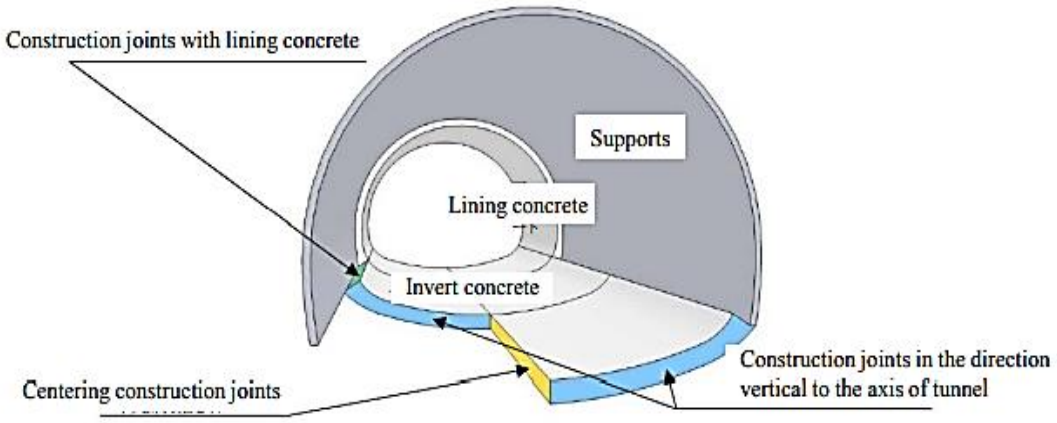

Figure 2.20: Example of Construction Joints in Invert Concrete (Source: Internet)

2.8 Effects of Ground Settlement

When a tunnel is constructed in soft ground, attention should be paid to how the soil characteristics effect ground settlement. It is necessary to consider the effects of ground settlement on the tunnel and the joints between the tunnel and the shaft. The effects of ground settlement on the tunnel can be studied in two ways:

i. Study of the effect of consolidation settlement on the tunnel in the transverse direction.

ii. Study of the effect of unequal settlement on the tunnel in the longitudinal direction.

When a tunnel is constructed in ground that is still undergoing consolidation, the tunnel experiences constraint displacement equivalent to the amount of settlement of the ground. In studying the effect of consolidation in the transverse direction, it is assumed that differential constraint displacement can be assigned to soil springs in the structural model for the tunnel's transverse direction. This displacement is generally evaluated by increasing the vertical earth pressure to examine the strength of the lining. In studying the effect of unequal settlement in the longitudinal direction, the amount of ground settlement in each position of the tunnel is assigned to the structural model in the longitudinal direction of the tunnel via soil springs, and countermeasures such as the reduction of the longitudinal rigidity of the tunnel, reduction in the amount of settlement by soil improvement, and expansion of the inner diameter of the tunnel should be considered. In general, the ground settlement in tunneling is thought to be caused by ground loss, which is defined as a difference between actual and theoretical excavation volume. The ground loss develops due to internal deformation of the tunnel during excavation, which makes the actual amount of excavation to be larger than the theoretical

amount. Hence, for TBM tunneling, ground loss can be divided into three categories to be consistent with the abovementioned ground settlement steps as called face loss, shield loss, and tail loss. The face loss is the ground loss caused by deformation of ground into tunnel face, and the shield loss is induced by the radial contraction of ground along the annular gap around the shield skin plate. The tail loss occurs along the annular void between ground and concrete segmental lining as a result of shrinkage or compression of backfill grout material. The components of the volume loss (radial loss of annulus and shield, and face loss) are shown in Figure 2.21.

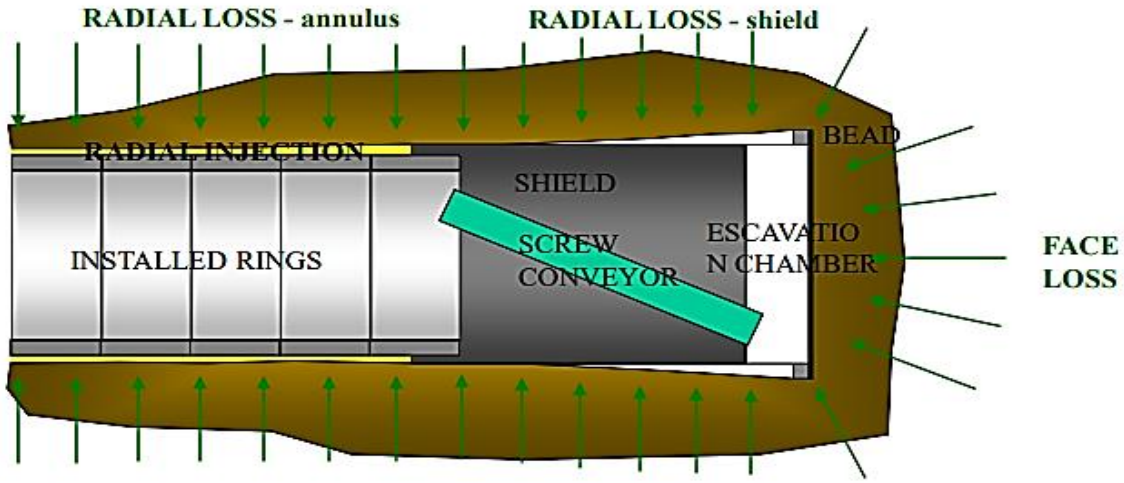

Figure 2.21: Components of the Volume Loss (Golpasand et al., 2016)

The causes and mechanisms of ground movements by EPB are as follows:

i. Unbalanced ground and groundwater pressures at the cutting face: If the pressure in the chamber is smaller than the ground pressure, surface settlement occurs. In the reverse situation, ground heave occurs. These phenomena are due to pressure release at the cutting face and elasto-plastic deformation by additional pressure.

ii. Ground disturbance during advancement and due to friction between plate of the machine and the ground may cause settlement.

iii. Due to the existence of the tail void, the ground which is supported by a skin plate, it causes elastic deformation caused by stress relief and ground settlement occurs.

iv. If joint bolts are not fully tightened, segmental rings may be deformed which causes deformation of primary lining and ground settlement increases.

v. If water flows from the cutting face, the groundwater table falls leading to ground settlement in the cohesive soil ground.

The ground movement due to shield advancement can be divided into five steps which is shown in Figure 2.22:

i. First step: Advancement settlement (heaving) prior to shield advancement
ii. Second step: Settlement (heave) in front of the machine face due to shield passing.
iii. Third step: At the tail of the shield passing or segment construction phase, settlement (heaving) at the shield machine face occurs.
iv. Fourth step: Due to tail void, settlement (heave) occurs.
v. Fifth step: Final settlement leads from subsequent settlement (heave)

In these circumstances, the hard soil may be pushed away from the face of the shield while the cohesionless soil runs into the openings in the cutterhead as the shield strives to cut the cohesive soil. In the case of a shield tunnel, the liner-soil interaction process is complex, given the nature by which the soil comes into contact with the liner, and the fact that the liner consists of bolted segments. The segmental nature of the liner leads to a flexibility that would not exist if the liner were continuous. The loads on the liner begin developing under the self-weight condition as the liner is erected in the tail of the shield. As the shield advances, and a ring of liner segments emerges from the shield, the liner is subjected to soil loads as the soil collapses through the tail void. Attempts to grout the tail void through the liner change the load distribution in an indeterminate fashion, although in the long run, creation of good contact between the soil and the liner through the grouting serves a positive purpose.

In Figure 2.23, the major movements occur as the soil is excavated at the tunnel heading, and before it can be supported by the application of the steel ribs and shotcrete. Minor movements occur after this as the liner is compressed under the ground stresses. There are no clear stages in the movement pattern as it occurs in the shield tunnel with closure of a tail void. For the NATM tunnel, the movements develop through a steady process instead of in increments. Loading on the initial ribs and shotcrete liner is created during the support installation and excavation process as the soil moves toward the opening. It is usually assumed in design that the shotcrete carries the load, and that the steel ribs are used to provide support to get the shotcrete in. While the steel ribs undoubtedly carry load, they are not normally figured in the load capacity of the initial liner since they are not positioned accurately enough to serve as

reinforcing. Loading on the final liner is assumed to develop with the gradual deterioration of the initial liner, and the final liner is designed to carry the full long-term load.

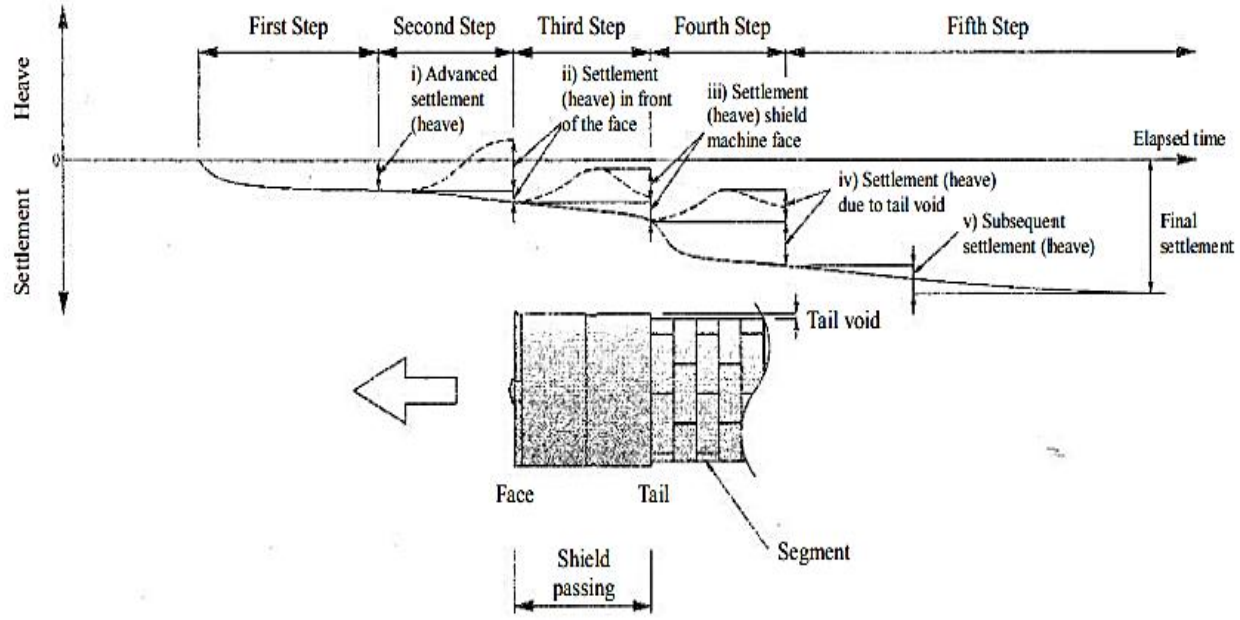

Figure 2.22: Classification of ground movement due to shield advancement (Tamagnini et al., 2022)

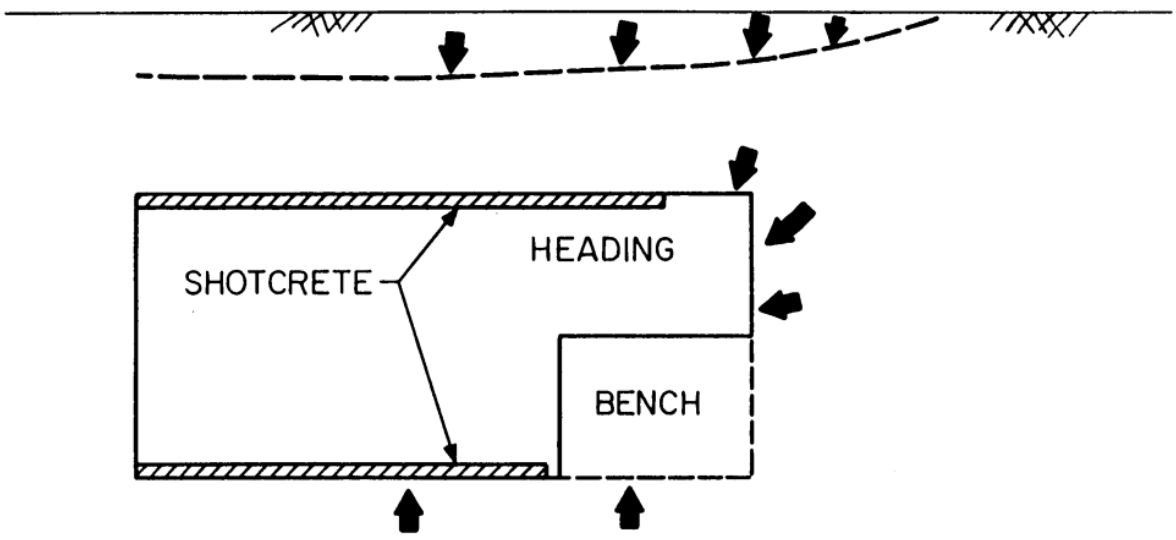

Figure 2.23: Pattern of Ground Movement due to NATM advancement (Yun, 2019)

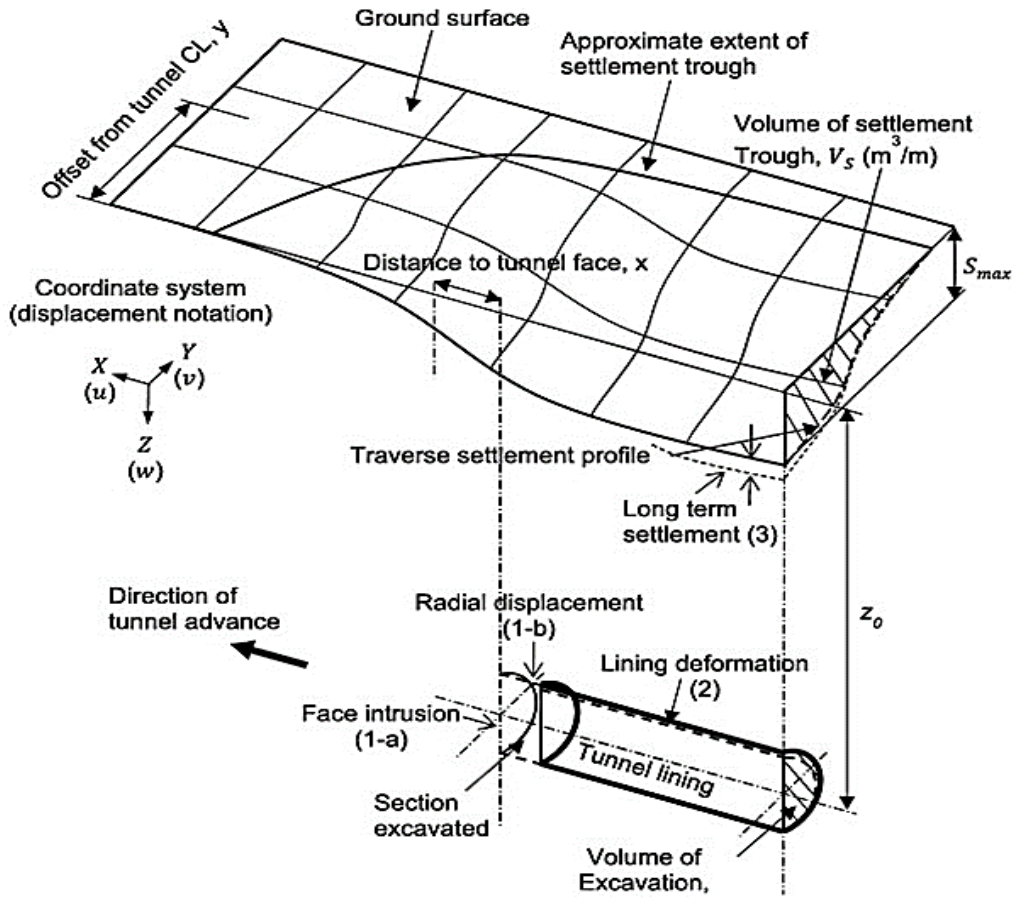

Figure 2.24: Geometry of the tunnel induced settlement trough (Attewell, 1986)

Figure 2.24 reproduces a complete 3D form of a tunnelling induced settlement trough, where x corresponds to the distance from the tunnel center-line in the transverse direction, y corresponds to the distance in the longitudinal direction relatively to the excavation face, and z is the depth below the ground surface. The displacements that compose the represented settlement trough will be analyzed individually, with S_V referring to vertical displacement, whereas S_{hx} and S_{hy} describe horizontal displacements in the transverse and in the longitudinal direction, respectively.

2.8.1 Surface Settlements: Transverse Displacements

Tunneling induced surface settlements gain more importance in tunneling as increasing number of tunnels are being constructed in urban areas. Methods to estimate the surface settlements should be developed and the mechanism under this phenomenon should be clearly investigated in order to minimize the effects of these settlements to the overlying structures. The most widely used method for estimating the surface settlements is the empirical method proposed

by (Peck, 1969). In this method the settlement profile is approximated by the Gaussian distribution curve:

$$S = S_{max}\ exp\ (-\frac{x^2}{2i^2}) \qquad (2.1)$$

Where S is the settlement, S_{max} is the maximum settlement above the tunnel centerline, i is the distance between tunnel centerline and the inflexion point of the curve and x is the horizontal distance from the tunnel centerline in the transverse direction. According to Franzius (Figure 2.25 and Figure 2.26), there are two settlement portions (sagging up to the point of inflexion and hogging) in transverse direction and maximum vertical settlement occurs in tunnel center point.

In 1995, Verruijt and Booker made a study on evaluating the settlements due to deformation of a tunnel with analytical methods. They extended the solution of Sagaseta (1987) by considering the ground loss not only for the incompressible case and by including the effect ovalization. This solution is based on the assumption of linear elastic soil and therefore it has some limitations. The settlements determined by using this method are generally larger than the observed ones. In 1998, Loganathan and Paulos made an attempt to find an analytical solution for tunneling induced ground movements in clays. They used the closed form solution derived by Verruijt and Booker by incorporating the redefined definition of the traditional ground loss parameter. Peck (1969) described that it was possible to deduce that the short-term transverse settlement trough in the greenfield could be approximated by a normal distribution or Gaussian curve. The empirical formula or trough curves used to fit transverse settlement patterns by different researchers are explained in Table 2.2.

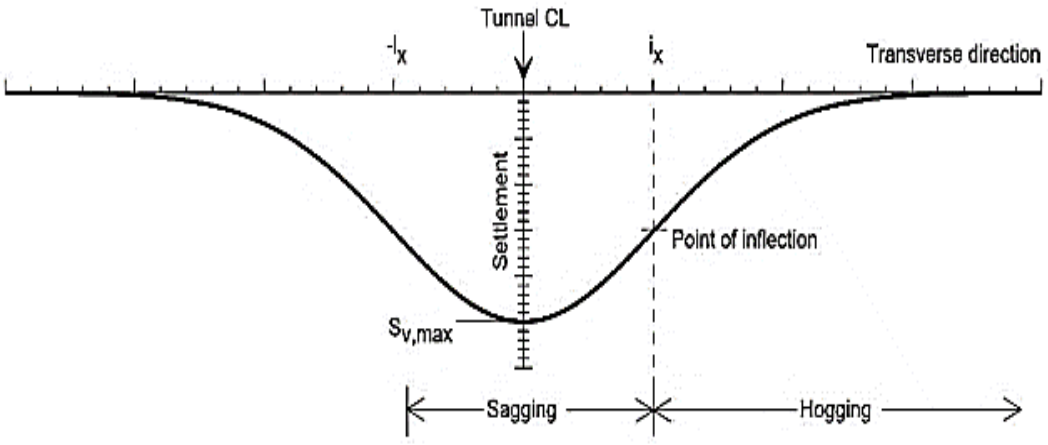

Figure 2.25: Transverse settlement trough (reproduced from Franzius, 2003)

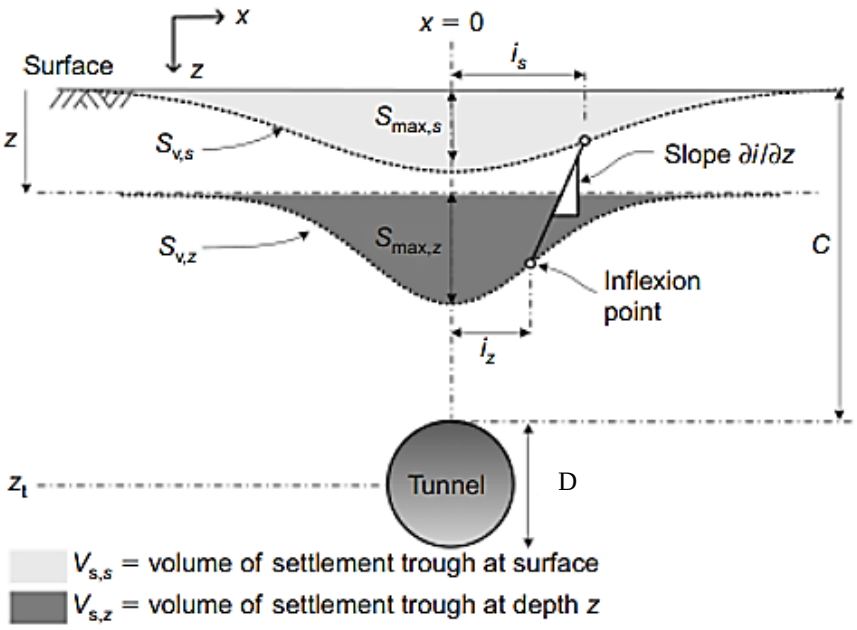

Figure 2.26: Greenfield Settlement Trough (Peck, 1969)

Table 2.2: Curves used to fit Settlement Trough Data above Tunnels

References	Equation of the Settlement	Additional Details
Peck, 1969	$S_{v(x)} = S_{max} \exp(-\frac{x^2}{2i^2})$	$S_{v(i)} = 0.606\, S_{max}$
Peck and Schmidt, 1969	$S_{v(x)} = \frac{V_s}{\sqrt{2\pi K Z_0}} \exp(-\frac{x^2}{2K^2 {Z_0}^2})$	Vs = volume of settlement trough per meter of tunnel advance (m^3/m) = percentage volume loss of the unit volume of the tunnel = 0.35% for low plastic soil K = trough width parameter = 0.5 for cohesive soil y = lateral distance from the tunnel centerline (m) Z_0 = depth of neutral axis from the surface
Jacobsz, 2004	$S_{v(x)} = S_{max} \exp(-\frac{1}{3}\frac{\lvert x \rvert}{2i})^{1.5}$	$S_{v(i)} = 0.717\, S_{max}$

Celestino, 2000	$S_{v(x)} = \frac{S_{max}}{1 + (\frac{\lvert x \rvert}{a})^b}$	
Vorster, 2005	$S_{v(x)} = \frac{nS_{max}}{(n-1) + \exp(a\left(\frac{x^2}{i^2}\right))}$	

2.8.2 Surface Settlements: Longitudinal Displacements

From Attewell and Woodman (1982) the longitudinal settlement profile can be derived by assuming a tunnel as a number of point sources in the longitudinal direction and therefore superimposing the settlement craters caused by each point source. If a Gaussian settlement profile is adjusted to the settlement crater, the longitudinal profile can be described by:

$$S_v(y)_{x=0} = S_{v,max}\varphi(\frac{y}{i}) \qquad (2.2)$$

Where, ϕ(y) is a cumulative probability curve and y is the longitudinal coordinate. Values of Φ(y) are listed in standard probability tables such as given by Attewell & Woodman (1982). According to Franzius and Luo and Chen, in the longitudinal profile, the vertical settlement occurs 0.5 of the maximum value at the position of tunnel face whereas it reduces in the ahead of the tunnel face and increases up to maximum value in behind the tunnel face. The deformation occurs inward at the tunnel face opposite to the direction of tunnel advancement. And radial deformation starts about 0.5 of tunnel diameter ahead of the advancing face, reaches one third of final value at the face and reaches the final maximum value at about 1.50 of tunnel diameter behind the face.

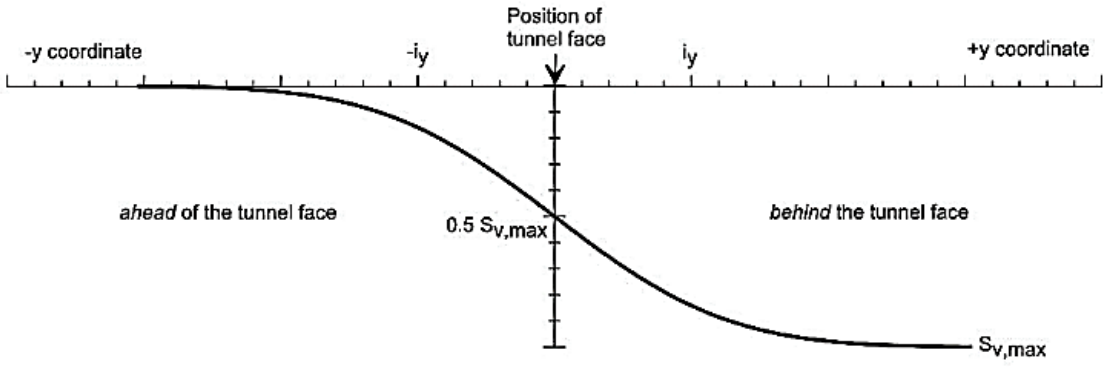

Figure 2.27: Longitudinal settlement profile (reproduced from Franzius, 2003)

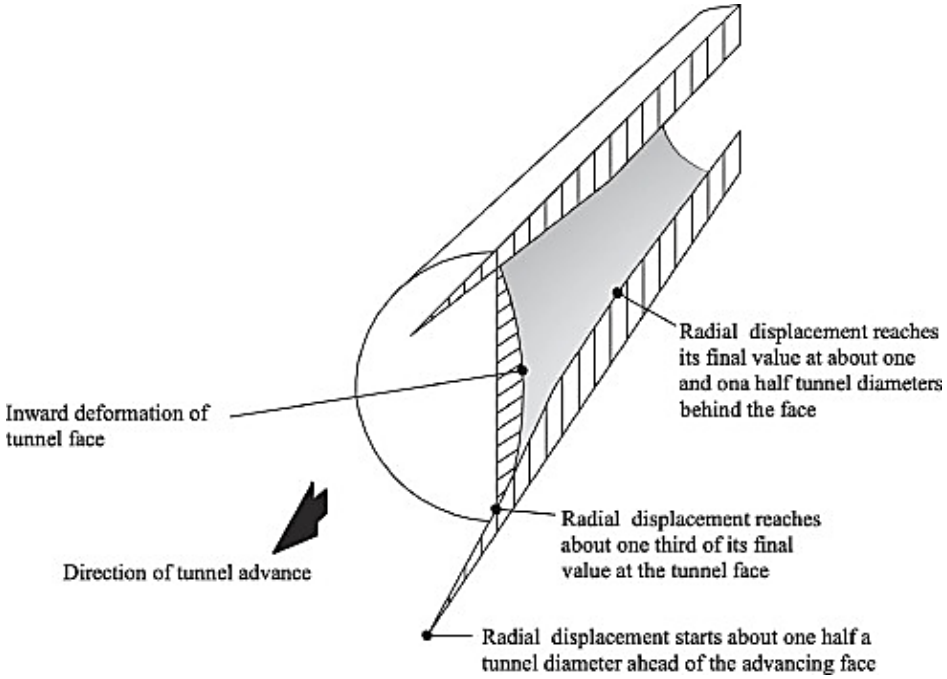

Figure 2.28: Longitudinal Deformation Profile (Luo et al., 2018)

Chow (1994) used elasticity solution to estimate the tunnel settlement, ignoring the effect of tunnel face and assuming the tunnel to have infinite length. The unloading of the excavated soil mass is modelled as a line load along the tunnel axis. It is not possible to obtain analytically the integral of the point load solution, so relative differences in vertical displacement are derived which cancel the insoluble part of the integral. The surface settlement over the tunnel is calculated as the settlement relative to some distance point on the surface which will in practice experience negligible settlement:

$$\delta_z = -\frac{\gamma D^2 z^2}{8G(x^2+z^2)} \qquad (2.3)$$

Where D is the tunnel diameter, γ is the unit weight of soil, G is the shear modulus of soil, x is the horizontal distance from tunnel's center, and z is the depth measured from tunnel's center.

Sagaseta (1987) suggested that in problems where the boundary conditions are only in terms of displacements, and only displacements are required for the solution, it is possible to eliminate the stresses from the governing equations and work in terms of strain for simple soil models. The advantage of Sagaseta's method is that the strain field obtained is independent of soil stiffness, and is valid for incompressible material even for fluid. Sagaseta showed that closed form solution for soil deformed due to ground loss (such as in tunnel excavation) can be obtained. Chow (1994) used this approach to derive the solution for vertical displacement at the surface as:

$$\delta_z = -\frac{\gamma D^2 z^2}{4G(x^2+z^2)} \quad (2.4)$$

The theoretical solutions provided by Sagaseta (1987), which other authors modified to predict soft ground deformations due to tunneling, is essentially based on incompressible soils. Hence, it might not accurately predict the deformations in soft ground. Elastic solutions are more applicable for hard rock conditions.

2.9 Finite Element Model

There are non-numerical ways of obtaining good predictions of the likely ground response to tunnelling and the likely loads in a tunnel lining. These conventional design tools are arguably cheaper and quicker to use. However, they are characteristically uncoupled, i.e., the loads are determined by one technique (usually an elastic solution), and movements by another (usually empirical) - not linked together. Moreover, the information gained from conventional analysis is often limited. In a real tunnel, however, the different facets are clearly coupled and the problem is complex, involving pore pressure changes, plasticity, lining deformations and existing structures. Numerical computations aim to analyze, i.e., reproduce, explain and predict the behavior and response of structures and media subjected to impacts from tunneling. Numerical procedures, such as the finite element technique, lend themselves to the analysis of such complex problems.

Potts (2001) state that the field conditions can be simulated more accurately if the utilized constitutive models can represent the soil behavior accurately and if the boundary conditions set are correct. Finite Element Method is one of the most widely used numerical methods in geomechanics and also in tunnel engineering. It is a continuum model but discontinuities can be also modeled individually. The reason of the popularity of FEM can be addressed to the fact that it was the first numerical method with enough ability to include the material non-homogeneity, complex boundary conditions and non-linear deformability. In the FEM, the subsurface is predominantly modeled as a continuum. The host ground is discretized into a limited number of elements connected at nodal points. Stress-strain deformation and relationship of the ground induced by changing the original subsurface condition for tunneling process. The analysis of the complex mathematical relationship between the interconnected elements is performed by solving the equation matrix (global stiffness matrix) of the mesh with limited number of elements. The capability of the FEM method includes the simulation of complex constitutive laws, non-homogeneities, and the impact of advance and time dependent characteristics of the construction methods.

The main idea of FEM is as follows: The hosting ground is discretized into a limited number of smaller elements. These elements are connected at nodal points. The stress, strain and deformation to be analyzed are caused by changing the original subsurface conditions (Gnilsen, 1989). The stresses and strains generated in one element effects the interconnected elements, and so forth.

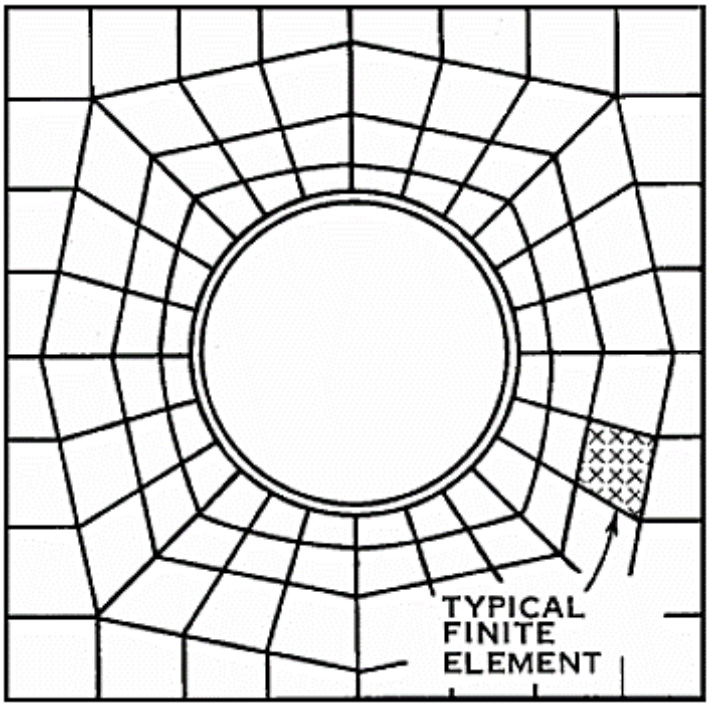

Figure 2.29: Typical Finite Element Model Formation for Tunnel (Luo et al., 2018)

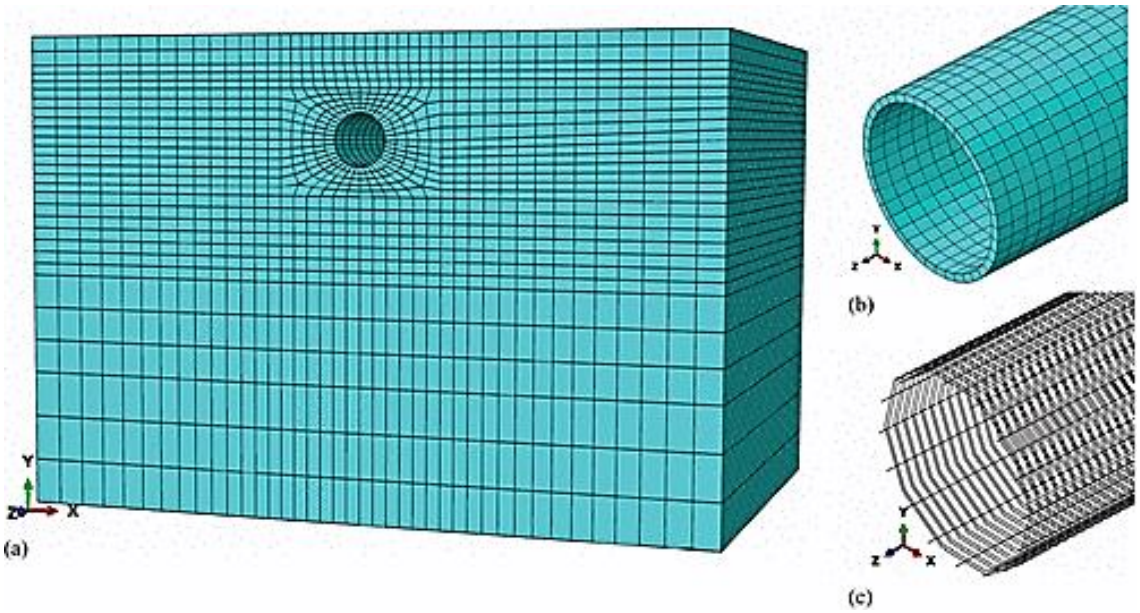

Figure 2.30: Typical Finite Element Model Simulation for Shield TBM Tunnel (Luo et al., 2018)

The stress-strain relationships of the elements are modeled mathematically by creating a global stiffness which relates the unknown quantities with known quantities and the results are obtained by solving this matrix. The equations to be solved are highly complex and as the number of the elements in the model increase, the calculation time and the storage capacity increase dramatically. When properly used, FEM method can produce realistic results which are of value to practical engineering problems. While using numerical methods like Finite Element Method for the solution of that kind of real three-dimensional problems, some approximations and simplifications are made to get the solution easier. By using FEM, complex conditions can be simulated due the capability of simulation of advanced constitutive models, non-homogeneities, stage by stage construction and time effect. Although there are many geotechnical problems that can be approximated to either plane strain or axi-symmetric conditions, some remain which are very three dimensional. Such problems will therefore require full three-dimensional numerical analysis. The output of the analysis is typically also complex and it makes the assessment of the results difficult. A post-processor may be utilized in order to overcome this difficulty.

2.9.1 Soil Behavior and Constitutive Material Modelling

Stress-strain behavior, strength parameters and failure surfaces are the key features of the stability problems in geotechnical engineering (Chen, 1975) There have been several models proposed in order to reflect the actual soil behavior.

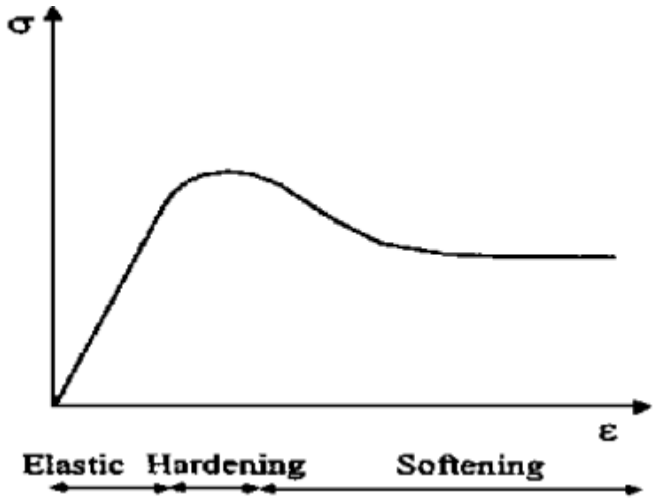

Figure 2.31: Real Soil Behavior involving hardening and softening (Potts, 2001)

This Figure represents an elasto-plastic behavior in which the elastic portion is assumed to be linear and includes strain hardening and softening. In the presented behavior, the strain

increments are dependent on the current stress level and therefore strain increments directions may not coincide with the incremental stress directions (Potts, 2001). The strain hardening and softening rules are not included in simple elastoplastic models and therefore they only reflect the peak strength and strain.

A material model is described by a set of mathematical equations that give a relationship between stress and strain. Material models implemented in PLAXIS are based on a relationship between the effective stress rates (infinitesimal increments of stress) and the strain rates (infinitesimal increments of strain). This relationship may be expressed in the form:

$$\sigma' = M\varepsilon \tag{2.5}$$

Where M is a material stiffness matrix. In this type of approach, pore pressures are explicitly excluded from the stress-strain relationship.

The simplest material model in PLAXIS is based on Hooke's law for isotropic linear elastic behavior. Two parameters are used in the model, the effective Young's modulus, E', and the effective Poisson's ration, υ'. According to Hooke's law, the relationship between Young's modulus E and other stiffness moduli, such as the shear modulus G, the bulk modulus K, and the oedometer modulus E_{oed}, is given by:

$$\begin{bmatrix} \dot{\sigma}'_{xx} \\ \dot{\sigma}'_{yy} \\ \dot{\sigma}'_{zz} \\ \dot{\sigma}'_{xy} \\ \dot{\sigma}'_{yz} \\ \dot{\sigma}'_{zx} \end{bmatrix} = \frac{E'}{(1-2\nu')(1+\nu')} \begin{bmatrix} 1-\nu' & \nu' & \nu' & 0 & 0 & 0 \\ \nu' & 1-\nu' & \nu' & 0 & 0 & 0 \\ \nu' & \nu' & 1-\nu' & 0 & 0 & 0 \\ 0 & 0 & 0 & \frac{1}{2}-\nu' & 0 & 0 \\ 0 & 0 & 0 & 0 & \frac{1}{2}-\nu' & 0 \\ 0 & 0 & 0 & 0 & 0 & \frac{1}{2}-\nu' \end{bmatrix} \begin{bmatrix} \dot{\varepsilon}_{xx} \\ \dot{\varepsilon}_{yy} \\ \dot{\varepsilon}_{zz} \\ \dot{\gamma}_{xy} \\ \dot{\gamma}_{yz} \\ \dot{\gamma}_{zx} \end{bmatrix} \tag{2.6}$$

$$G = \frac{E}{2(1+\vartheta)} \tag{2.7}$$

$$K = \frac{E}{3\,(1-2\vartheta)} \tag{2.8}$$

$$E_{oed} = \frac{(1-\vartheta)E}{(1-2\vartheta)(1+\vartheta)} \tag{2.9}$$

2.9.2 PLAXIS 3D Program for Material Modelling

Plaxis 3D Tunnel program consists of four basic components; namely Input, Calculation, Output and Curves. In the Input program the boundary conditions, geometry of the problem, all structural components such as retaining walls, tunnel lining, geogrids or anchors with

appropriate material properties are defined. The soil and the interfaces can be modeled with different levels of complexity. The plates can be used to model walls, tunnel and liners. The plates are modeled with Mindlin Beam theory. In this theory, shear deformations are also calculated in addition to the out-of-plane bending. The Shear Stiffness is calculated based on the assumption that the plate has a rectangular section.

According to Brinkgreve et al. (Figure 2.32), The volume elements are 15-node wedge elements and they are composed of 6-node triangles in x-y direction and 8-node quadrilaterals in z-direction. Higher order element types are not employed in 3D analysis since it would result in a dramatic increase in the memory consumption and calculation time. The plates, walls and shells are modeled with 8-node plate elements and 16-node interface elements are used to model the soil-structure interaction (PLAXIS Material Models Manual, 2018). The 2D mesh generation in PLAXIS is fully automatic and the 3D mesh generation is semi-automatic. The size of the mesh elements can be adjusted by using a general mesh size varying from very coarse to very fine and also by using local refinements (follow sample configurations of meshing in Figure 2.33).

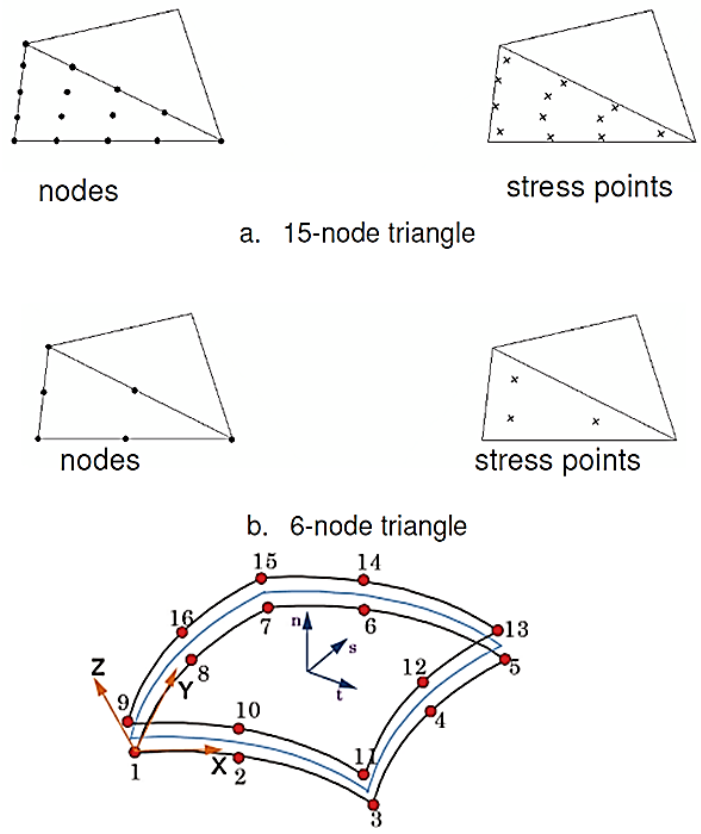

Figure 2.32: Topology of 15 node wedge elements, 6 node triangles and 16 node interface elements in PLAXIS 3D (Galavi et al., 2013)

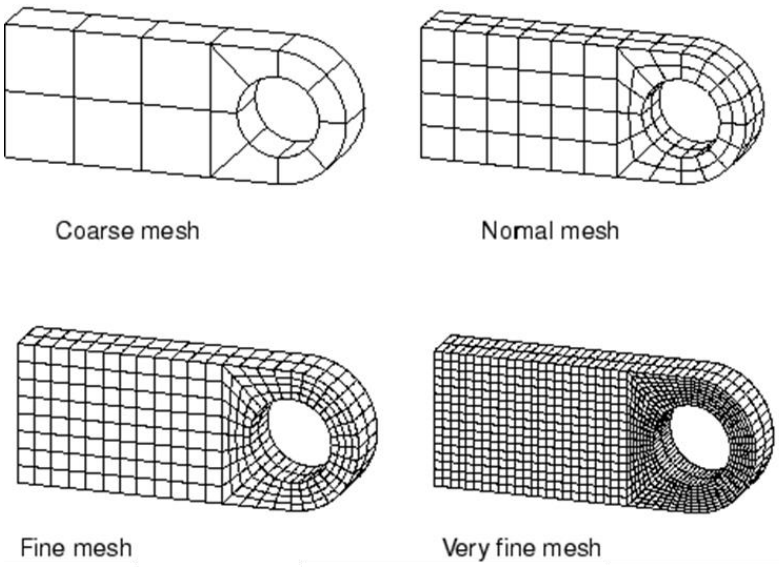

Figure 2.33: Sample Refinements of Mesh in PLAXIS 3D (Source: Internet)

After fully defining the geometry and generating the mesh in 3D, initial stresses are applied by using either the Ko-procedure or gravity loading. The calculation procedure can be performed automatically but there is also an option for manual control. The stages of the construction are defined by activating and deactivating the objects in the slices and a simulation of the construction process can be achieved. A construction period can also be specified for each construction stage. However, the material model type for the soil should have been specified as Hardening-soil model. The number of the iterations can be specified both as manually and automatically. The most important calculation type in PLAXIS 3D tunnel is the staged construction as far as the tunnel construction simulation is concerned. In order to carry out this type of calculation, a 3D model with all active and inactive structural and geotechnical objects should be defined. In every 42 stage of the calculation the material properties, the geometry of the problem, loading type and water pressures can be redefined. These changes generally cause substantial out-of-balance forces. These out of balance forces are stepwise applied to the finite element mesh using a Load advancement ultimate level procedure. During these calculations, a multiplier that controls the staged construction process (ΣM_{stage}) is increased from zero to the ultimate level which is generally 1.0. The constructions which are not completed fully can be modeled by using this feature.

2.9.2.1 Mohr-Coulomb Model

The basic principle of elastoplasticity is that strains and strain rates are decomposed into an elastic part and a plastic part. According to the classical theory of plasticity, plastic strain rates

are proportional to the derivative of the yield function with respect to the stresses (the stress-strain relationship diagram is shown in Figure 2.34 for Mohr-Coulomb model).

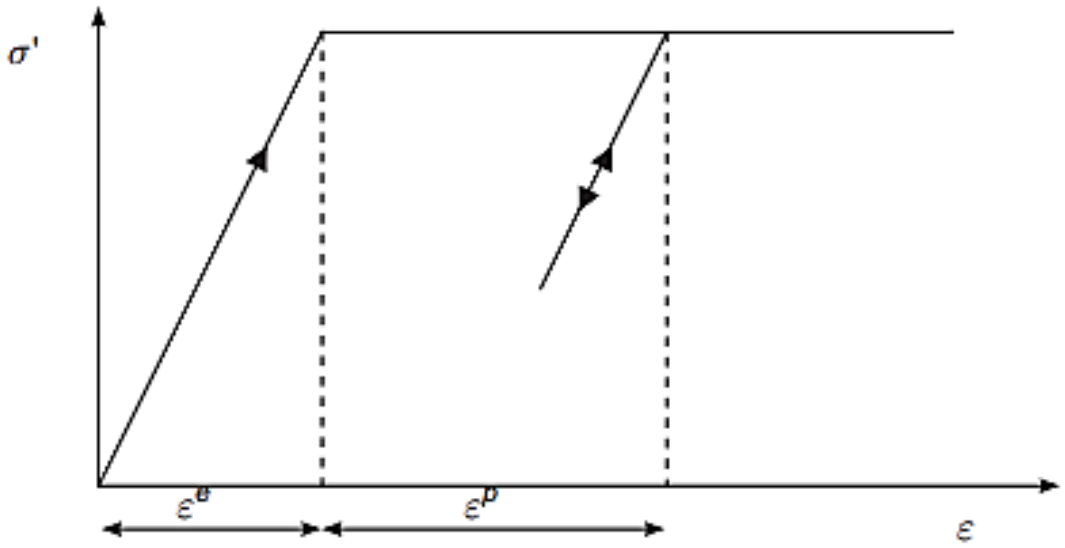

Figure 2.34: Basic Idea of an Elastic Perfectly Plastic Model (Bentley, 2018)

The Mohr-Coulomb yield condition is an extension of Coulomb's friction law to general states of stress. The full Mohr-Coulomb yield condition consists of six yield functions when formulated in terms of principal stresses:

$$
\begin{aligned}
f_{1a} &= \frac{1}{2}(\sigma_2' - \sigma_3') + \frac{1}{2}(\sigma_2' + \sigma_3')\sin\varphi - c\cos\varphi \le 0 \\
f_{1b} &= \frac{1}{2}(\sigma_3' - \sigma_2') + \frac{1}{2}(\sigma_3' + \sigma_2')\sin\varphi - c\cos\varphi \le 0 \\
f_{2a} &= \frac{1}{2}(\sigma_3' - \sigma_1') + \frac{1}{2}(\sigma_3' + \sigma_1')\sin\varphi - c\cos\varphi \le 0 \\
f_{2b} &= \frac{1}{2}(\sigma_1' - \sigma_3') + \frac{1}{2}(\sigma_1' + \sigma_3')\sin\varphi - c\cos\varphi \le 0 \\
f_{3a} &= \frac{1}{2}(\sigma_1' - \sigma_2') + \frac{1}{2}(\sigma_1' + \sigma_2')\sin\varphi - c\cos\varphi \le 0 \\
f_{3b} &= \tfrac{1}{2}(\sigma_2' - \sigma_1') + \tfrac{1}{2}(\sigma_2' + \sigma_1')\sin\varphi - c\cos\varphi \le 0
\end{aligned}
\qquad (2.10)
$$

The two plastic model parameters appearing in the yield functions are well-known friction angle ϕ and the cohesion c. The condition $f_i = 0$ for all yield functions together (where f_i is used to denote each individual yield function) represents a fixed hexagonal cone in principal stress space which is shown in Figure 2.35 and Figure 2.36.

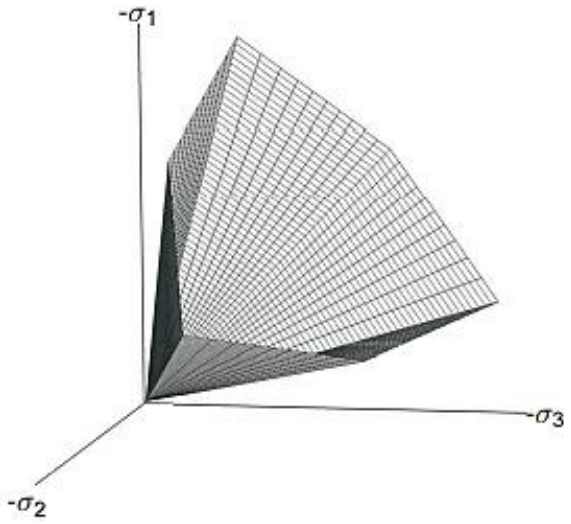

Figure 2.35: The Mohr Coulomb yield surface in principal stress space (c=0) (Bentley, 2018)

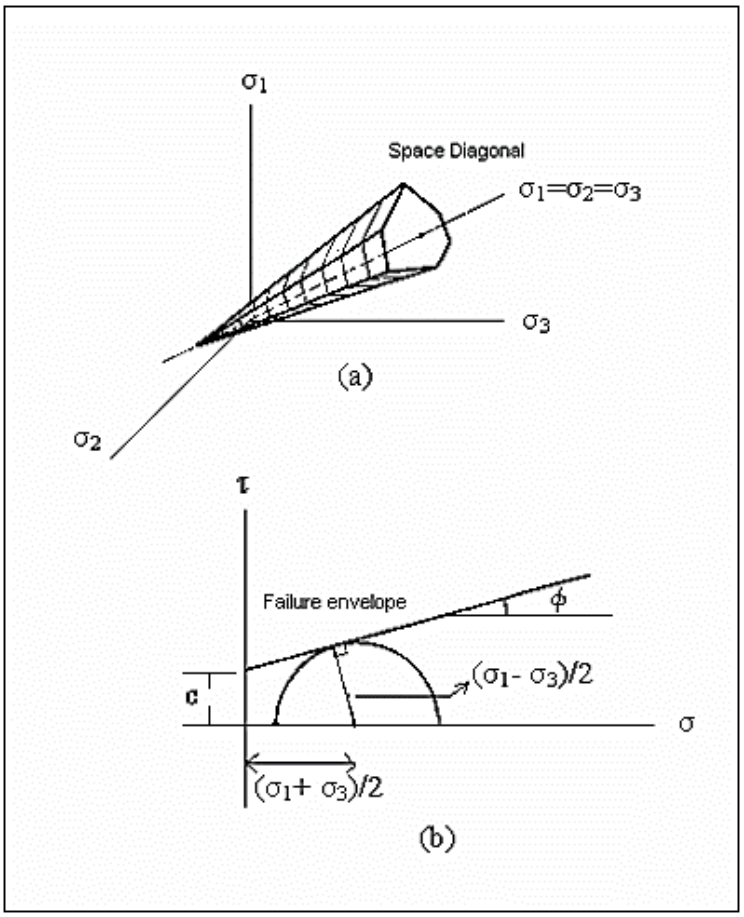

Figure 2.36: Mohr-Coulomb criteria in principal stress space and Mohr's diagram. a) Principal stress space, b) Mohr's diagram (Bentley, 2018)

The plastic potential functions contain the dilatancy angle, ψ, as the third plasticity parameter, which is required to model positive plastic volumetric strain increments (dilatancy) as actually observed for dense soils. For c>0, the standard Mohr-Coulomb criterion allows for tension. In reality, soil can sustain none or only very small tensile stresses which can be included in PLAXIS analysis by introducing a tension cut-off. In triaxial testing of soil samples the initial slope of the stress-strain curve (tangent modulus) is usually indicated as E_0 (for materials with a large linear elastic range) and the secant modulus at 50% strength is denoted as E_{50} (for loading of soils). Considering unloading problems, as in case of tunneling and excavations, unload-reload modulus (E_{ur}) is used instead of E_{50}. The definition of E_0, E_{50} and E_{ur} for drained triaxial test results can be depicted as shown in Figure 2.37. Standard drained triaxial tests may yield a significant rate of volume decrease at the very beginning of axial loading and a low initial value of Poisson's ration (υ). However, in general, when using Mohr-Coulomb model the use of a higher value is recommended. For loading conditions other than one-dimensional compression, values in the range between 0.3 and 0.4 can be used and for unloading conditions, it is more appropriate to use values in the range between 0.15 and 0.25. To avoid complications, it is advised to enter at least a small value for the cohesion in soil layers near the ground surface (c > 0.2 kPa) (Bentley, 2018).

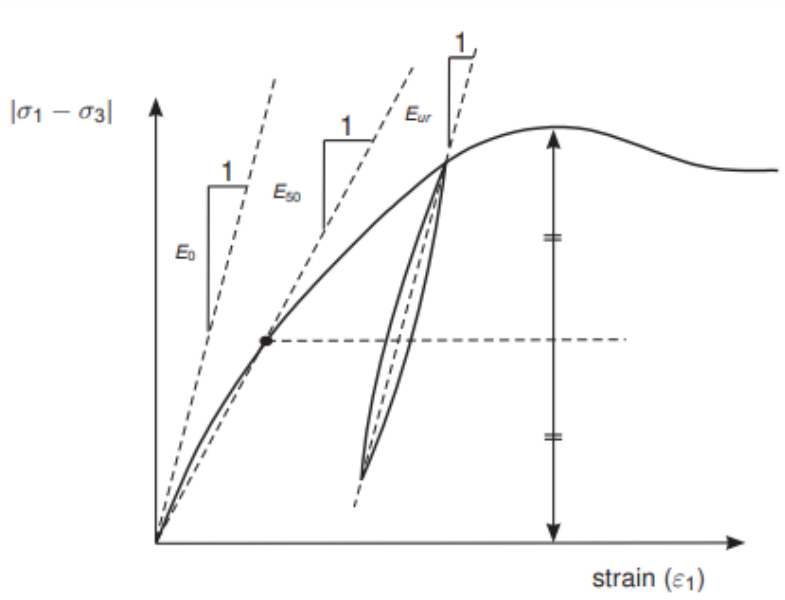

Figure 2.37: Definition of E_0, E_{50} and E_{ur} for drained triaxial test results (Bentley, 2018)

2.9.2.2 The Hardening Soil Model

The Hardening Soil model (HS) proposed by (Schanz et al., 2019) is an appropriate model to simulate the mechanical behavior of soft and stiff soils. The shear failure in this model obeys Mohr-Coulomb failure criterion while the plasticity is governed by a double hardening law that acts on a cone-cap yield surface. In contrast to MC model, the yield surface of HS model can be isotopically expanded due to plastic straining. The yield surface of a hardening plasticity model is not fixed in principal stress space, but it can expand due to plastic straining. Both types of hardening, shear hardening (used to model irreversible strains due to primary deviatoric loading) and compression hardening (used to model irreversible plastic strains due to primary compression in oedometer loading and isotropic loading) are contained in the present model. When subjected primary deviatoric loading, soil shows a decreasing stiffness and simultaneously irreversible plastic strains develop. In the special case of a drained triaxial test, the observed relationship between the axial strain and the deviatoric stress can be well approximated by a hyperbola. For oedometer conditions of stress and strain, the model implies the relationship $E_{oed} = E_{oed}^{ref}(\frac{\sigma}{p^{ref}})^m$. There is also a simple relationship between the modified compression index λ*, as used in models for soft soil and the oedometer loading modulus.

$$E_{oed}^{ref} = \frac{p^{ref}}{\lambda^*}, where\ \lambda^* = \lambda/(1+e_0) \tag{2.11}$$

Where p^{ref} is a reference pressure. Here we consider a tangent oedometer modulus at a particular reference pressure p^{ref}. Hence, the primary loading stiffness relates to the modified compression index λ* or to the standard Cam-Clay compression index λ. The unloading-reloading modulus relates to the modified swelling index, κ* or to the standard Cam-Clay swelling index, κ.

$$E_{ur}^{ref} = \frac{2p^{ref}}{\kappa^*}, where\ \kappa^* = \frac{\kappa}{1+e_0} \tag{2.12}$$

The relationship applies in combination with the input value m=1.

The parameter E_{50} is the confining stress dependent stiffness modulus for primary loading and is given by the equation:

$$E_{50} = E_{50}^{ref}(\frac{c\cos\varphi - \sigma_3' \sin\varphi}{c\cos\varphi + p^{ref}\sin\varphi})^m \tag{2.13}$$

Where, E_{50}^{ref} is a reference stiffness modulus corresponding to the reference confining pressure p^{ref} (In PLAXIS, the value is 100 stress units). In order to simulate a logarithmic compression

behavior, as observed for soft clays, the power should be taken equal to 1.0. It is appropriate to set $E_{ur}^{ref} = 3E_{50}^{ref}$. The definition of E_0, E_{50} and E_{ur} for drained triaxial test results along with hyperbolic stress strain relationship can be depicted as shown in Figure 2.38. The yield surface of HS model and the position of Mohr-Coulomb failure line showing elastic region in stress-pressure relationship is shown in Figure 2.39.

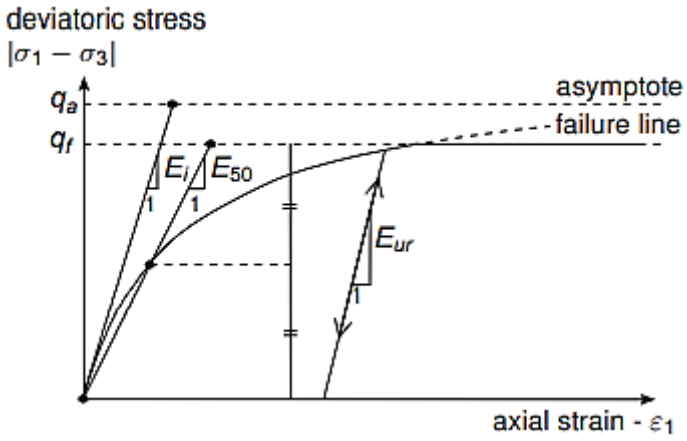

Figure 2.38: Hyperbolic stress strain relation in primary loading for a standard drained triaxial test (Bentley, 2018)

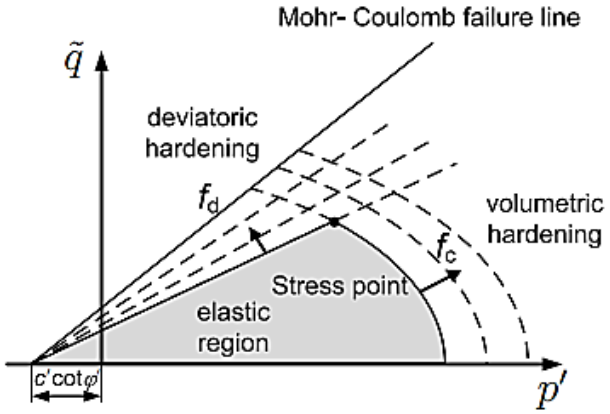

Figure 2.39: Yield surface of HS model, after (Galavi et al., 2013)

The advantage of the HS model over the MC model is not only the use of a hyperbolic stress-strain curve instead of a bi-linear curve, but also the control of stress level dependency. When using the Mohr-Coulomb model, a fixed value of Young's modulus has to be selected whereas for real soils this depends on the stress level. With HS model, this cumbersome selection of input parameters is not required. E_{50}^{ref} is the secant stiffness at 50% of the maximum deviatoric stress, at a cell pressure equal to the reference stress p^{ref} (the program uses 100kN/m^2). The

definition of E_{50}^{ref} and E_{ur}^{ref} for drained triaxial test results and total yield contour of the HS model for cohesionless soil are shown in Figure 2.40 and Figure 2.41.

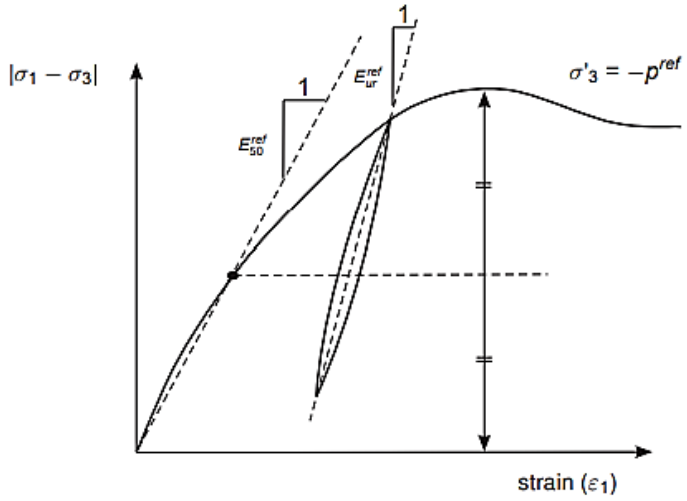

Figure 2.40: Definition of E_{50}^{ref} and E_{ur}^{ref} for drained triaxial test results (Galavi et al., 2013)

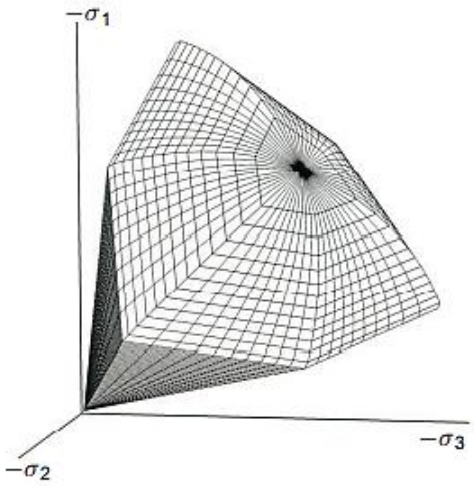

Figure 2.41: Representation of total yield contour of the HS model in principal stress space for cohesionless soil (Galavi et al., 2013)

2.9.2.3 Modified Cam-Clay Model

Cam clay is an elasto-plastic constitutive model developed by Roscoe and Schofield (1963). The modified Cam clay model is then proposed by Roscoe and Burland (1968). The Cam clay and modified Cam clay models are formulated for a soil which is subjected to triaxial test.

In the modified Cam-Clay model (MCC), a logarithmic relation is assumed between void ratio, e and the mean effective stress, p' in virgin isotropic compression, which can be formulated as:

$$e - e^0 = -\lambda\, ln(\frac{p'}{p^0})$$ (Virgin isotropic compression) (2.14)

The parameter λ is the Cam-Clay isotropic compression index, which determines the compressibility of the material in primary loading. When plotting this relation in a e-ln p' diagram one obtains a straight line. During unloading and reloading, a different line is followed, which can be formulated as:

$$e - e^0 = -\kappa\, ln(\frac{p'}{p^0})$$ (Isotropic unloading and reloading) (2.15)

The parameter κ is the Cam-Clay isotropic swelling index, which determines the compressibility of the material in unloading and reloading. In fact, an infinite number of unloading and reloading lines exists in p'-e plane each corresponding to a particular value of the preconsolidation stress p_p.

The yield function of the MCC model is defined as:

$$f = \frac{q^2}{M^2} + p'(p' - p_p)$$ (2.16)

The behavior of soil sample under isotropic compression and position of virgin consolidation line and swelling lines are shown in Figure 2.42. The difference between Cam clay yield curve and Modified Cam clay yield curve is shown in Figure 2.43. The yield surface (f=0) represents an ellipse in p'-q plane. The yield surface is the boundary of the elastic stress states. Stress paths within this boundary only give elastic strain increments, whereas stress paths that tend to cross the boundary generally give both elastic and plastic strain increments. In p'-q plane, the top of the ellipse intersects a line that can be written as:

$q = Mp'$, this line is called the critical state line and gives the relation between p' and q in a state of failure. The constant M is the tangent of the critical state line and determines the extent to which the ultimate deviatoric stress, q, depends on the mean effective stress, p'. The value of M can be obtained from ϕ:

$$M = \frac{6\ sin\varphi}{3-sin\,\varphi}$$ (for initial compression stress states) $(\sigma_1' \leq \sigma_2' = \sigma_3')$ (2.17)

$$M = \frac{6\ sin\,\varphi}{3+sin\,\varphi}$$ (for triaxial extension stress states) $(\sigma_1' = \sigma_2' \leq \sigma_3')$ (2.18)

$$M \approx \sqrt{3}\, sin\,\varphi$$ (for plane strain stress states) (2.19)

Poisson's ratio in this model is usually in the range between 0.1 and 0.2.

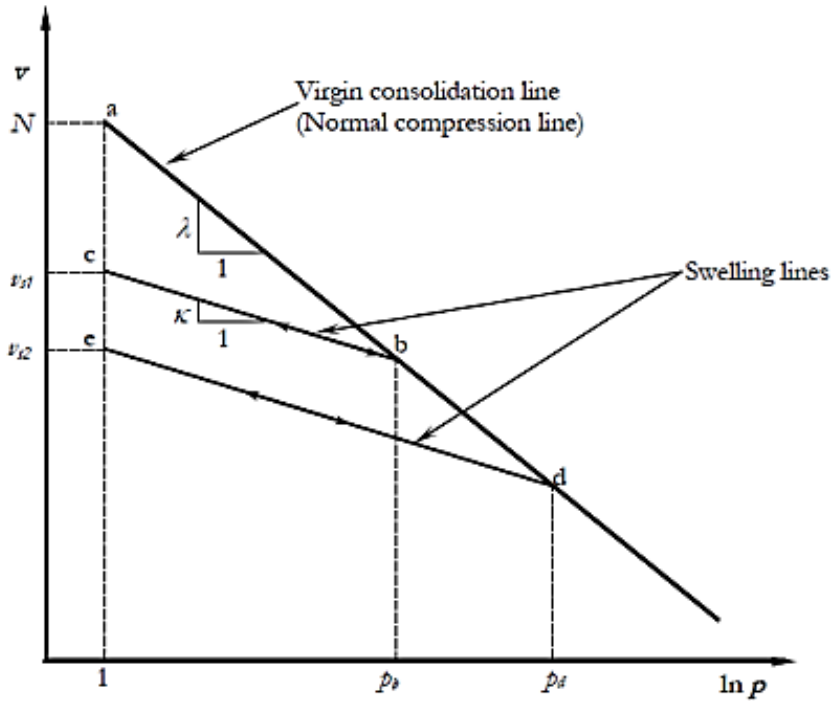

Figure 2.42: Behavior of Soil Sample under Isotropic Compression (Wood, 1990)

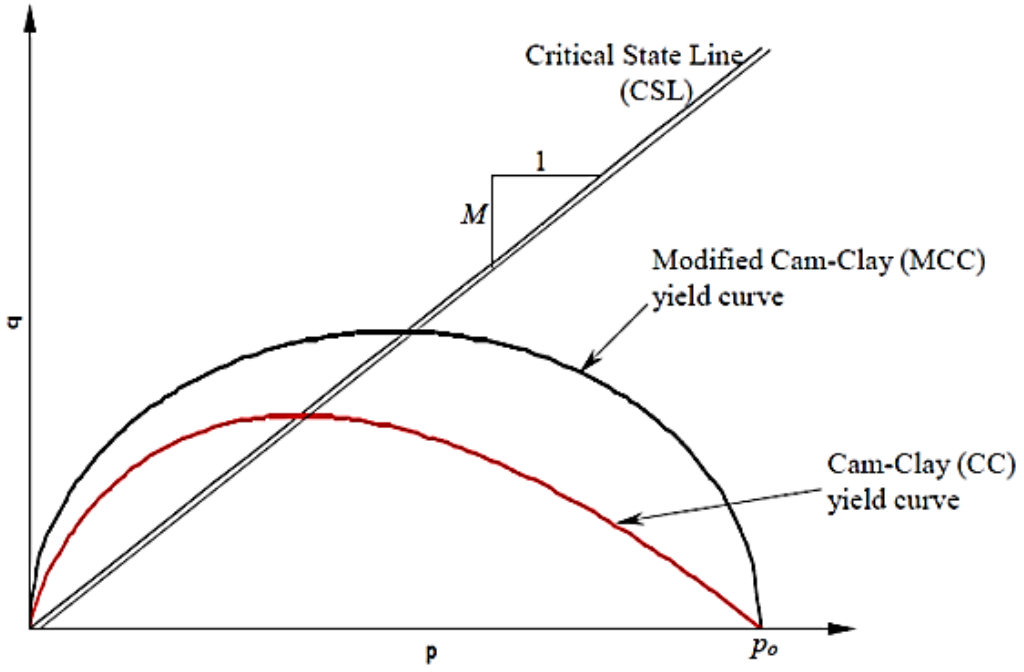

Figure 2.43: Cam Clay and Modified Cam Clay Yield Surfaces (Wood, 1990)

2.9.3 Applicability of the Material Models (from PLAXIS manual)

The mechanical behavior of soils and rocks may be modelled at various degrees of accuracy. Hooke's law of linear, isotropic elasticity, may be thought of as the simplest available stress-strain relationship. The linear elastic Mohr-Coulomb may be considered as a first order approximation of soil or rock behavior. However, PLAXIS includes more advanced material models involving specific features such as stress- dependency of stiffness, strain hardening/ softening, memory of pre-consolidation, critical state, anisotropy, creep, swelling and shrinkage. An overview of the applicability of the material models are given in Table 2.3 and Table 2.4.

Table 2.3: Applicability of Material Models Considering Different Types of Applications (considering also types of soil)

Model	Foundation	Excavation	Tunnel	Embankment	Slope	Dam	Offshore	Other
Linear Elastic Model	C		C					
Mohr-Coulomb Model	C	C	C	C	C	C	C	C
Hardening Soil Model	B	B	B	B	B	B	B	B
HS small Model	A	A	A	A	A	A	A	A
UBC3D-PLM Model	B	B	B	B	B	B	B	B
Soft Soil Creep Model	B	B	B	A	A	B	B	B
Soft Soil Model	B	B	B	A	A	B	B	B

Model	Foundation	Excavation	Tunnel	Embankment	Slope	Dam	Offshore	Other
Jointed Rock Model	B	B	B	B	B	B	B	B
Modified Cam-Clay Model	C	C	C	C	C	C	C	C
NGI-ADP Model	B	B	B	A	A	B	A	B
UDCAM-S Model							A	
Hoek-Brown Model	B	B	B	B	B	B	B	B
Concrete Model	A	A	A	A	A	A	A	A

Here,

A: The best standard model in PLAXIS for this application

B: Reasonable modelling

C: First order (crude) approximation

Notes: Soft soil creep model in case time dependent behavior is important. UBC3D-PLM model for dynamic analysis of sandy soils involving liquefaction. As an alternative PM4Sand is available as a user-defined soil model upon request.

Table 2.4: Applicability of Material Models Considering Different Types of Materials

Model	Concrete	Rock	Gravel	Sand	Silt	OC Clay	NC Clay	Peat (org)
Linear Elastic Model	C	C						
Mohr-Coulomb Model	B	B	C	C	C	C	C	C
Hardening Soil Model			B	B	B	B	B	

Model	Concrete	Rock	Gravel	Sand	Silt	OC Clay	NC Clay	Peat (org)
HS small Model			A	A	A	A	B	
UBC3D-PLM Model			B	B	B			
Soft Soil Creep Model							A	A
Soft Soil Model							A	A
Jointed Rock Model		A						
Modified Cam-Clay Model							C	C
NGI-ADP Model						A	A	A
UDCAM-S Model						A	A	A
Hoek-Brown Model		A						
Concrete Model	A							

Here,

A: The best standard model in PLAXIS for this application

B: Reasonable modelling

C: First order (crude) approximation

Notes: Soft soil creep model in case time dependent behavior is important. UBC3D-PLM model for dynamic analysis of sandy soils involving liquefaction. NGI-ADP model for short-term and UDCAM-S model for cyclic analysis, in case only undrained strength is known. Jointed Rock model in case of anisotropy and stratification; Hoek-Brown for rock in general.

2.10 **Summary**

i. Tunneling through soft ground requires special concern as the interaction and redistribution effects between tunnels and soil may cause serious issues with adjacent structures.

ii. Depending on the excavation factors and geotechnical soil properties, tunnel construction methods need to be chosen.

iii. NATM (New Austrian Tunneling Method) was created and named over 50 years ago in 1960s by Rabcewicz initially developed for rock tunnel. Improvements and

modifications have been concurred to make it adaptable for soft ground tunnels in urban environments and the first application was in Frankfurt, Germany (1968).

iv. The TBM-EPB method can give satisfactory results if the excavated materials have good plastic deformation, pulpy to soft consistency, low inner friction, and low permeability.

v. Effect in settlement is considered in transverse and longitudinal direction which results in constraint displacement of the ground. In TBM, face loss, shield loss and tail loss are three categories of ground loss caused by ground deformation into tunnel face, annular gap around the shield skin plate and annular gap between ground and lining. Unbalanced ground and groundwater pressure, advancement of tunnel, elastic deformation due to tail void, deformation in segmental rings, etc. can be reason to ground settlement.

vi. In numerical procedure (FEM) field conditions can be simulated accurately with constitutive models and boundary conditions. The plate elements and the volume elements are composed of 8 node plate elements and 16 node interface elements and 6 node triangles in x-y direction and 8 node quadrilaterals in z direction consecutively.

vii. After defining the geometry and generating the mesh (coarse, medium, fine, and very fine), initial stresses are applied using either K0 procedure or gravity loading method.

viii. The Mohr-Coulomb model is based on the principle of elastoplasticity and the important parameters for this model are cohesion, friction angle, dilatancy angle, modulus of elasticity, Poisson's ratio, etc.

ix. The Hardening soil model is based on the principle of double hardening law (shear and compression hardening) that acts on a cone cap yield surface. The important parameters of HS model are: stress dependent stiffness, plastic straining, primary compression, and elastic unloading/ reloading.

x. The Modified Cam Clay model is based on the principle of the relationship between void ratio and mean effective stress in virgin isotropic compression. The basic parameters of MCC model are: Poisson's ratio, swelling index, compression index, tangent of CSL, and initial void ratio.

Chapter 3

MODEL VALIDATION

2.11 Introduction

This chapter emphasizes on the validation of two metro rail lines of Iran and Delhi with PLAXIS 3D. For Mashhad Metro Line 2, each section of the ground was modeled by two constitutive models, namely MCC and Mohr-Coulomb (MC). Numerical modeling was originally performed by FLAC3D software. Afterwards, the results of two types of numerical analyses and empirical data were compared with each other. Based on the transverse and longitudinal sections settlement, the MCC model showed high capabilities of predicting the surface settlement in comparison to the MC model. And also, the deviated values are less for both of the models for O'Reily & New relationships. Originally, a 2D numerical model has been developed using finite element software OptumG2 to replicate the Delhi Metro Phase 3 tunnel project. An elastoplastic model of the tunnel at a standard depth of 18 m has been analyzed. After comparing results of two types of numerical analyses and empirical data of Peck & Schmidt formula, the vertical surface settlement shows relatively closer values for both PLAXIS 3D and OptumG2.

2.12 General Information about Line 2 Metro of Mashhad

Mashhad Metro Line 2 is the second metro line that is being developed to facilitate passengers' transport in Mashhad, Iran. This metro line is situated beneath the street level in a tunnel running in a Northeast-Southwest direction, as seen in Figure 3.1. In total, this line includes 12 stations. Furthermore, Metro Line 2 is connected to Mashhad Metro Lines 1 and 3 as well as the national railway line in Iran. The total length of Line 2 is about 14.3 km. A part of the tunnel running from Station A2 through L2 and going further to the TBM exit shaft is going to be constructed with mechanized tunneling methods, such as the Tunnel Boring Machine or TBM. The TBM excavates the ground in front of the cutter head while pushing itself forward. The tunnel is built up inside the TBM from concrete segments. Figure 3.2 shows the section of ground stratifications and tunnel's location along with water level position.

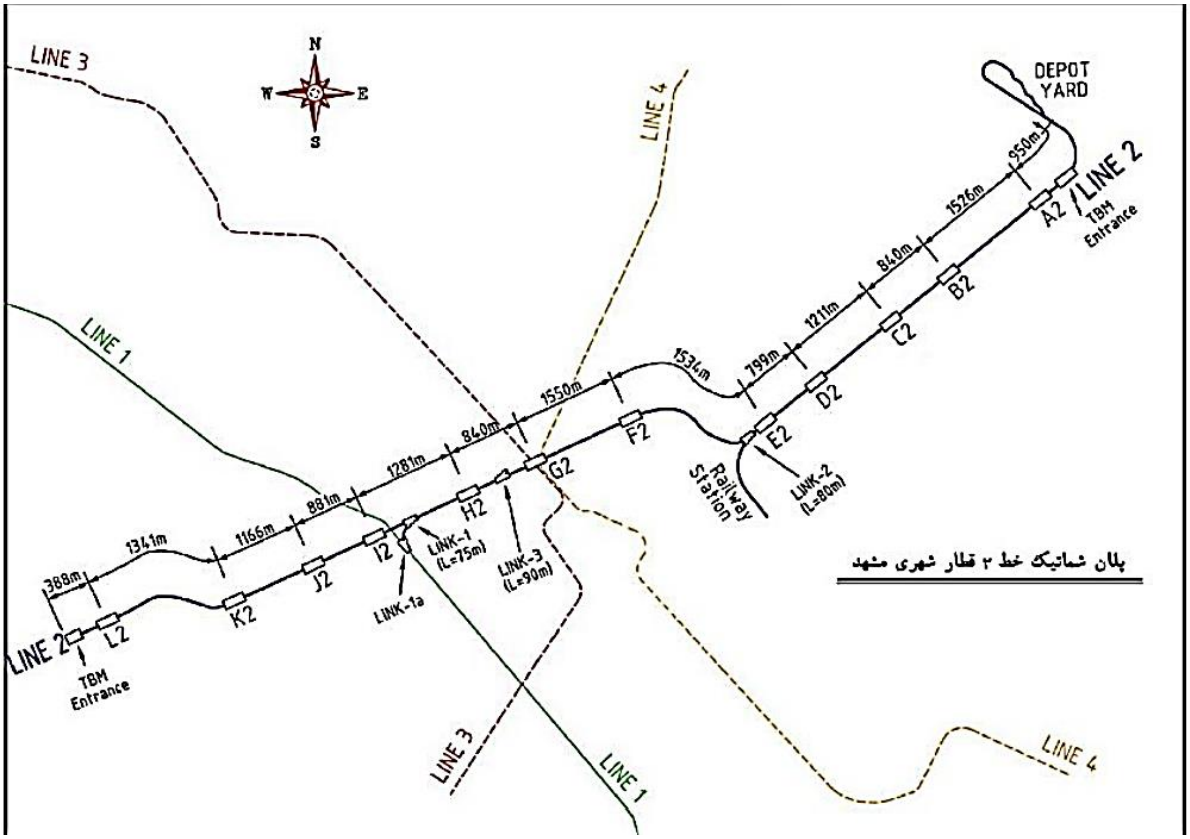

Figure 3.1: Plan of Line 2 Metro of Mashhad (Eslami et al., 2020)

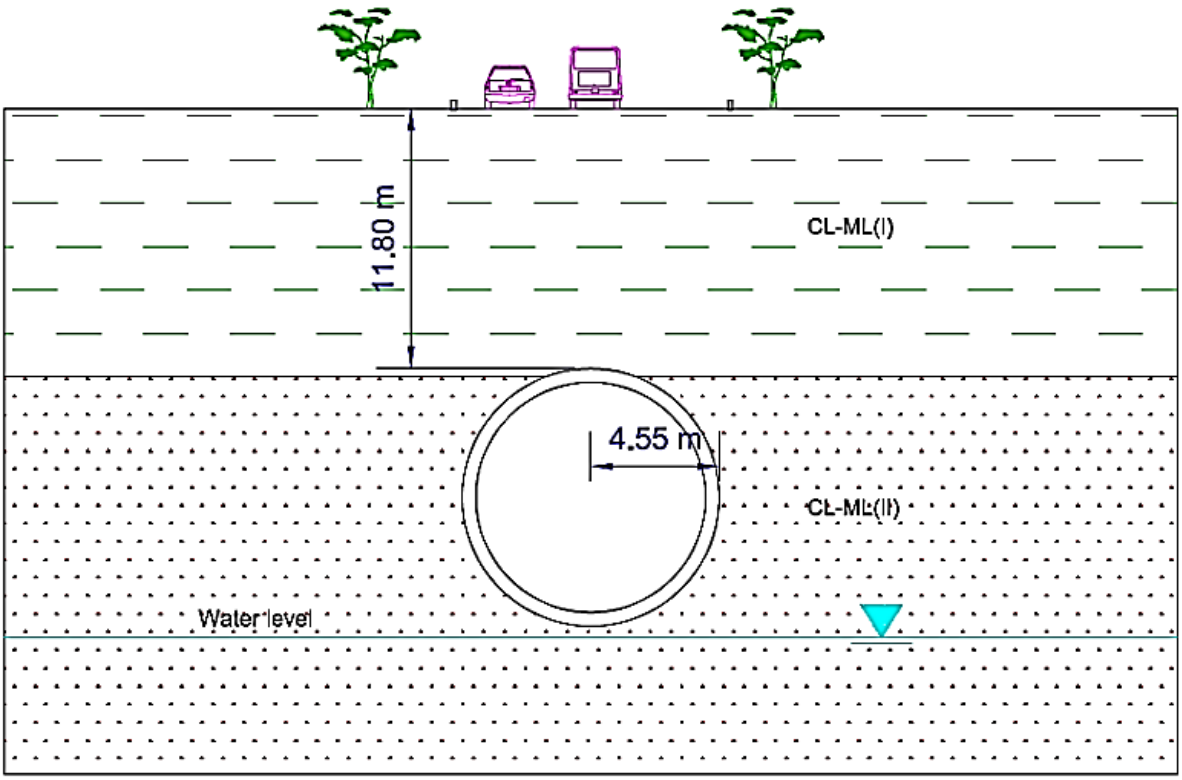

Figure 3.2: Section of ground line 2 Metro of Mashhad (Eslami et al., 2020)

3.2.1 Soil Condition

The detailed geotechnical investigations were performed by the excavation of 61 boreholes (a total length of 2,487.7 m) and 16 test pits (a total length of 296.95 m). These investigations mainly included some field tests and surveys, laboratory tests, and desk studies. The field tests included a plate loading test (PLT), in-situ shear test, pressure meter test, standard penetration test (SPT), Lufran permeability test, and in-situ density test. The laboratory tests comprised the direct shear test, triaxial test, particle size analysis, Atterberg limits test, consolidation, permeability, and the Los Angeles Abrasion test. The desk studies included the collection of the existing data such as previous reports, in-situ test results, and data processing and analyzing. The geological section of the project is illustrated in Figure 3.3. The soil sample for testing is considered from DH-09 Borehole.

The characteristics of Mashad's soil are illustrated in Table 3.1.

i. Medium clay-silt (CL-ML l): The uppermost layer is the soft clay soil by low plasticity and low moisture percentage. The average thickness is about 10 m in most areas.
ii. Medium clay-silt (CL-ML ll): The low layer is the soft clay soil by high plasticity and high moisture percentage. This layer can be found at depths of 10-35 m.

Table 3.1: Characteristics Profile of Mashhad's Soil

Layer No.	Notation	Depth	Dry Density	Moisture Content	Cohesion	Friction Angle	Undrained Cohesion	Undrained Friction Angle
		(m)	(kN/m^3)	(%)	kPa	deg	kPa	deg
I (A)	CL-ML I	0 ~ 10	17.00	17.00	10	25	10	25
I (B)	CL-ML II	10 ~ 35	17.50	18.00	30	23	12	20

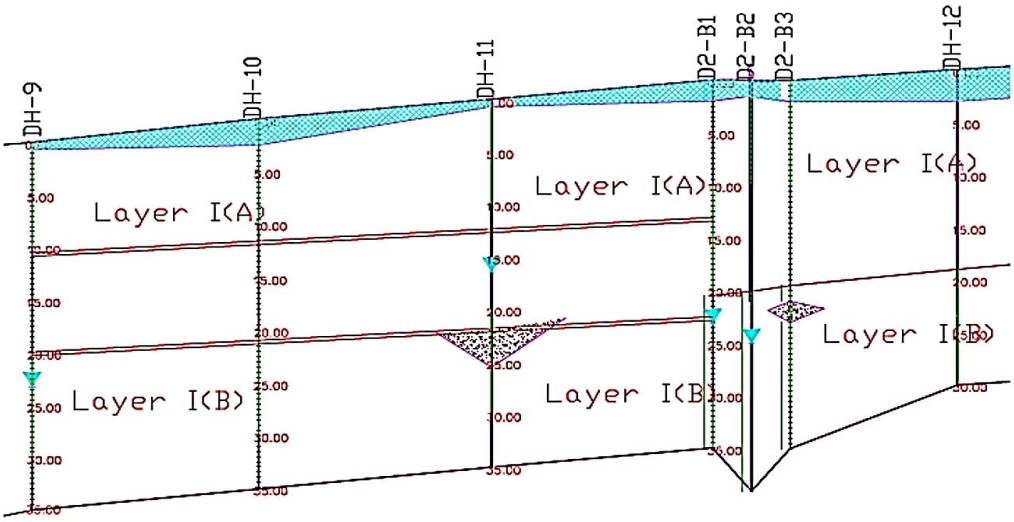

Figure 3.3: Geological Section of Mashhad Metro Line 2 (12+500km) (Eslami et al., 2020)

The calculation of the MCC parameter was performed based on the elasticity rule:

$$G = \frac{E}{2(1+\vartheta)} \quad (3.1)$$

$$K = \frac{E}{3(1-2\vartheta)} \quad (3.2)$$

$$\kappa = C_s . ln\, 10 \quad (3.3)$$

$$\lambda = C_c . ln\, 10 \quad (3.4)$$

$$\vartheta_0 = 1 + \vartheta \quad (3.5)$$

Table 3.2: Soil characteristics and the respective parameters for MCC Model

Parameter	**Description**	**Values for Soil Layer**	
		I (A)	II (A)
E (MPa)	Young Modulus	100	120
G (MPa)	Shear Modulus	40	48
ρ (kN/m^3)	Density	19.85	20.65
M	Frictional Constant	0.983	0.898
K	Slope of Swelling line	0.0345	0.044
υ	Poisson ratio	0.27	0.27

3.2.2 Numerical Modeling

For accurate modeling of a tunnel in soft ground by FEM methods, some of key parameters that affect the surface settlement such as constitutive soil model, tunnel lining, over excavation, and shield element should be considered. In this study, the result of field tests, in situ measurements, and laboratory data is utilized to describe two different constitutive models. Since there is a complicated correlation between the target parameter (surface settlement) and other factors, the input parameters of constitutive models should be considered accurately.

To obtain a rational result, all main elements of mechanized excavation should be modeled such as: TBM's shield, concrete tunnel lining, support face pressure, tail void grouting, and over excavation. Therefore, FLAC3D (Version 3.0) code, a commercial software package based on the generalized finite difference method, was used to develop the numerical simulation. The standard dimensions followed for the numerical modeling is displayed in Figure 3.4 in FLAC3D.

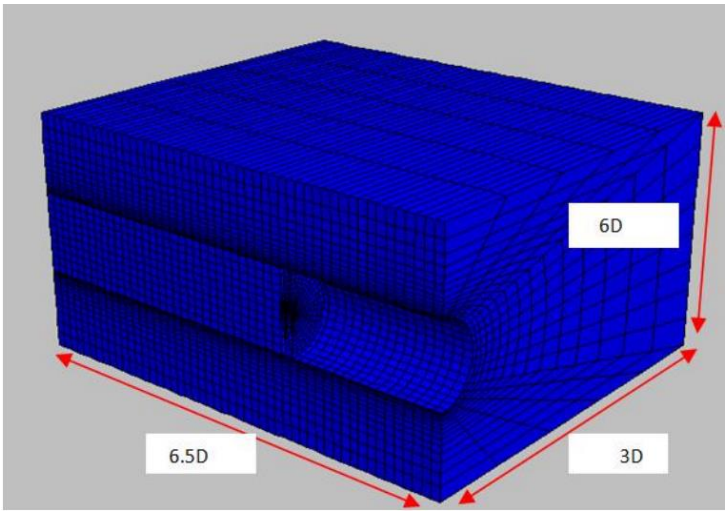

Figure 3.4: Dimension of the 3D Simulation in FLAC3D (Eslami et al., 2020)

For validation purpose, PLAXIS 3D software is used to compare the result with the literature's numerical and empirical results. The shield of TBM was modeled using a plate element and a simplified cylindrical geometry is considered. The segmental lining and shield elements are modeled by the elastic constitutive model. The effect of virtual boundary on the results were neglected because the model has a longitudinal dimension (y direction) of 6.5D, an extension under the tunnel axis (z direction) of 3D, and a transverse extension of 4D, where D is the tunnel diameter. As the underground water table in this project is lower than the project line, all analyses have been performed in drain condition. The tunnel length of 15m (1/1000th of

actual length), radius of 4.55m and depth of 14m have been considered for simplified modelling.

The order of excavation integrated into the models is as follows:

Step 1: Excavation of tunnel (about 1.5m)

Step 2: Application of face pressure by the TBM on the new excavation face of the tunnel

Step 3: Excavation of the tunnel by driving the EPB machine

Step 4: Generation of both the gap filling and segment elements performed after excavation of the tunnel

Step 5: Removing the previous face pressure on the tunnel face.

Step 6: Repeating the steps 1 to 5 until the TBM reaches its destination

3.2.3 Distribution of Surface Settlements in Transverse Section

The semi-empirical relation of Peck was obtained in following equations, showing the shape of transverse settlement:

$$S = S_{max} e^{\left(-\frac{y^2}{2i^2}\right)} = \frac{V_L}{i\sqrt{2\pi}} e^{\left(-\frac{y^2}{2i^2}\right)} \quad (3.6)$$

$$V_S = \int_{-\infty}^{+\infty} S_{max}\, e^{\left(-\frac{y^2}{2i^2}\right)} = \sqrt{2\pi} i S_{max} \quad (3.7)$$

$$V_L = \frac{V_S}{V_0} * 100 \quad (3.8)$$

Here,

S = vertical surface settlement at y location (m)

y = distance of the considered point from the tunnel axis (m)

Vs = volume of settlement per meter of tunnel advancement (m^3/m)

i = trough width parameter ($i = kZ_0$, where k is a dimensional constant depending on soil type and Z_0 is the depth of the tunnel axis below surface

V_L = volume of settlement per unit length expressed as a percentage of the total excavated volume of the tunnel

V_0 = volume required to construct the tunnel

In Figure 3.5, three-dimensional view of a tunnel is shown where the tunneling direction is considered along X-axis and settlement trough is considered to be deformed along vertically downward Z-axis. The distance between ground surface and center of the tunnel is considered Z_0. The inflection point where the sagging stops and hogging starts is considered the horizontal distance, i, from center point (maximum settlement), which is clearly shown in the A-A cross sectional view.

O'Reily & New showed that point of inflection (trough width parameter) i had a linear relation with depth of tunnel and they suggested equations:

$$i = 0.43Z_0 + 1.1 \text{ (For cohesive soil)} \quad (3.9)$$

$$i = 0.28Z_0 - 0.1 \text{ (For granular soil)} \quad (3.10)$$

A summary of all relations suggested by different researchers is presented in Table 3.3. The behavior of the surface settlement in transverse section follows the Gaussian distribution and based on this assumption, a Gaussian curve is fitted to the data monitoring outputs. As a result, the Gaussian distribution is analyzed for obtaining trough width parameter, i, which is about 7.41m and this value is very close to the O'Reily & New relation whose deviated value was about 3.91% (less deviation of all). In our numerical analyses, the deviated value for this relationship is also less than others. The deviated percentages are approximately 1.66% and 4.81% for MC and MCC models consecutively. The transverse profile of the surface settlement was compared with the numerical results obtained from the MCC model and the MC model. It can be clearly seen that results of the MCC model have the best fit to the data points. According to the literature, the MC model substantially differs from data monitoring outputs, thus the elasto-plastic model (e.g., the MCC model) is considered to be suitable for this type of soils. In the literature, comparing the maximum settlements of numerical analyses and Peck formula, about 9.6% and 41% deviations were found for MC and MCC models respectively. In our comparative analyses of Plaxis, the values are 11.11% and 44.4% for MC and MCC models respectively.

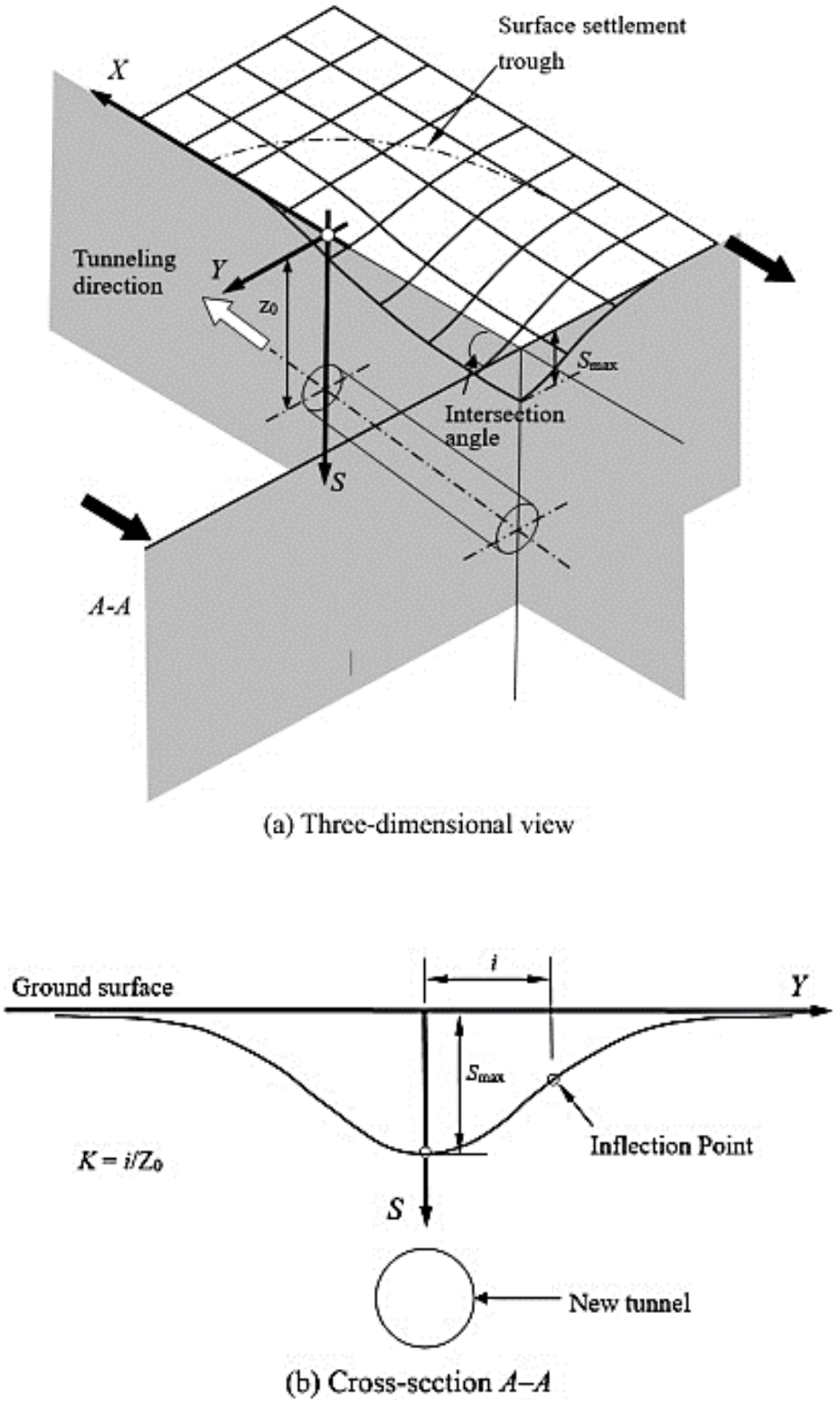

Figure 3.5: Distribution of Surface Settlement Trough (a) Three-dimensional view (b) Cross Sectional view (Transverse Section) (Lu et al., 2019)

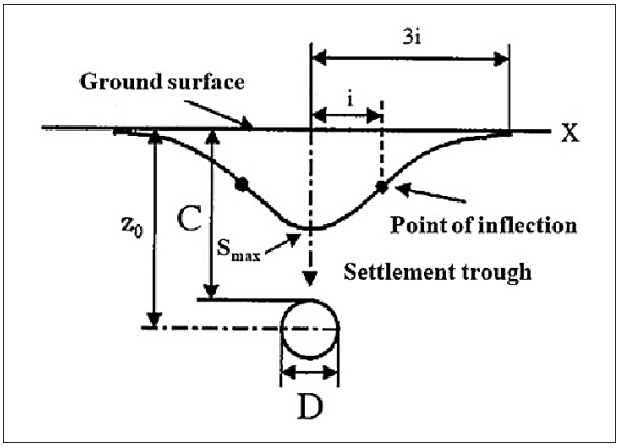

Figure 3.6: Relevant parameters for relations (Eslami et al., 2020)

Table 3.3: Empirical Relations based on different researchers

Researchers	**Empirical Relations**
Peck, 1969	$\frac{i}{R} = (\frac{Z_0}{2R})^n \ (n = 0.8 - 1)$
Clough & Schmidt, 1981	$\frac{i}{R} = (\frac{Z_0}{2R})^n \ (n = 0.8)$
Atkinson & Potts, 1977	$i = 0.25 \ (1.5Z_0 + 0.5R)$
O'Reily & New, 1982	$i = 0.43Z_0 + 1.1$
Mair & Taylor, 1999	$i = (0.4 - 0.5)Z_0 + 1.1$
Attewell & Farmer, 1974	$\frac{i}{R} = (\frac{Z_0}{2R})$

To predict the surface settlement, the MCC model is proposed in soft clay with a low over consolidation ratio or normal consolidation similar to the soil in this site. In other words, where the shear modulus is independent of the shear strain, the surface settlement has a wide and shallow profile. Since the over consolidation clay exhibits non-linear stress strain behavior at the small strain prior to crossing the plastic yielding, it is very important to consider the behavior of these kinds of soils under small strain condition. Nevertheless, the shear modulus in the MC model is constant and the shear strain doesn't change with shear stress; this is probably the main reason for the difference between the results. Based on the results of Bolton for the prediction of surface settlement, strain non-linearity within the elastic domain must be implemented. The MCC model has a relatively precise prediction of the surface displacement in clay, either by normal consolidation or low OCR value.

In Table 3.4, the results are shown after calculating the distance of inflexion point from center based on different researchers' empirical formulas for both MC and MCC models of TBM method. And after analyzing, the deviated percentage from PLAXIS and literature is marked in O'Reily & New relationship as it shows the lowest deviated percentages (%) among all. Also, the maximum transverse settlement and settlement at inflection point do not vary a lot from literature's perspective. Therefore, for measuring the distance, i, O'Reily & New formula can be reliable to use which is validated in this chapter.

From the comparative analysis of Mashhad Metro Line 2, it can be seen that O' Reily & New empirical relation shows closest values (3.91%, 1.66% and 4.81% deviation with FLAC 3D, MC model in PLAXIS 3D and MCC model in PLAXIS 3D respectively).

Table 3.4: Calculation of inflexion point distance from center based on different researchers for MC and MCC Models (TBM method) and Comparison with Numerical Analysis (for literature and PLAXIS both)

Model Type	Researchers	Tunnel depth	Tunnel Radius	Distance to Point of Inflexion, i	Value from PLAXIS	Deviated Value	Value from Literature	Deviated Value	Difference in inflexion point	Max Settlement from PLAXIS	Max Settlement from literature	Settlement at inflexion (Plaxis)	Settlement at inflexion (Literature)
		m	m	m	m	%	m	%		mm	mm	mm	mm
MC	Peck	14	4.55	6.42	7.24	3.31	7.41	5.53	0.17	-8.0	-7.0	-5.0	-4.0
	Clough & Schmidt	14	4.55	6.42	7.24	11.32	7.41	13.33	0.17	-8.0	-7.0	-5.0	-4.0
	Atkinson & Potts	14	4.55	5.82	7.24	19.64	7.41	21.47	0.17	-8.0	-7.0	-5.0	-4.0
	O' Reily & New	14	4.55	7.12	7.24	1.66	7.41	3.91	0.17	-8.0	-7.0	-5.0	-4.0

Model Type	Researchers	Tunnel depth	Tunnel Radius	Distance to Point of Inflexion, i	Value from PLAXIS	Deviated Value	Value from Literature	Deviated Value	Difference in inflexion point	Max Settlement from PLAXIS	Max Settlement from literature	Settlement at inflexion (Plaxis)	Settlement at inflexion (Literature)
	Mair & Taylor	14	4.55	5.60	7.24	3.31	7.41	5.53	0.17	-8.0	-7.0	-5.0	-4.0
	Attewell & Farmer	14	4.55	7.00	7.24	3.31	7.41	5.53	0.17	-8.0	-7.0	-5.0	-4.0
MCC	Peck	14	4.55	6.42	7.48	6.42	7.41	5.53	0.17	-5.0	-4.0	-4.0	-3.0
	Clough & Schmidt	14	4.55	6.42	7.48	14.14	7.41	13.33	0.17	-5.0	-4.0	-4.0	-3.0
	Atkinson & Potts	14	4.55	5.82	7.48	22.21	7.41	21.47	0.17	-5.0	-4.0	-4.0	-3.0
	O' Reily & New	14	4.55	7.12	7.48	4.81	7.41	3.91	0.17	-5.0	-4.0	-4.0	-3.0
	Mair & Taylor	14	4.55	5.60	7.48	25.13	7.41	5.53	0.17	-5.0	-4.0	-4.0	-3.0
	Attewell & Farmer	14	4.55	7.00	7.48	6.42	7.41	5.53	0.17	-5.0	-4.0	-4.0	-3.0

In Figure 3.7, the transverse settlement profile from PLAXIS, FLAC3D and Peck's empirical formula is plotted in graphical form, where it can be seen that every curve follows the Gaussian distribution curve. Curves for MC (PLAXIS and FLAC3D both) tends to show similar pattern

as the Peck's curve and settlement values are larger in MC than MCC models. The center of the tunnel is depicted as 0 in X-axis of the graph. Different findings of distance of inflection point from center from PLAXIS values and empirical relations established by various researchers is shown in Figure 3.8, where it can be indicated that the O'Reily & New formula gives comparatively closer value of numerical findings among all. The distribution of total displacement in PLAXIS 3D for MC and MCC model are represented in Figure 3.9 and Figure 3.10 respectively.

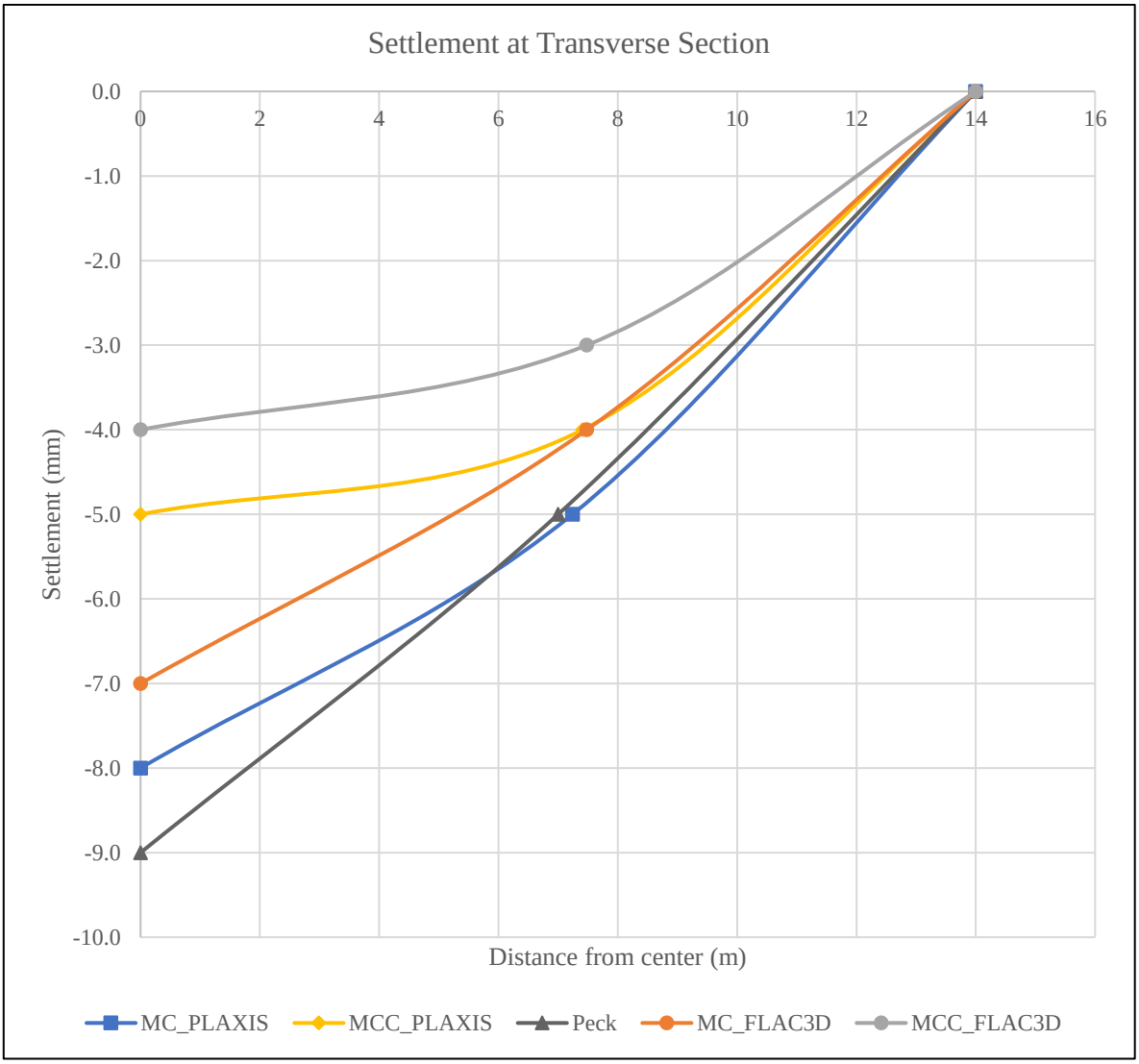

Figure 3.7: Comparison of Settlement at Transverse Section between PLAXIS 3D, FLAC 3D and Peck's Formula

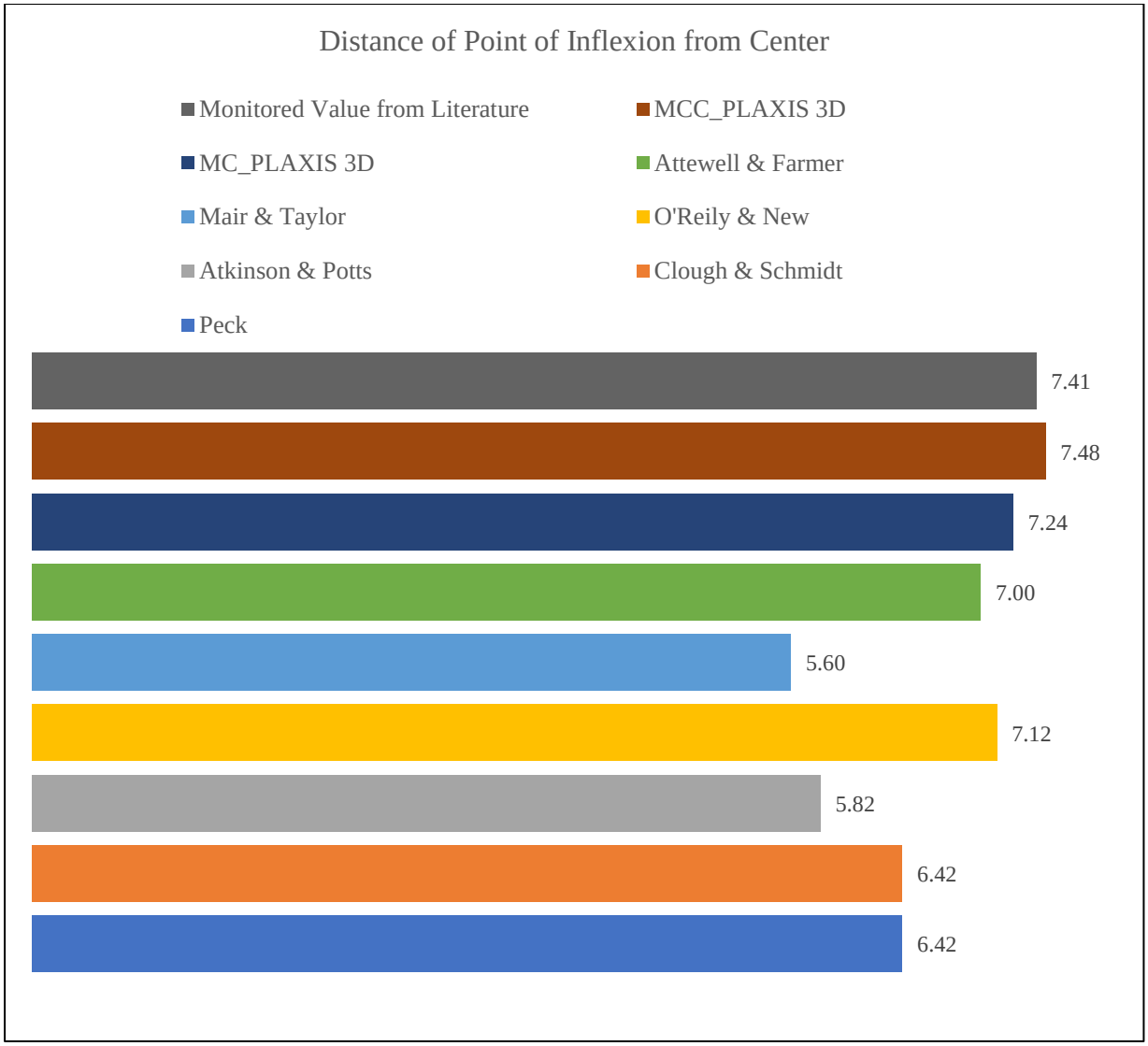

Figure 3.8: Comparison between Different Findings of Distance of Point of Inflexion from Center

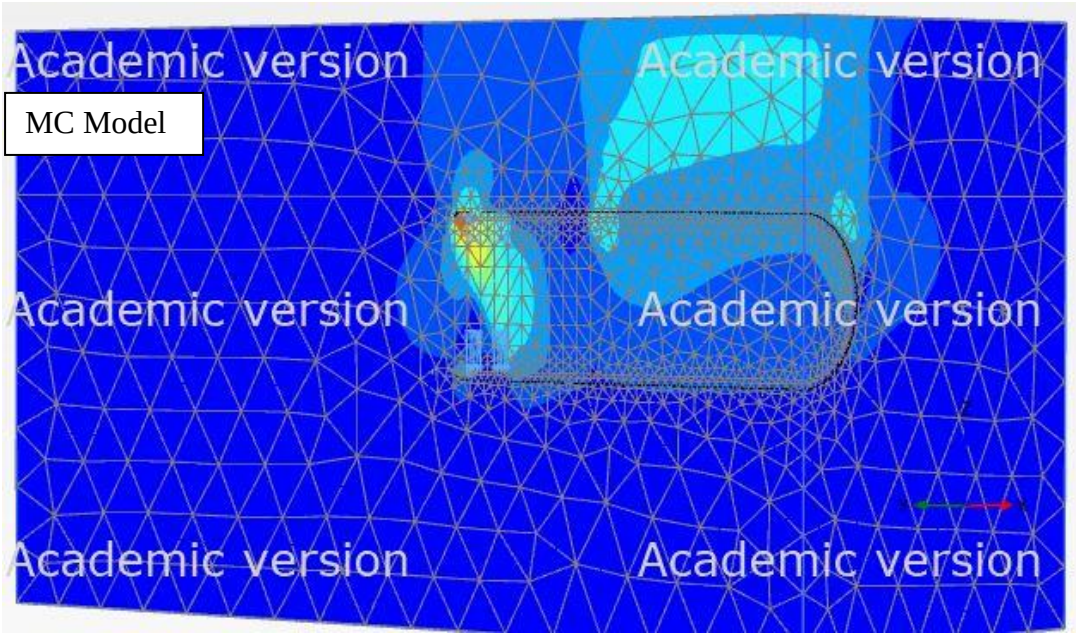

Figure 3.9: Representation of Distribution of Total Displacement of Mashhad Metro in PLAXIS 3D (MC Model)

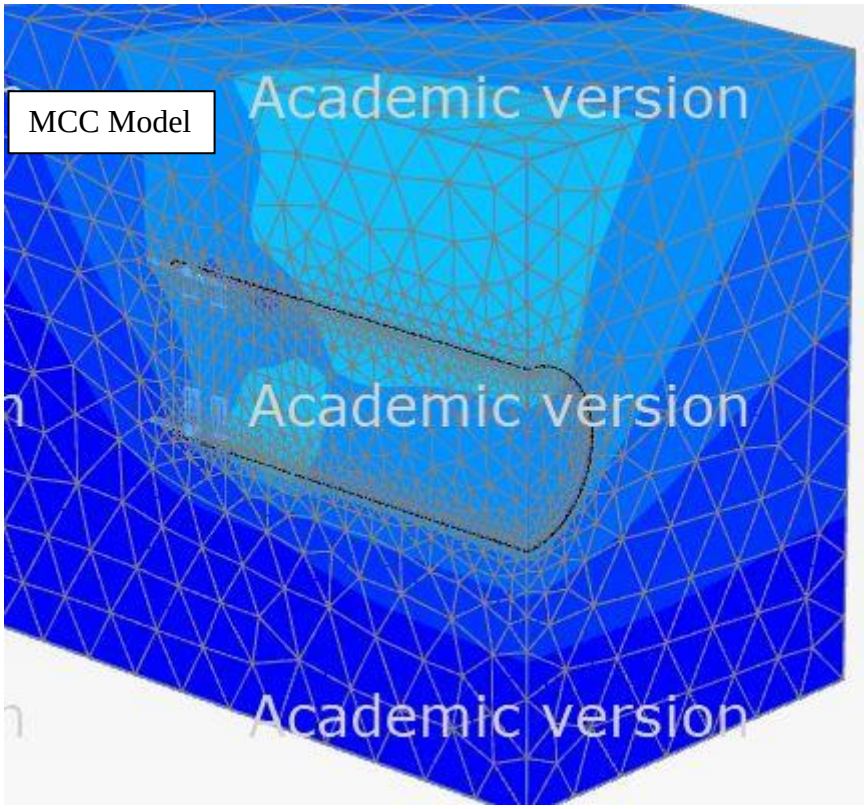

Figure 3.10: Representation of Distribution of Total Displacement of Mashhad Metro in PLAXIS 3D (MCC Model)

3.3 General Information about Delhi Metro Phase 3, India

In Delhi Metro Phase-3, a record of 30 TBMs was used to bore about 80km of underground tunnels in total (combining the length of both way tunnels). The total length of the underground corridor in this phase is about 54km. The new tunnels passed below existing operational elevated viaducts, an operational tunnel of DMRC, the rocky Aravalli ranges, heritage monuments, and densely populated areas. The tunnel passed underneath the old dilapidated buildings, which were undergoing reconstruction or repairs. The Figure 3.11 represents the proposed plan of Delhi Metro Phase 3.

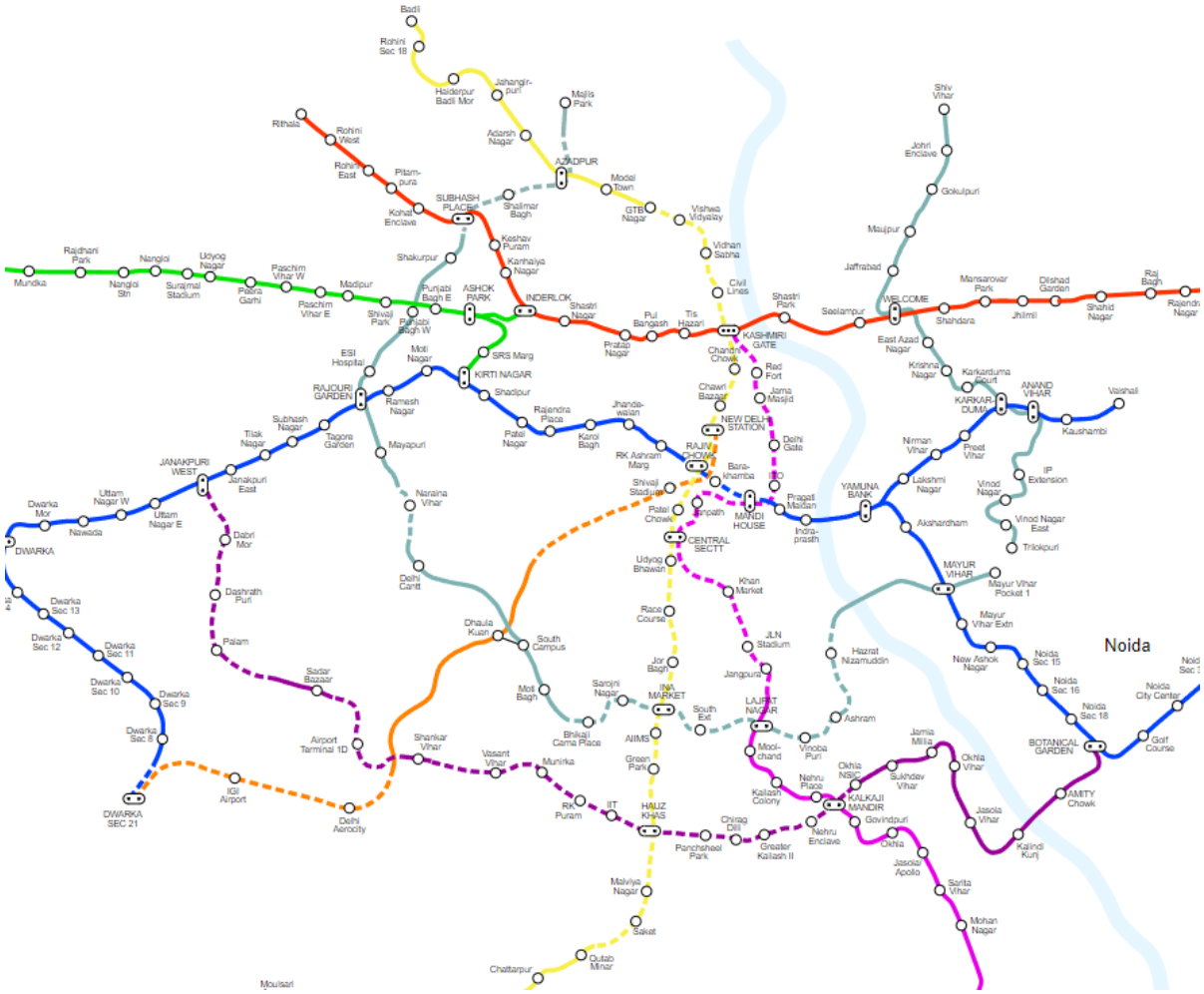

Figure 3.11: Proposed Plan of Delhi Metro Phase 3 Line (Dotted Lines are Underground portions) (Naqvi et al., 2021)

3.1.1 Soil Condition and Parameters

The soil used in this analysis was Delhi silty sand. The properties of soil and concrete tunnel lining are given in Table 3.5 and Table 3.6.

Field data shows that the cohesionless of soil of Delhi has horizontal stratification with the variation in Young's modulus at various depths. To replicate the field condition, the Young's modulus of soil is linearly varied from top to bottom, with 7.5 MPa at top and 50 MPa at the bottom. In Figure 3.12, the variation in Young's modulus with depth is shown for clear view. The location of tunnel and tunnel specification is defined in Figure 3.13.

Table 3.5: Soil and Concrete Lining Properties found from Soil Test Data

Delhi Silty Sand		
Bulk Density	kN/m^3	18
Saturated Density	kN/m^3	20
Poisson's Ratio		0.25
Friction Angle		35
Dilatation Angle		5
Concrete Lining		
Density	kN/m^3	25
Young's Modulus	kPa	3.16×10^7
Poisson's Ratio		0.15
Sectional Area	cm^2/m	2500
Plastic Section Modulus	cm^3/m	15625
Moment of Inertia	cm^4/m	130208.33
Yield Strength	MPa	30
Weight	kg/m/m	625

Table 3.6: Young's Modulus of Delhi Silty Sand at Various depths

Depth (m)	Young's Modulus (kPa)
0 ~ 10	7500
10 ~ 20	15000
20 ~ 35	30000
35 ~ 50	40000
50 ~ 60	50000

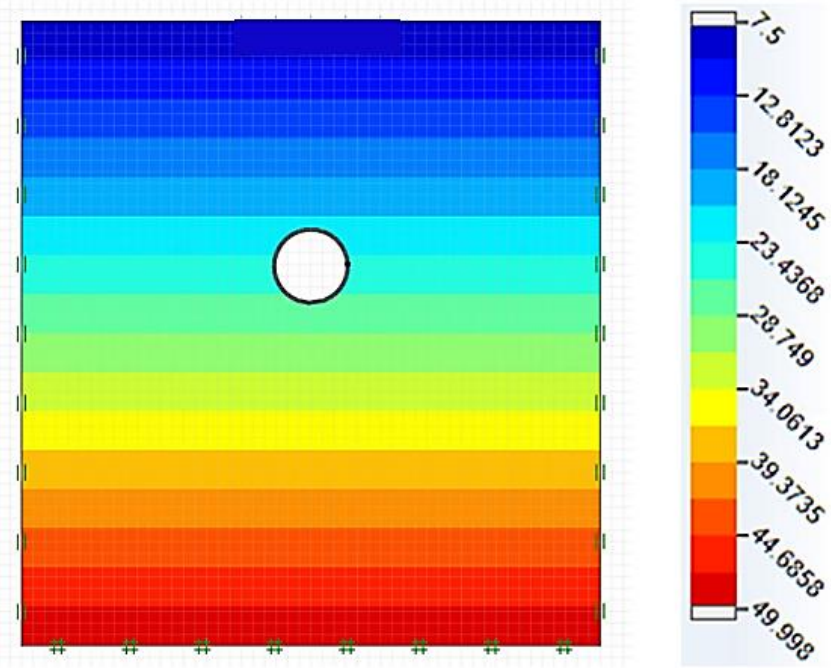

Figure 3.12: Representation of Young's Modulus of Delhi Silty Sand at Various depths (Naqvi et al., 2021)

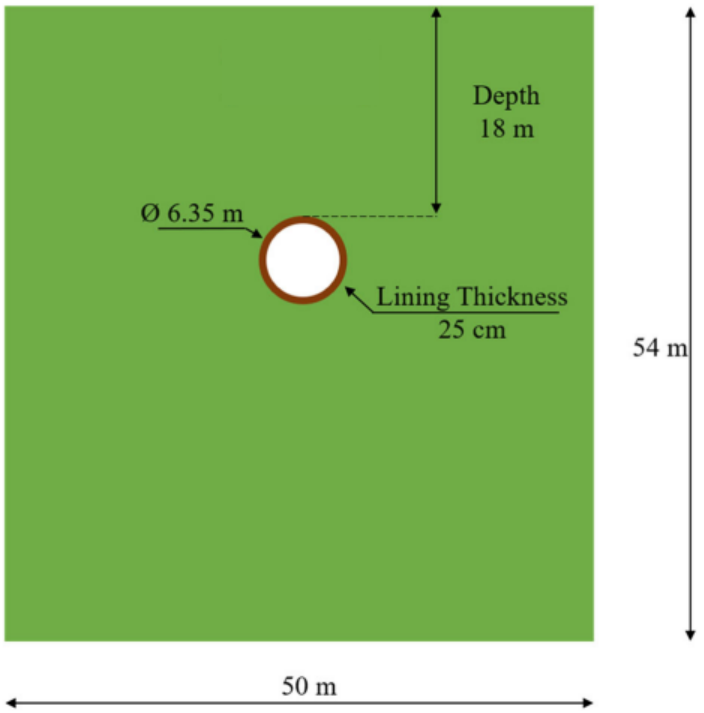

Figure 3.13: Schematic Representation of Model Parameters (Naqvi et al., 2021)

3.1.2 Numerical Modelling

2D plain strain model has been a model using commercially available finite element software Optum G2. The elastoplastic model of soil was modelled using the Mohr-Coulomb criterion. The dimensions of the soil model are considered as 50 m width and 54 m height. The range of depth of tunnel found in the Delhi Metro Phase 3 project is 12–30 m. Depth 18m was chosen for simplification of modeling. The excavated diameter of the tunnel is kept 6.35 m. In order to avoid the boundary effect in numerical analysis, the outer boundary was placed at a distance of 3 diameters away from the center of the tunnel. The thickness of the concrete lining used for the modelling was kept 25 cm. Tunnel length of 54m ($1/1000^{th}$ of actual length) and radius of 3.175m have been considered.

3.1.3 Stages of Analysis

The analysis was performed in below mentioned stages to simulate the real field conditions as follows:

Stage 1: A Greenfield condition having soil modelled similarly to field conditions. The analysis performed in this stage, known as initial stress analysis.

Stage 2: A second stage where the tunnel is excavated. The tunnel perimeter is here fully supported.

Stage 3: The lining was inserted in the third stage, and all supports around the tunnel perimeter were removed and were replaced by a plate to model the lining. The elastoplastic analysis was then carried out.

For the validation of the present numerical analysis, the surface settlement has been calculated through established empirical formulas and compared with the numerical results of OptumG2 in literature and of PLAXIS 3D in this research. A closed-form solution had been proposed by Peck and Schmidt (1969) to calculate the surface settlement in soil due to an underground opening.

$$S_v = \frac{V_s}{\sqrt{2\pi}KZ_0} e^{-\frac{y^2}{2K^2{Z_0}^2}} \quad (3.11)$$

Where Vs is the volume of the settlement trough per meter of tunnel advance (m^3/m), defined as a percentage volume loss of the unit volume V of the tunnel, and was taken as 0.35% for low plastic silty soil, K is trough width parameter and was taken as 0.5 for ML soil, y is the lateral distance from the tunnel centerline (m), and Z_0 is the depth of the neutral axis from the

surface. Vertical settlement profile of ground from the center of model (point above crown) to the lateral boundary was plotted using the above two formula and numerical results obtained from Optum G2 and PLAXIS 3D. The variation or deviation percentage between numerical analysis and peck formula was considered approximately 13% in literature whereas in our computation after numerical analysis, the deviations are approximately 15%. This comparison of settlement values of Peck's empirical formula, OptumG2 and PLAXIS 3D numerical analyses for MC model type are shown in Table 3.7 and Figure 3.14. In Figure 3.15, Figure 3.16, and Figure 3.17, the meshing condition in Optum G2, the meshing condition in PLAXIS 3D and distribution of vertical surface settlement in PLAXIS 3D are shown.

It can be seen from the validation result of PLAXIS 3D, Optum G2 and Peck formula, the difference percentage between Optum G2 and Peck's formula is 12.69% whereas the difference percentage between PLAXIS 3D and Peck's formula is 14.93% and the difference percentage between PLAXIS 3D and Optum G2 is 4.81%.

Table 3.7: Calculation of Vertical Surface Settlement based on Peck & Schmidt Formula and Comparison with Numerical Analysis Data

Model Type	**Tunnel Depth, Z_0**	**Radius, R**	**Vertical Surface Settlement (from Peck formula)**	**Vertical Surface Settlement (from Optum G2)**	**Vertical Surface Settlement (from PLAXIS)**	**Difference between Optum G2 and Empirical Formula**	**Difference between PLAXIS and Empirical Formula**	**Difference between PLAXIS and Optum G2**
	(m)	(m)	(mm)	(mm)	(mm)	(%)	(%)	(%)
MC	18	3.175	34.10	29.70	31.20	12.69	14.93	4.81

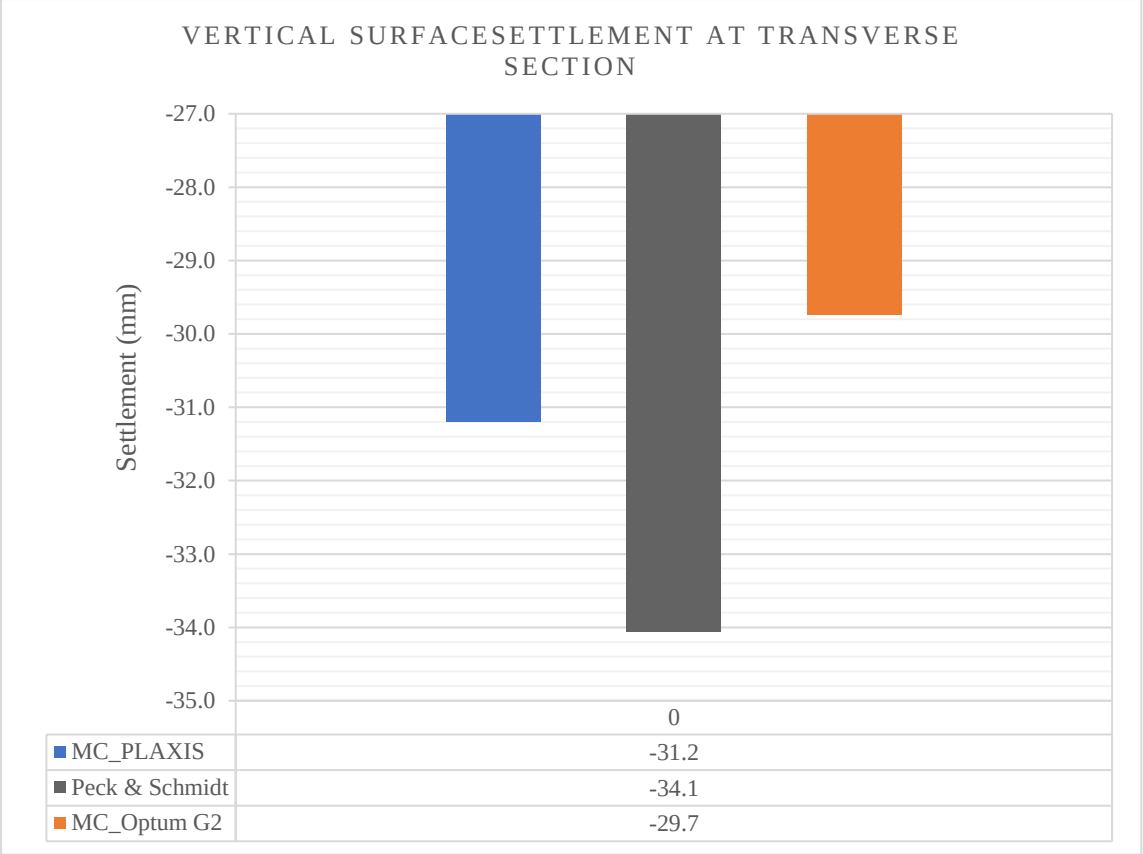

Figure 3.14: Comparison of Vertical Surface Settlement between PLAXIS 3D, Optum G2 and Peck & Schmidt Formula

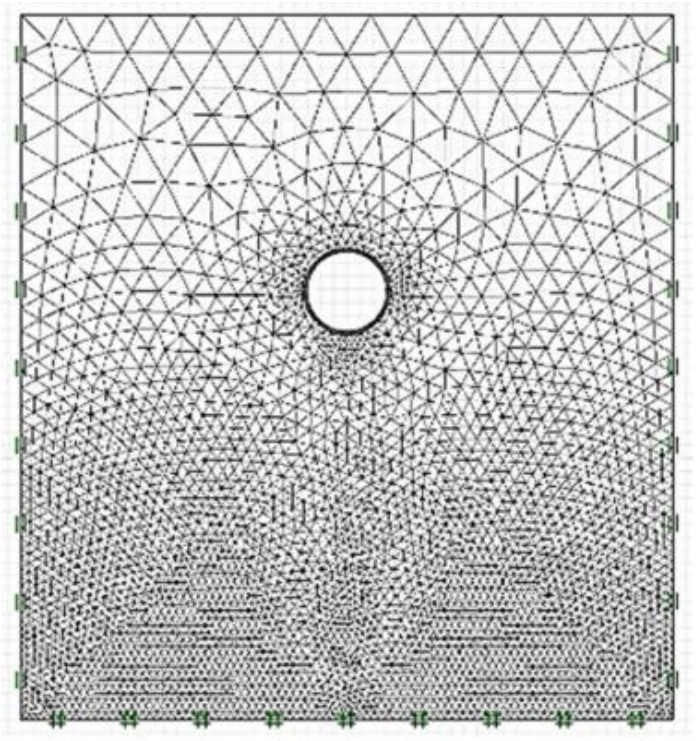

Figure 3.15: Meshing Condition in Optum G2

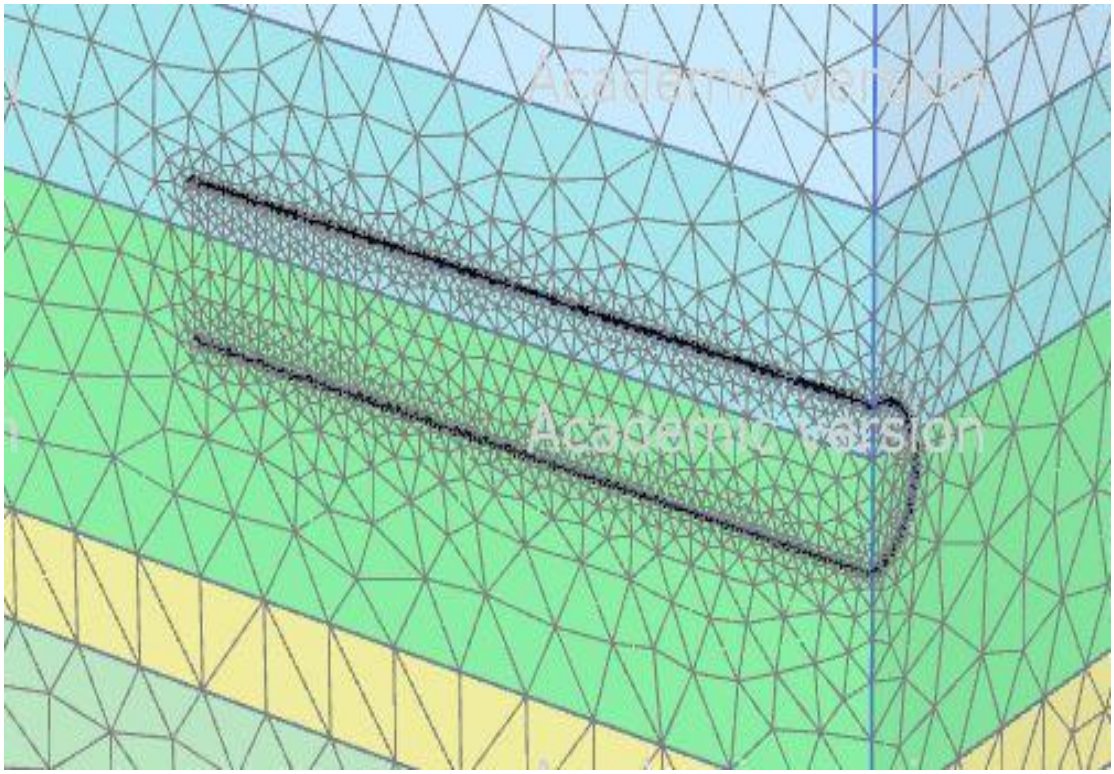

Figure 3.16: Meshing Condition in PLAXIS 3D

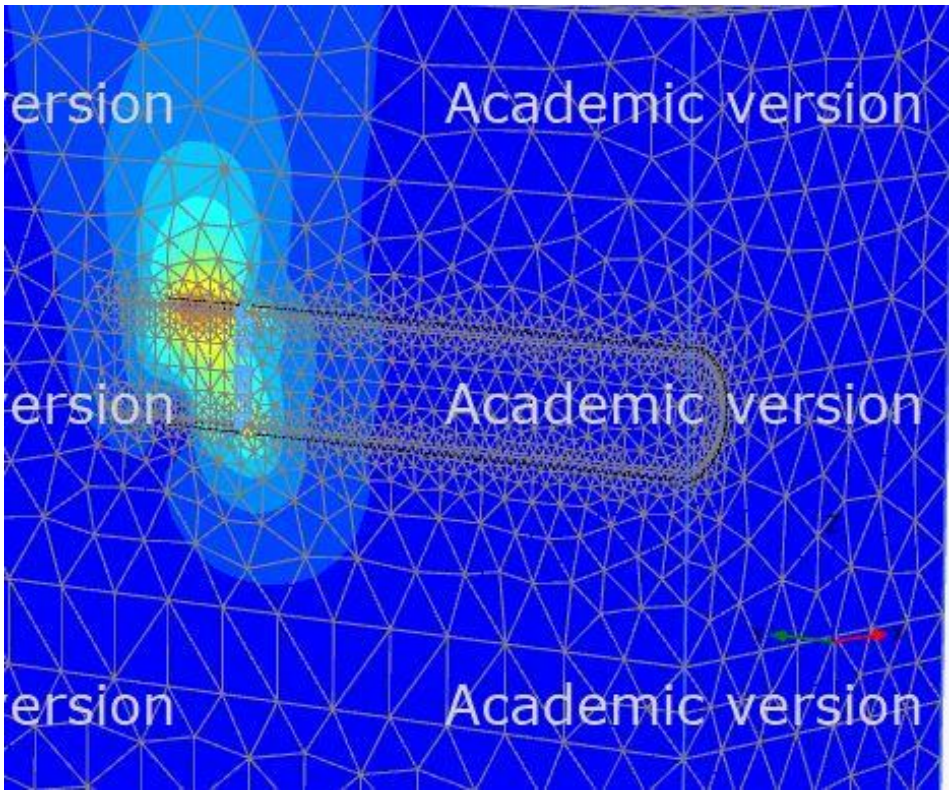

Figure 3.17: Distribution of Vertical Surface Settlement in PLAXIS 3D

3.4 Summary

i. The detailed geotechnical investigation report of Mashhad Metro Line 2 has been implied in PLAXIS 3D to validate the researcher's result with the numerical result. The researchers used FLAC 3D for numerical analysis and compared the result with empirical relations.

ii. From the empirical relations suggested by the researchers, it can be seen that O'Reily and New relations show better error value than others. Also, in our numerical analyses with PLAXIS 3D, the error values for this relationship are 1.66% and 4.81% for MC and MCC models respectively which are comparatively less than other relationships.

iii. Comparing the FLAC 3D result and Peck formula for maximum settlement, 9.6% and 41% error were found for MC and MCC models respectively, whereas comparing PLAXIS 3D and Peck formula for maximum settlement, 11.11% and 44.4% were found for MC and MCC models respectively which is approximately close to the literature.

iv. From the comparative analysis of Mashhad Metro Line 2, it can be seen that O' Reily & New empirical relation shows closest values (3.91%, 1.66% and 4.81% deviation with FLAC 3D, MC model in PLAXIS 3D and MCC model in PLAXIS 3D respectively).

v. The detailed geotechnical investigation report of Delhi Metro Phase 3 has been implied in PLAXIS 3D to validate the researcher's result with the numerical result. The researchers used Optum G2 for numerical analysis and compared the result with empirical relations.

vi. The variation percentage between numerical analysis of Optum G2 and Peck's formula was approximately 13% whereas in PLAXIS 3D and Peck's formula was approximately 15% which is approximately close.

vii. It can be seen from the validation result of PLAXIS 3D, Optum G2 and Peck formula, the difference percentage between Optum G2 and Peck's formula is 12.69% whereas the difference percentage between PLAXIS 3D and Peck's formula is 14.93% and the difference percentage between PLAXIS 3D and Optum G2 is 4.81%.

Chapter 4

NUMERICAL MODELING AND ANALYSIS

3.2 Introduction

In this chapter, the outline of proposed MRT line 1 project, the detailed route of underground part, and geology and soil condition of the selected study area are described with appropriate maps. The field study investigation including physical and laboratory tests of soil samples are done in accordance with the ASTM standards which are also discussed and a longitudinal soil profile for the study area is created with the help of the field study data. The different test results of the field study investigation are mentioned in this chapter and in Appendix which are collected from secondary sources. FEM analysis (numerical modelling) is done by PLAXIS 3D for both NATM and TBM methods for different types of models (MC, MCC and HS) are described in details in this chapter.

3.3 Context of Underground Part of Dhaka Mass Rapid Transit Line 1

The length of the MRT line 1 will be 28.2 km with 19 stations and one depot in Purbachal area. As per the plan, the MRT line 1 consists of two lines, one being the route that connects Kamalapur with the Hazrat Shahajalal International Airport (hereafter the "Airport Line"). The line will be runs through underground tunnel, starts at the Kamlapur station of Bangladesh National Rail (BR), travels westward under the Outer Circular Road, northward under the Rampura DIT Road and Pragati Sharani Road, crosses the Kuril flyover, and proceeds under the New Airport Road to its destination at Dhaka International Airport. Out of total 28.2 km, the airport line will be 14.8 km underground line comprising total 12 underground stations. Construction of the underground running section shall be done by Tunnel Boring Machine (TBM) and stations will be constructed either by Cut and Cover method. The outer diameter of the tunnel is 7m and standard length of station is 250m. The metro tunnels will range from 20m to 50m below the ground in different locations with average depth of 35 meter (NKDOS Consortium Proposal, 2019). The Figure 4.1 represents the alignment map of MRT Line 1 where green line, red line, green labels and red labels are represented as underground section, elevated section, underground stations, and elevated stations respectively. The Table 4.1 specifies the underground stations' names, station types and tier type or connectivity locations with other stations.

Table 4.1: List of Underground Stations in MRT Line 1

SL. No.	Underground Stations	Station Type	Special Consideration
1	Kamlapur	Standard	
2	Rajarbagh	Narrow/Deep	Two-tier Station
3	Malibagh	Narrow/Deep	Two-tier Station
4	Rampura	Standard	
5	Hatirjheel East	Standard	Connectivity with Line 5 South Station
6	Badda	Standard	
7	North Badda	Standard	
8	Natun Bazar	Wide Station	Connectivity with Line 5 North Station and proper protection for existing DWASA pipe line
9	Nadda	Double/Deep	Two-tier Station
10	Khilkhet	Standard	
11	Airport Terminal - 3	Standard	Connectivity with New Airport Terminal 3
12	Airport	Standard	Connectivity with BR Station and Extension Line 1

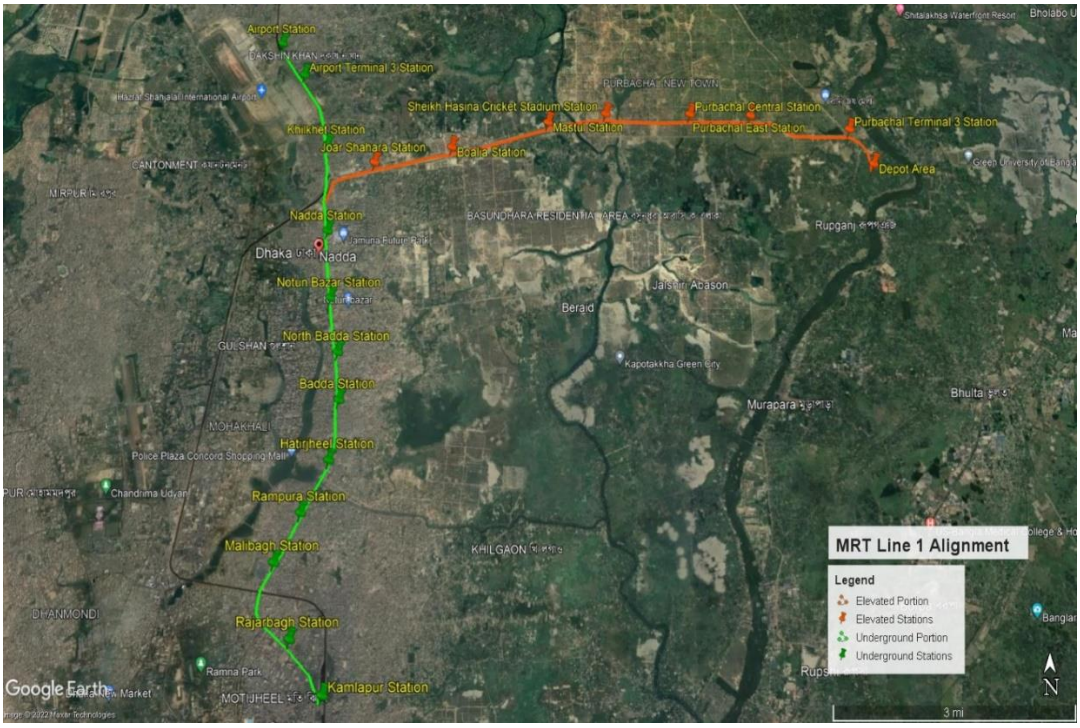

Figure 4.1: Map showing the MRT Line 1 Alignment with Stations Location (NKDOS Consortium Proposal, 2019)

3.3.1 Geology and Soils

Dhaka lies in the extreme south of the Madhupur Tract, which is situated in the central-eastern part of Bangladesh. The planning area is covered mainly by the Pleistocene Madhupur Clay, a yellowish brown to the highly oxidized reddish brown silty clay; and by Holocene sediments to the south, west and east made up of alluvial silt and clay and marshy clay and peat. The moisture content and liquid limit results obtained for the Madhupur clay show that it is normally consolidated to slightly over-consolidated, perhaps due to groundwater pumping. The clay has intermediate to high plasticity, and is overlain by the Dupi Tila formation of medium to coarse sand. The incised channels and depressions within the city are floored by recent alluvial flood plain deposits. The project location in geology of Bangladesh map is shown in the Figure 4.2.

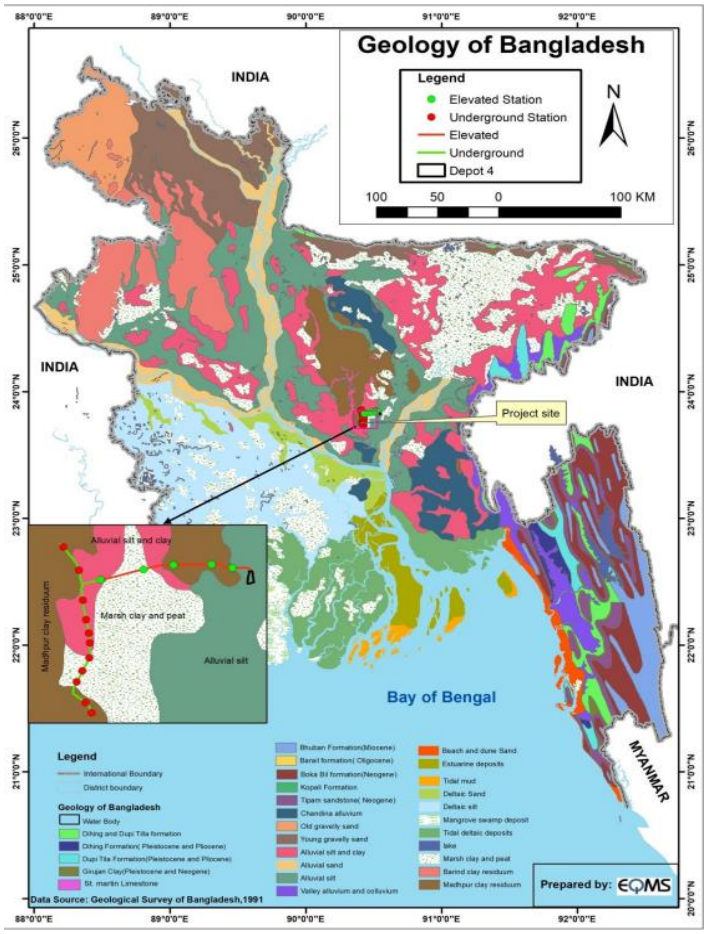

Figure 4.2: MRT Line 1 Location in Geology of Bangladesh Map (NKDOS Consortium Proposal, 2019)

According to the soil maps of Bangladesh (Figure 4.3), the project site falls under the shallow red-brown terrace soil and deep red-brown terrace soil. The shallow red-brown soils are

imperfectly to moderately well drained. The topsoil of deep red-brown terrace soils usually is 8-10 cm thick and has a brown to yellow brown color, loam to clay loam texture and rusty stains along root channels. The subsoil usually is 60-120 cm thick.

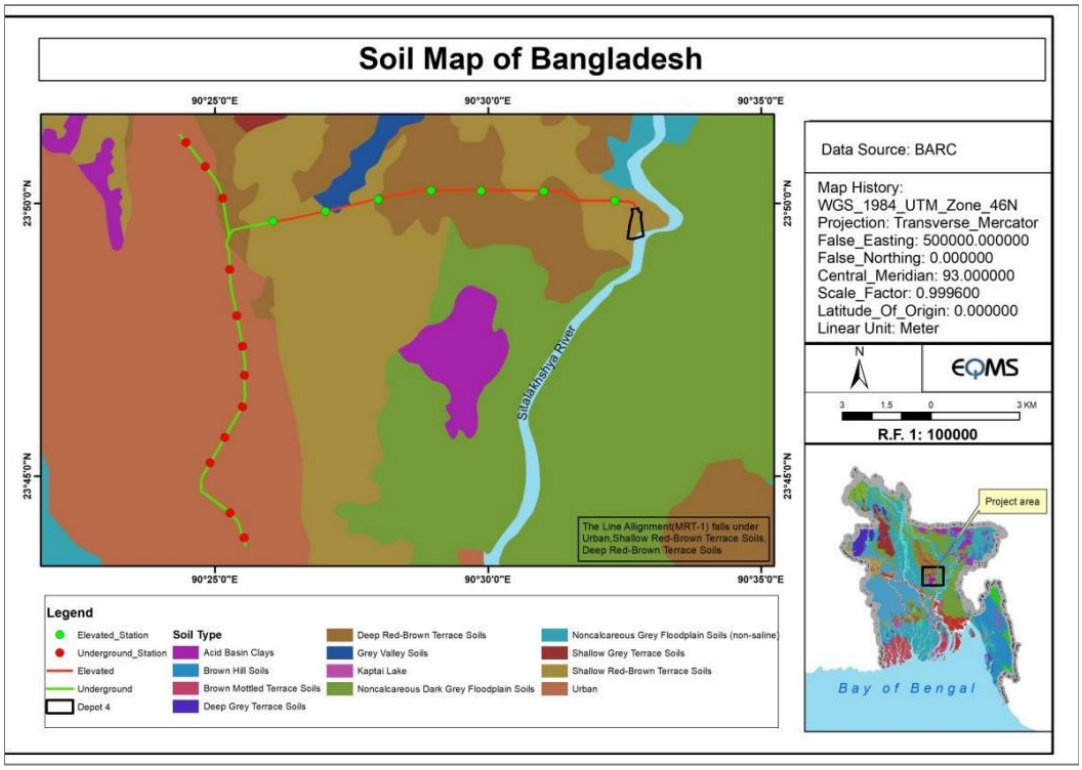

Figure 4.3: MRT Line 1 Location of Soils of Bangladesh Map (NKDOS Consortium Proposal, 2019)

Dhaka city falls in seismic zone II of the seismic zoning map of Bangladesh which means the city is at moderate risk (basic seismic coefficient is 0.5 g). Neotectonic movement in and around the city has been reported widely. The Madhupur Tract as a whole is a structural high in which the Dhaka-Tongi block is the most uplifted part. The boundaries of the tract to the west, south and east are characterized by step faulting. The high land area which varies up to 100ft shows low relief. The high lands are composed of Pleistocene Madhupur Clay and Sand formation where the low lands are recent floodplain deposits. The studied area is mostly consisted of clayey soil than the sandy soils. There are some sandy soils interbedded between these clay layers. The upper part comprises grayish to brownish stiff to medium stiff clayey soil and brownish medium dense soil of Basabo silty clay formation and lower brownish very dense sand and hard clayey soil below it can be of from Madhupur clay and sand formation. The degree of concentration and thickness of clayey soil is also influenced by the neo-tectonics of this region, which causes undulation of ground surface. The surface elevation of the area Dhaka are ranges between 1 and 14m and most of the built-up areas located at the elevations

of 6-8m (Follow Figure 4.4). The drainage system will be hampered due to construction activities like as infilling, construction of the depot, construction yards and haul routes. A major impact during construction stage is due to suspended solids entrained in runoff that can bring soil surfaces and clog drainage system. Underground tunnel construction may impact on ground water quality and depth of the underground water level. Potential impacts on groundwater are insignificant. In Dhaka City, Ground Water extraction started from a depth of 100m and in some extreme condition the well goes up to 300 meters to reach the main aquifer.

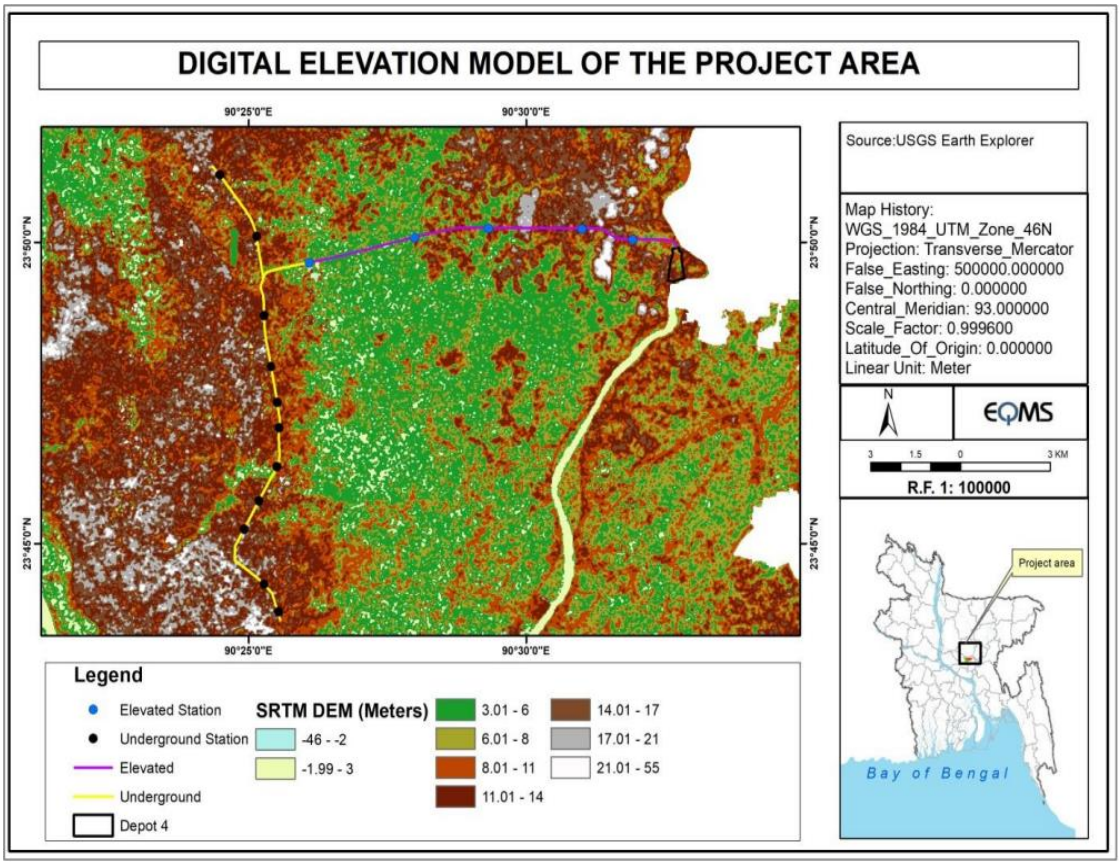

Figure 4.4: Elevation Map of the Project Area (NKDOS Consortium Proposal, 2019)

3.3.2 Field Investigation of the Study Area

The objectives of the geotechnical survey are to obtain physical and mechanical properties of soil and soil design parameters through field and laboratory tests. In field, in-situ tests, such as standard penetration tests and pressure meter tests were conducted and index and mechanical properties tests such as compression, consolidation tests etc. were conducted in the laboratory. The investigation program was consisted of soil boring and sampling at desired intervals for subsequent observation and laboratory testing (ProSoil Geotechnical Survey, 2019). The soil

report and physical and mechanical properties of soil are collected from secondary data sources.

The selected borehole's location (BH-24) is marked in the route map in Figure 4.5 and Table 4.2. The portion of longitudinal soil profile (geotechnical) of the Airport route and soil stratification of BH-24 is presented in Figure 4.6. The physical description of soil strata with SPT values and depth range are mentioned in Table 4.3.

Figure 4.5: Location of Selected Borehole (BH-24) for Investigation (NKDOS Consortium Proposal, 2019)

Table 4.2: Identification of Borehole 24

Borehole No.	24
Location	Under Kuril Flyover (In front of Walton Showroom)
Coordinates	23.82075N, 90.42077E
RL	+8.313m

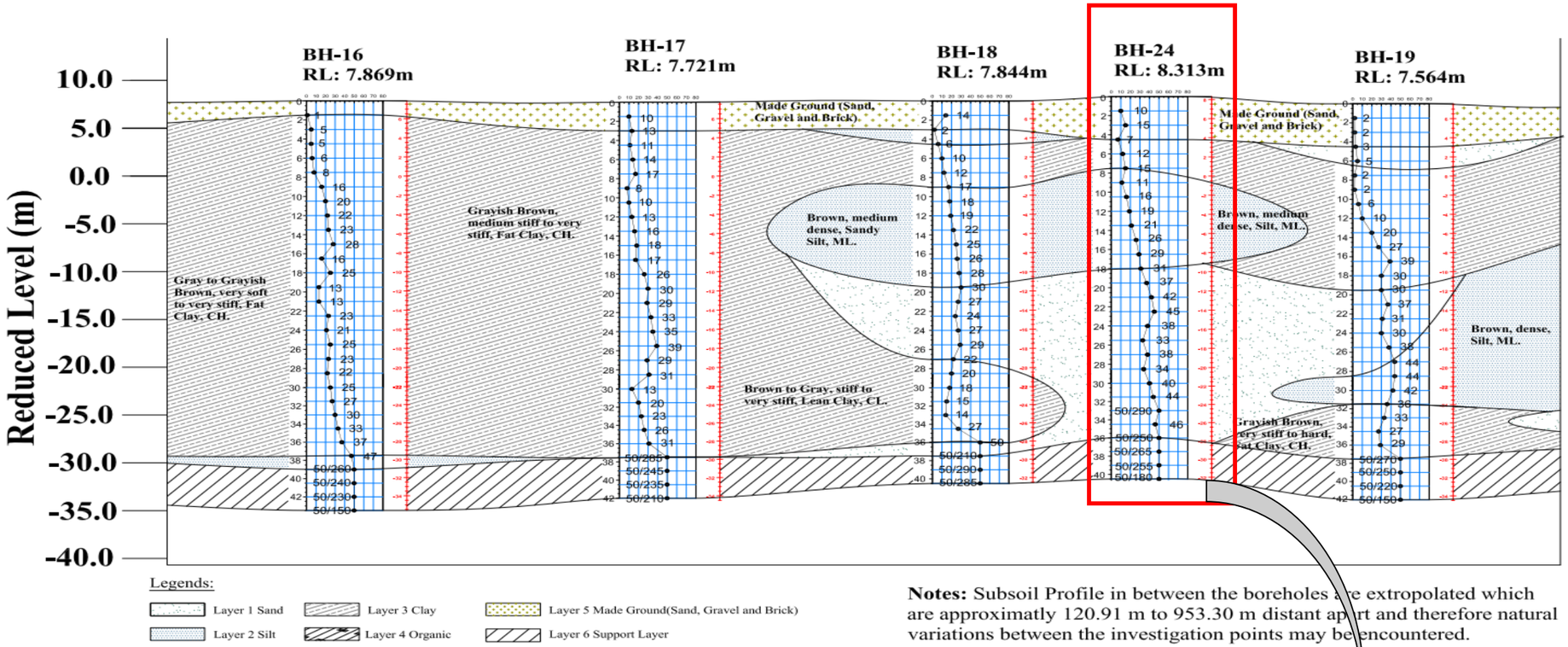

Notes: Subsoil Profile in between the boreholes are extropolated which are approximatly 120.91 m to 953.30 m distant apart and therefore natural variations between the investigation points may be encountered.

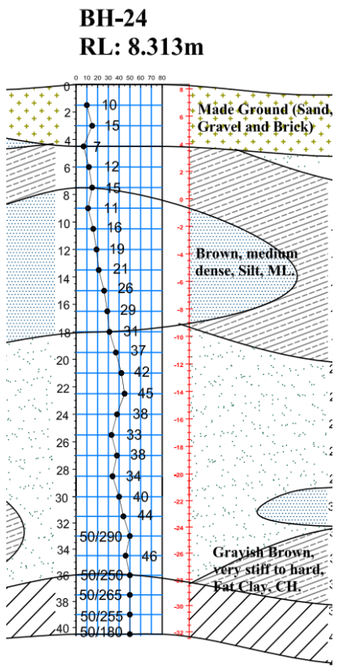

Figure 4.6: Subsoil Stratification of BH-24

Table 4.3: Description of Soil Layers from SPT Test Result (BH-24)

SL. No.	Soil Layer Notation	Description	Soil Consistency and Relative Density	Soil Color	Depth Range (m)	SPT Range
1	SF	Made Ground		Gray, Gray to Reddish Gray, Reddish Gray	0 – 4.5	10-15
2	AC3	Lean Clay	Medium Stiff	Gray, Reddish Gray, Gray to Yellowish Gray, Brown	4.5 – 5.0	7
3	AC4	Fat Clay	Stiff	Brown, Gray, Gray to Yellowish Gray, Grayish Brown to Gray, Gray to Brown, Grayish Brown	5.0-6.0	12
4	AC4	Lean Clay	Stiff	Brown, Gray, Gray to Yellowish Gray, Grayish Brown to Gray, Gray to Brown, Grayish Brown	6.0-7.5	15
5	AS3	Sandy Silt	Medium Dense	Gray, Yellowish Gray, Yellowish Gray to Brown, Brown	7.5 – 9.0	11
6	AS3	Silt		Gray, Yellowish Gray, Yellowish Gray to Brown, Brown	9.0-12.0	16
7	AC5	Lean Clay	Very Stiff	Yellowish Gray, Yellowish Gray to Reddish Brown, Brown to Gray, Gray, Gray to Reddish Gray, Reddish Brown, Brown, Dark Gray, Reddish Gray, Gray to Yellowish Gray, Red, Grayish Brown, Black, Gray to Brown, Brown to Brownish Gray, Brownish Gray to Brown	12.0 – 13.5	19 – 21
8	AS3	Silt		Gray, Yellowish Gray, Yellowish Gray to Brown, Brown	13.5 – 16.5	21-29
9	AS3	Sandy Silt	Medium Dense	Gray, Yellowish Gray, Yellowish Gray to Brown, Brown	16.5 – 18	31

SL. No.	Soil Layer Notation	Description	Soil Consistency and Relative Density	Soil Color	Depth Range (m)	SPT Range
10	AS4	Silty Sand	Dense	Gray, Yellowish Gray, Brown, Gray to Brown, Brown to Grayish Brown, Yellowish Gray to Brown, Gray, Reddish Gray, Brownish Gray to Gray	18 – 21	37
11	AS4	Sandy Silt	Dense	Gray, Yellowish Gray, Brown, Gray to Brown, Brown to Grayish Brown, Yellowish Gray to Brown, Gray, Reddish Gray, Brownish Gray to Gray	21 – 22.5	42 – 45
12	AS5	Silty Sand	Very Dense	Gray, Brown, Gray to Brown, Yellowish Brown, Yellowish Gray, Reddish Gray, Brown to Grayish Brown, Red, Grayish Brown to Brown, Brownish Gray to Gray	22.5 – 41	38 – 50

Unconfined compression test results, UU triaxial test results for determining undrained shear strength, secant modulus, angle of friction, and cohesion are included in this chapter and summary test result sheet collected from secondary source is mentioned in Appendix A. As the soil was found unsaturated, the angle of friction was found deviated from zero.

Loading Rate (mm/min)	Unconfined Compressive Strength qu (kPa)	Undrained Shear Strength Cu (kPa)	% Strain at qu max	Secant Modulus E_{50} (kPa)
2	106.00	53.00	15.00	3.53

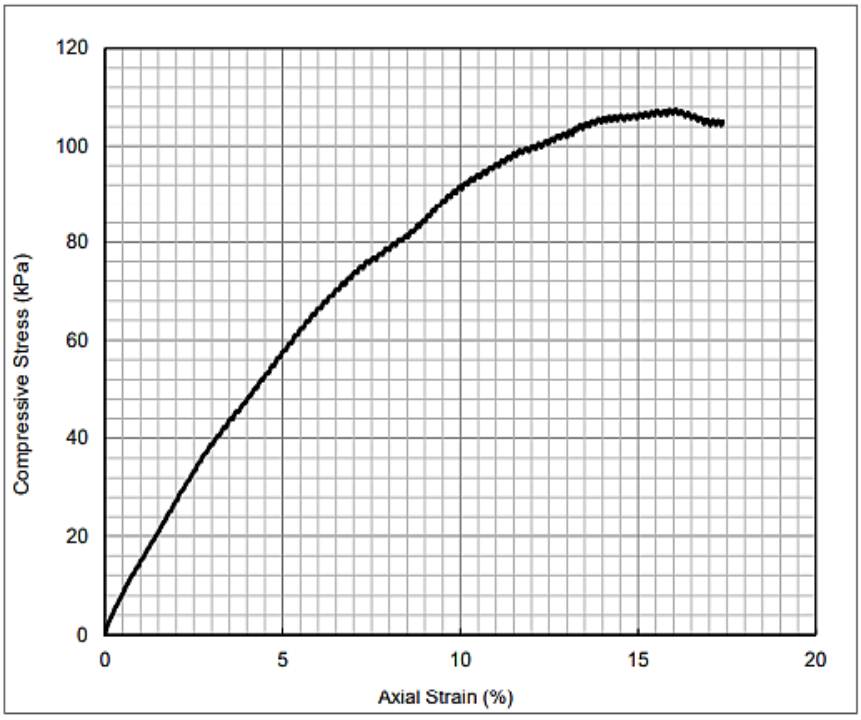

ASTM D-2166

Figure 4.7: Unconfined Compression Test Result (Depth 5.0-6.0m) – Soil Type: Fat Clay

Shear Strength Properties	
Angle of Friction , Φ	Cohesion, C (kPa)
5.1	48.0

Specimen ID	Initial Moisture Content (%)	Final Moisture Content (%)	Avg Initial Diameter (mm)	Avg Initial Height (mm)	Initial Bulk Density (gm/cm³)	Initial Dry Density (gm/cm³)	Deviator Stress (KPa)	Minor Principal Stress (δ_3') (kPa)	Major Principal Stress (δ_1') (kPa)
A	26.00	25.09	37.13	76.27	1.67	1.33	115	50	165
B	25.26	24.46	37.77	76.73	1.83	1.46	126	100	226

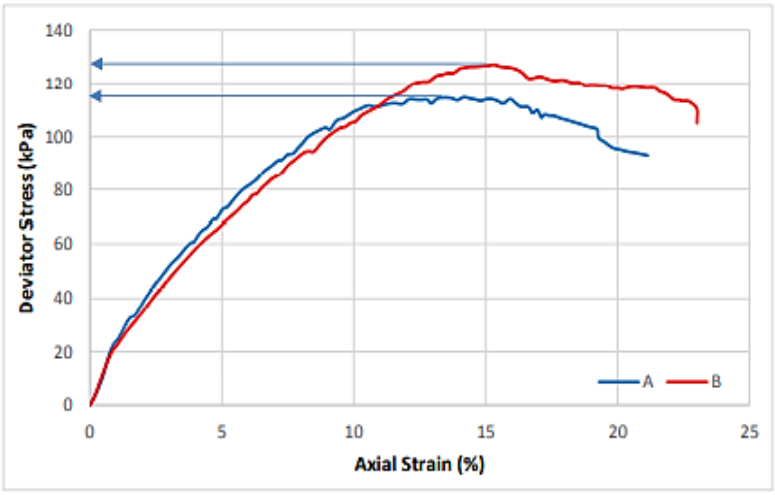

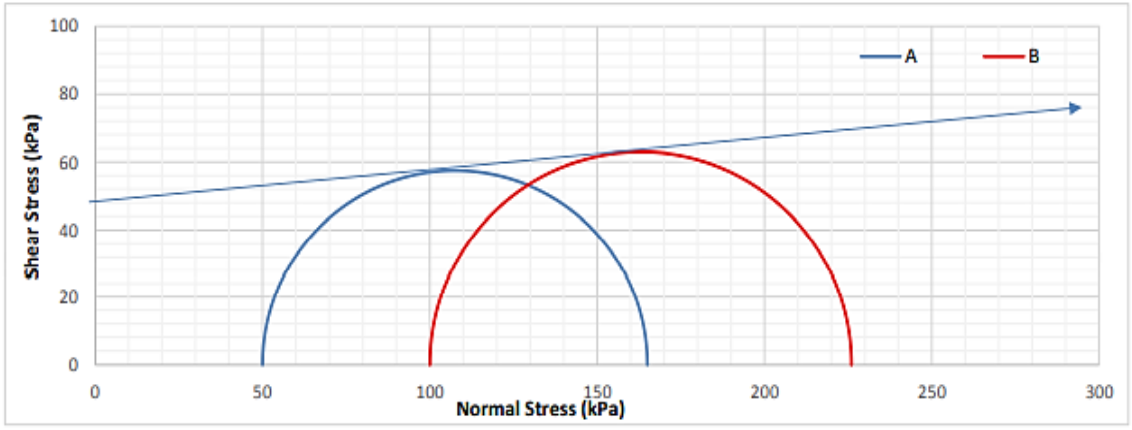

ASTM: D 2850-95

Figure 4.8: UU Triaxial Test Result (Depth 5.0-6.0m)

3.4 Numerical Modeling

To evaluate the settlement or displacement of tunnel under static condition, the numerical modelling in PLAXIS 3D can simulate the significant results which is difficult to conduct in laboratory or field or empirical conditions. In this investigation, the study area is filled with clayey type soil and sandy silt type soil in between. Therefore, there is a minimal chance of having liquefaction effect in seismic condition in this area. The FEM model is calibrated with the field and laboratory tests data. The result of TBM and NATM tunnels are shown using MC, MCC and HS soil models. The effect of varying tunnel depths and diameters is shown for TBM methods. At the end a comparison is made between NATM and TBM method in respect to settlement for three different models. Assumptions used in the estimations are as follows:

i. Cross-section of the tunnel is almost circular.

ii. Undulation in existing ground level is ignored.

iii. Tunnel is considered to move along a straight line.

iv. Tunnel is deep enough (35m from EGL) for avoiding the effect of adjacent structures and foundations.

v. Tunnel passes through clayey soil formation.

vi. Tunneling method is both NATM and TBM.

vii. Estimations are valid for completed primary support

viii. Long term consolidation settlement is ignored.

ix. Static and Dynamic loading effects are ignored.

3D model is chosen because for 2D FE models, it is not so easy to estimate pre-relaxation factors (sometimes called stress reduction factors), which is fraction of load effecting on tunnels, and purely based on practical experience. With the 3D model, estimation of pre-relaxation factor is no longer required when excavation stages can be modelled not only in cross-section but also in the longitudinal section, e.g., excavation of the bench and invert can be modelled in the actual distance behind the excavation of the top heading.

Limitations:

i. Existing ground surface abruption and ground water level effect (flow water condition) is not considered.

ii. Due to considering one borehole data, the soil properties and division of layers are kept equal all along the assumed length.

iii. Diameter (7m) is considered according to the feasibility report of MRT line 1 Project. Though for TBM analysis, variations in diameter (up to 5m) have been considered.

3.5 FEM Model in PLAXIS 3D (TBM Method)

The lining of a shield tunnel is often constructed using prefabricated concrete ring segments, which are bolted together within the TBM to form the tunnel lining. During the erection of the tunnel lining the TBM remains stationary. Once a tunnel lining ring has been fully erected, excavation is resumed, until enough soil has been excavated to erect the next lining ring. As a result, the construction process can be divided into construction stages with a length of a tunnel ring, often about 1.5m long. In each of these stages, the same steps are repeated over and over again. In order to model this, a geometry consisting of slices each 1.5m long was used. The calculation consists of a number of plastic phases, each of which models the same parts of the excavation process; the support pressure at the tunnel face needed to prevent active failure at the face, the excavation of soil and pore water within the TBM, the installation of the tunnel lining and the grouting of the gap between the soil and the newly installed lining. This tunnel advancement process is illustrated in Figure 4.9. In each phase the input for the calculation phase is identical, except for its location, which will be shifted by 1.5m each phase.

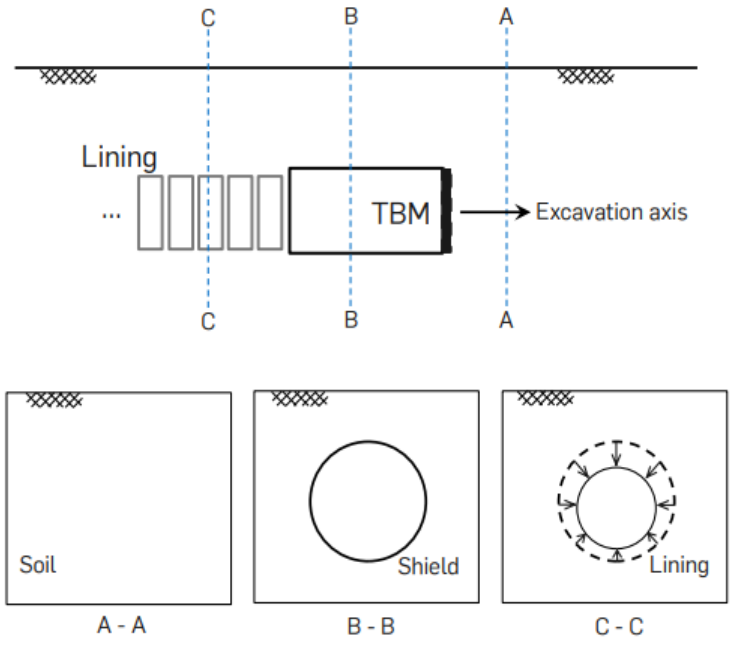

Figure 4.9: Schematic illustration of tunneling simulation process (Bentley, 2018)

3.5.1 Geometry

In the model, only one symmetric half is included. The model is 25m wide, it extends 60m in the y-direction and it is 41m deep. These dimensions are sufficient to allow for any possible collapse mechanism to develop and to avoid any influence from the model boundaries. The subsoil consists of 11 layers. The soil layers with depth and soil conditions with parameters for all models are given below. The tunnel excavation is carried out by a tunnel boring machine (TBM) which is 10m long and 7m diameter with 0.25m concrete lining. The TBM was considered to be advanced 25m into soil. Subsequent phases will model an advancement by 1.5m each. The locations of tunnels considered in simulation are 30m, 32m, and 35m depth from ground surface (Figure 4.10).

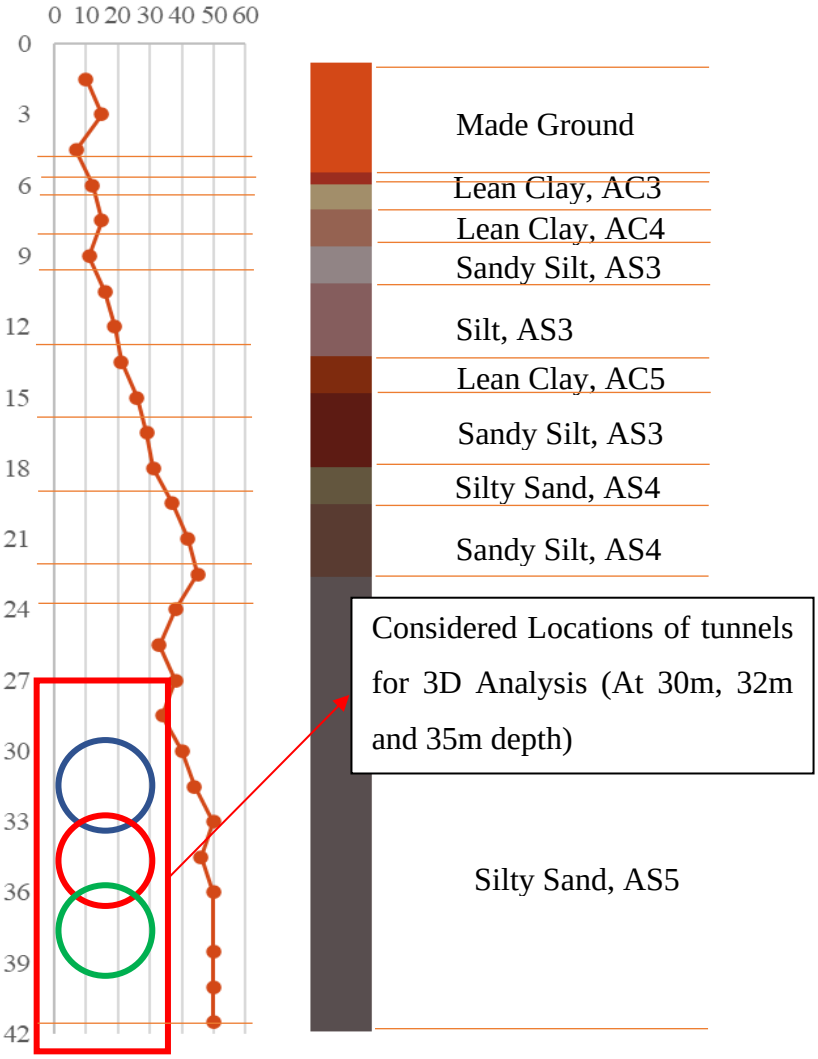

Figure 4.10: Locations of TBM machines in Soil (NKDOS Consortium Proposal, 2019)

3.5.2 Definition of Structural Elements

A soil structure interaction has to be added on the outside of the tunnel due to the slight cone shape of the TBM. Typically, the cross-sectional area at the tail of the TBM is about 0.5% smaller than the front of the TBM. The reduction of the diameter is realized over the first 7.5m length of the diameter while the last 1.5m to the tail has the constant diameter. So, in modeling, uniform and incremental contraction has been considered according to the advancement of the TBM. The surface load representing the grout pressure is constant during the building process. In the specifications of the tunnel boring process, it is given that the grout pressure should be -100kN/m^2 at the top of the tunnel and should increase with -20kN/m^2/length. The tunnel face pressure is a bentonite pressure (Bentonite slurry) or an earth pressure (Earth Pressure balance) that increases linearly with depth.

For the initial position of the TBM and the successive four positions when simulating the advancement of the TBM, a tunnel face pressure was defined. In order to simplify the definition of the phases in Staged construction mode, the sequencing of the tunnel was defined. The soil in front of the TBM will be excavated, a support pressure will be applied to the tunnel face, the TBM shield will be activated, and the conicity of the shield will be modelled, at the back of the TBM the pressure due to the backfill grouting will be modelled as well as the forces of the hydraulic jacks driving the TBM exert on the already installed lining, and a new lining ring will be installed. In the mesh mode, medium mesh was used to generate. Since water levels will remain constant the flow conditions mode was skipped. The excavation of the soil and the construction of the tunnel lining was modelled in the staged construction mode. The first phase differs from the following phases, as in this phase the tunnel is activated for the first time. In the Table 4.4, parameters are defined for HS, MC and MCC model types for TBM construction method. The soil parameters depicted are:

i. Dry and Wet Density, Initial Void Ratio, Cohesion (c_{ref}), Internal Friction (ϕ)
ii. Secant Modulus at 50% strength (E_{50}^{ref}), Modulus for Oedometer conditions (E_{oed}^{ref}), Unload-Reload Modulus (E_{ur}^{ref})
iii. Cam Clay isotropic compression index (λ), Cam Clay isotropic swelling index (κ), Tangent of the critical state line (M)
iv. Young's Modulus (E'), Poisson's Ratio (υ)

3.6 FEM Model in PLAXIS 3D (NATM Method)

NATM is characterized by the fact that a tunnel is excavated in different parts (crown, bench, and invert), where subsequent parts are executed at a certain distance (lag) behind the previous part. After each excavation part the tunnel contour is secured by means of a temporary lining of sprayed concrete. A final lining can be installed later if the long-term soil conditions require such. As per the real tunnel excavation, in the modelling excavation of three parts were included. The model is basic and medium in order to restrict the computation time and memory consumption.

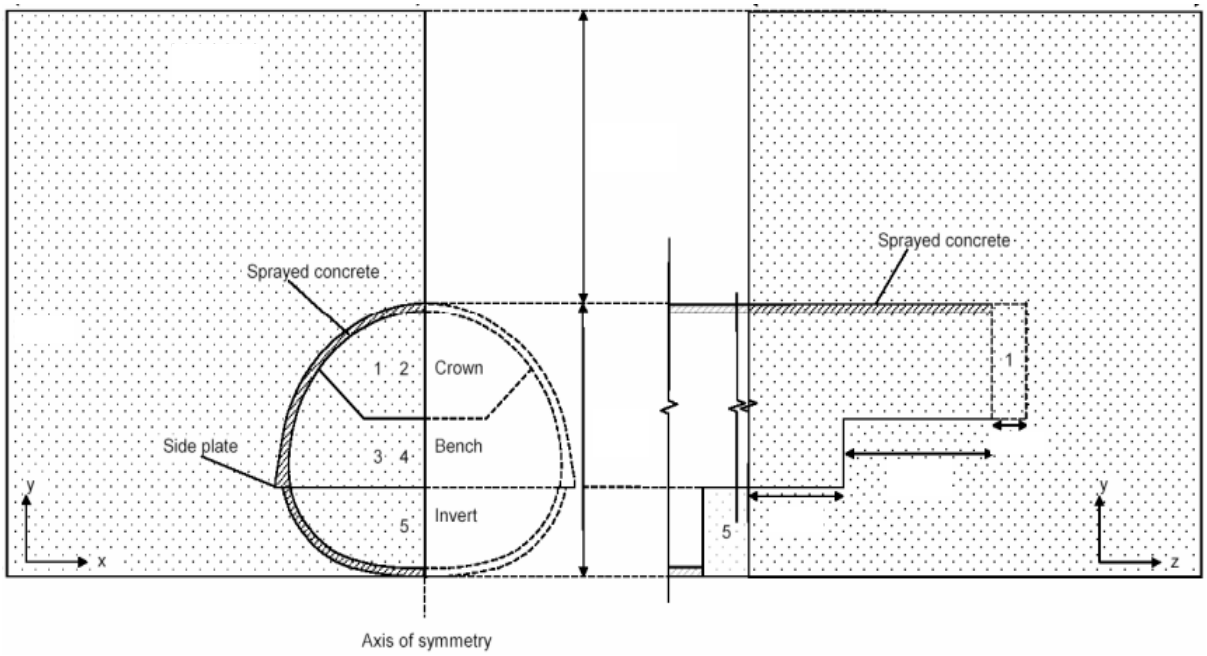

Figure 4.11: Basic NATM method assuming for Numerical Modelling (Sinha, 1989)

4.5.1 Geometry

The top of the tunnel is 35m below the ground surface considered. The full tunnel has the height of 7m and a width of 10m. The crown was excavated in a section of 1.0m length. After the excavation the surrounding soil was secured with sprayed concrete. The excavation of the bench is always some meters behind the heading. A length of 9m behind the bench excavation was included in the model to create the starting situation. The invert is much further behind and it is of almost 5m behind the benching. For reasons of symmetry, only half of the geometry is modelled, whereas symmetry conditions were adopted at the center plane. The model is extended 25m sideways (in y direction) from the center plane, 60m in x direction and -40m in z direction.

4.5.2 Definition of Structural Elements

The mesh is generated automatically (usually medium) and some refinements was applied by PLAXIS in order to get smaller mesh sizes in the tunnel vicinity where the stresses and deformations are concentrated. The mesh for the 3D model consists of the default 10-node tetrahedron elements. For plates used to simulate tunnel linings, 6-node plate elements are applied which are compatible with the 6-node face of a soil element. Moreover 12-node interface elements are used to simulate soil-structure interaction behavior. In the staged construction, the advancement of top heading, bench and invert excavations are assumed to 2m. Although this value is a little bit higher than the common practice, shorter advancements, i.e., shorter slice lengths, result in excessive run times and memory consumption. The tunnel length is taken as 19m which is suitable for displaying deformations and stresses due to surface excavation and construction along the tunnel of actual length of MRT Line-1.

The excavation process was divided in two different stages for each advance: the first stage simulates the excavation and the second stage the application of the concrete lining. It was assumed that the soil and initial ground support deforms to equilibrium after each 1 m advance before the primary sprayed lining is applied, furthermore no time effects were taken into account for the PLAXIS plastic calculations. The hosting media is assumed to be consisting of 11 layers of soil. It is assumed that no water table is encountered in the problem domain. All the analyses are performed by considering the drained condition. The tunnel is modelled with three different types of models (MC, MCC and HS), where modulus of elasticity (initial, unloading/reloading, oedometer, etc.) are chosen satisfactorily and according to the soil test results. The elasticity modulus of the soil is stress dependent and the loading history has a great influence on the soil non-linear behavior. Interfaces were applied only to the negative side of the tunnel lining, meaning only in the contact places with the soil mass, and not on the inside of the tunnel, where the soil volume is excavated. The shotcrete is modeled as a linear elastic material. The main parameter for the linear elastic materials in PLAXIS 3D tunnel is the Young's modulus. The modulus for shotcrete has been evaluated by using the empirical formula suggested by American Concrete Institute which relates the Young's modulus with the compression strength of the concrete:

$$E = 4900\sigma^{0.5} \tag{4.1}$$

Where σ is the 28-day compression strength of the concrete.

The final lining of the tunnels is actually not the main load carrying components in short term. They are designed for the long term since the shotcrete is degraded in time and it loses its load carrying capacity. The final lining is assumed to be reinforced concrete. After the K0 procedure, which is the initial phase, the phases of excavation and primary lining installation are modelled in a sequence as it would happen in site. The main idea behind the staged excavation modelling is to simulate the real construction procedure and thus take the arching effect and the effects of the sequential construction to the 3D model into account. After each of the excavation phase, a so-called nil step is used to regenerate equilibrium for the next calculation which reduces the instability of the model. Plastic calculations are executed in order to calculate the unfactored deformations and pressures to allow a fair comparison. The analyses have been made for excavation depth 35m and diameter 7m.

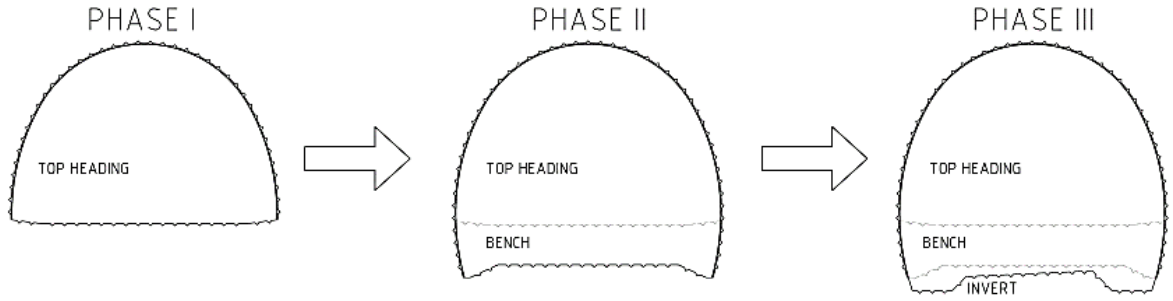

Figure 4.12: Phases of construction used for PLAXIS 3D modelling (Sinha, 1989)

The soil layers for different depths are specified along with soil condition parameters in Table 4.4. In the Table, parameters are defined for HS, MC and MCC model types for NATM and TBM construction method. The soil parameters depicted are: Dry and Wet Density, Initial Void Ratio, Cohesion (c_{ref}), Internal Friction (ϕ), Secant Modulus at 50% strength (E_{50}^{ref}), Modulus for Oedometer conditions (E_{oed}^{ref}), Unload-Reload Modulus (E_{ur}^{ref}), Cam Clay isotropic compression index (λ), Cam Clay isotropic swelling index (κ), Tangent of the critical state line (M), Young's Modulus (E'), Poisson's Ratio (υ).

In Table 4.5, the stage construction phases followed for numerical modelling in NATM and TBM construction methods are emphasized. And in Figure 4.13 and Figure 4.14, the deformation patterns in PLAXIS 3D for NATM method and TBM method (depth 35m and diameter 7m) for HS, MC and MCC models are depicted. The depth variation and diameter variation has been considered also in calculation which is not shown in this report.

Table 4.4: Soil Layers with Depth Range and Soil Condition Parameters using in NATM and TBM Methods

General Information								HS Model			MCC Model			MC Model	
SL. No.	Description	Depth Range (m)	Dry Density (kN/m^3)	Wet Density (kN/m^3)	Initial Void Ratio	c_{ref}	ϕ (deg)	E_{50}^{ref} (kN/m^2)	E_{oed}^{ref} (kN/m^2)	E_{ur}^{ref} (kN/m^2)	λ	κ	M	E’	υ
1	Lean Clay	4.5 – 5.0	17.50	21.04	0.60	48	10	$282.4*10^3$	$272.2*10^3$	$1.05*10^6$	0.40	0.10	0.90	$282.4*10^3$	0.20
2	Fat Clay	5.0-6.0	17.10	20.72	0.57	48	20	$282.4*10^3$	$222*10^3$	$1.01*10^6$	0.78	0.17	0.80	$282.4*10^3$	0.20
3	Lean Clay	6.0-7.5	17.50	21.04	0.60	48	10	$282.4*10^3$	$272.2*10^3$	$1.05*10^6$	0.41	0.10	0.90	$282.4*10^3$	0.20
4	Sandy Silt	7.5 – 9.0	18.70	21.71	0.44	30	25	$282.4*10^3$	$228.7*10^3$	$1.05*10^6$				$282.4*10^3$	0.20
5	Silt	9.0-12.0	18.67	21.76	0.45	30	27	$282.4*10^3$	$223*10^3$	$1.05*10^6$				$282.4*10^3$	0.20
6	Lean Clay	12.0 – 13.5	17.50	21.04	0.60	48	10	$282.4*10^3$	$272.2*10^3$	$1.05*10^6$	0.41	0.10	0.90	$282.4*10^3$	0.20
7	Silt	13.5 – 16.5	18.67	21.76	0.45	30	27	$282.4*10^3$	$223*10^3$	$1.05*10^6$				$282.4*10^3$	0.20
8	Sandy Silt	16.5 – 18	18.70	21.71	0.44	30	25	$282.4*10^3$	$225.7*10^3$	$1.05*10^6$				$282.4*10^3$	0.20
9	Silty Sand	18 – 21	17.85	20.22	0.32	30	30	$282.4*10^3$	$224.7*10^3$	$1.05*10^6$				$282.4*10^3$	0.20
10	Sandy Silt	21 – 22.5	18.70	21.71	0.44	30	25	$282.4*10^3$	$225.7*10^3$	$1.05*10^6$				$282.4*10^3$	0.20
11	Silty Sand	22.5 – 41	17.85	20.22	0.32	30	30	$282.4*10^3$	$224.7*10^3$	$1.059*10^6$				$282.4*10^3$	0.20
	Concrete		24		0.50				$31.11*10^6$					$28.0*10^6$	0.20

Table 4.5: Stage Construction Phases for both NATM and TBM

Method	Phase	Calculation Type	Action Taken
NATM	Initial	K0 procedure	
	Phase 1	Plastic	Crown excavation, bench excavation, invert excavation, Lining installed in the excavated portions
	Phase 2	Plastic	Crown excavation
	Phase 3	Plastic	Crown excavation
	Phase 4	Plastic	Bench excavation, lining installed in previous crown excavation
	Phase 5	Plastic	Bench excavation, lining installed in previous bench excavation
	Phase 6	Plastic	Invert excavation, lining installed in previous bench excavation
	Phase 7	Plastic	Crown excavation, lining installed in previous invert excavation
	Phase 8	Plastic	Crown excavation, lining installed in previous crown excavation
	Phase 9	Plastic	Bench excavation, lining installed in previous crown excavation
	Phase 10	Plastic	Bench excavation, lining installed in previous bench excavation
	Phase 11	Plastic	Invert excavation, lining installed in previous bench excavation
	Phase 12	Plastic	Invert excavation, lining installed in invert excavation
TBM	Initial	K0 procedure	
	Phase 1	Plastic	Excavation for TBM launching
	Phase 2	Plastic	Concrete Lining installation for the excavated portion, excavation stepping ahead, activation of negative interface, contract pressure, surface load
	Phase 3	Plastic	Excavation stepping ahead and concrete lining installation for previous excavation, activation of negative interface, contract pressure, surface load
	Phase 4	Plastic	Excavation stopped and concrete lining installation for previous excavation, activation of negative interface, contract pressure, surface load

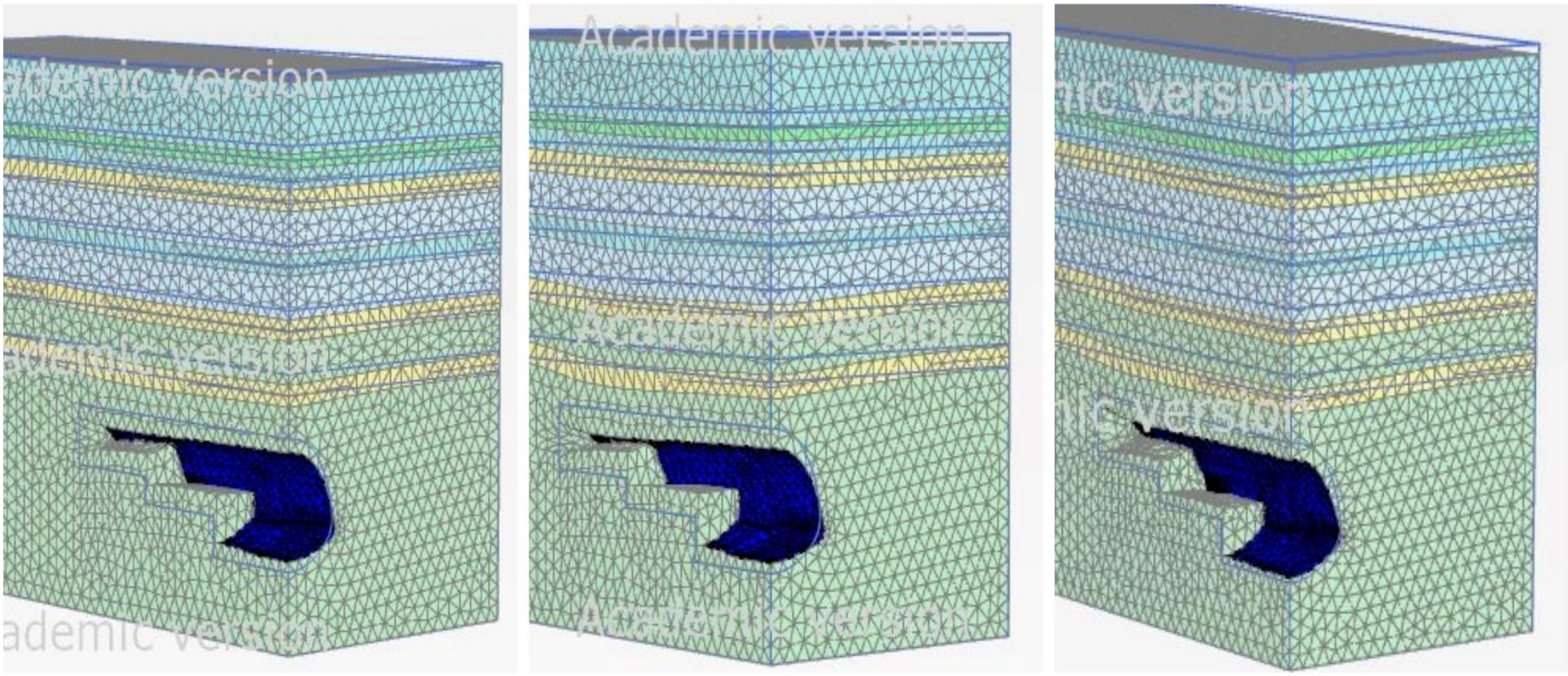

Figure 4.13: NATM Method (MC, MCC, HS model): Depth 35m and Diameter 7m

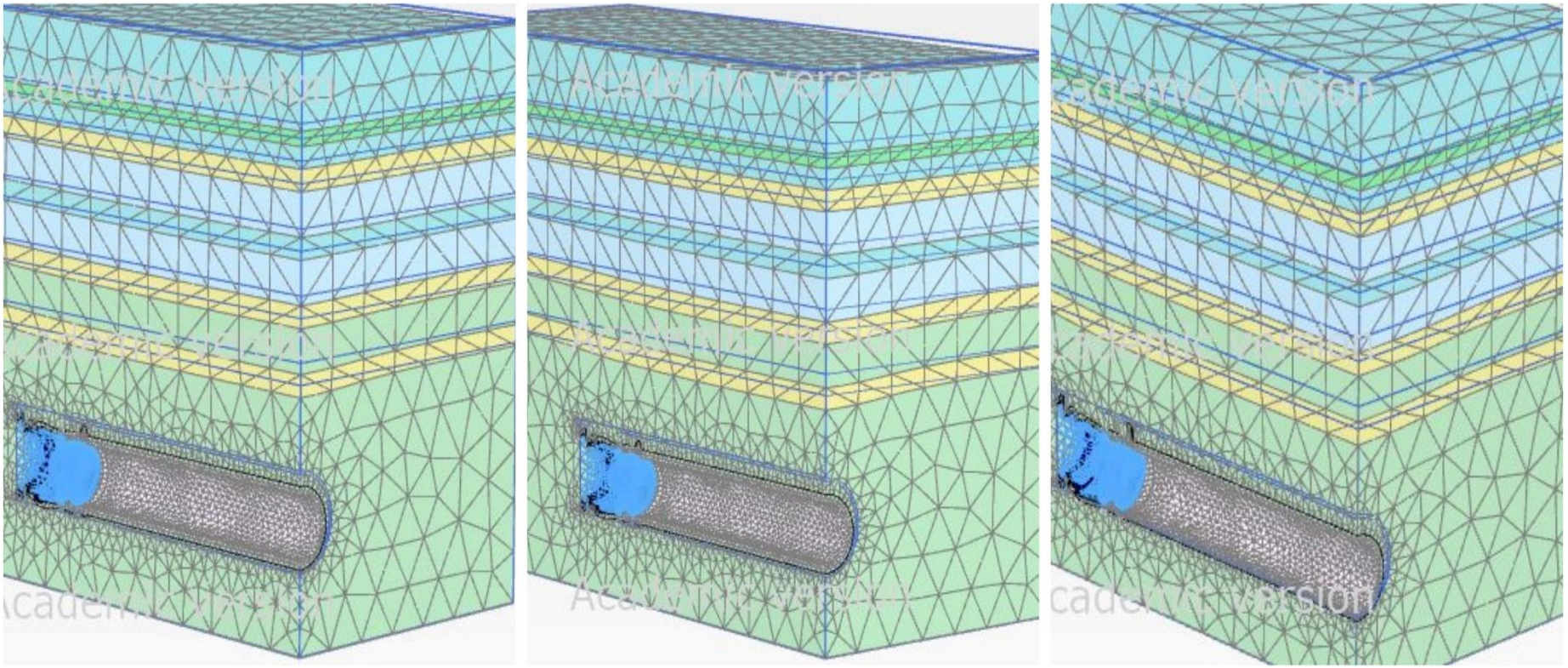

Figure 4.14: TBM Method (MC, MCC, HS model): Depth 35m and Diameter 7m

3.6 Effect of Meshing in Maximum Settlements for NATM and TBM Methods

FEA is the process of dividing geometry into smaller pieces (elements), applying loads and boundary conditions to those elements, and then solving the matrix equations assembled from the mesh. Theoretically, the more elements used in the model, the closer the results get to the actual behavior (as modeled), but it may take more computational time. It is found in Yaning Li and Tomasz Wierzbicki's research that the stress and strain fields have high gradients in the localization zone and the continuing application of the classical stress-strain relation in the localization zone is the cause for mesh size effects in Finite Element simulations. The smaller elements in a finer mesh can more accurately capture stress gradients across the element.

When the geometry model is fully defined the geometry has to be divided into the finite elements to perform finite element calculations. Very fine meshes should be avoided since this will lead to excessive calculation times. The basic soil elements of the 3D finite element mesh are the 10-node tetrahedral elements. The mesh generator in PLAXIS 3D requires a global meshing parameter that represents the target element size, l_e, which is based on the relevant element size factor (r_e). The values of this parameter for the element distributions predefined in the program are: very coarse = 2.0, coarse = 1.5, medium = 1.0, fine = 0.7, and very fine = 0.5. The exact number of elements depend on the shape of the geometry and optional local reinforcement settings. By default, the element distribution is set to Medium (1.0) but for this research, this value has been changed to coarse (1.5) and fine (0.7) also for comparing the analysis results for tunnel depth = 35.0m and diameter =7.0m for both NATM and TBM models.

From Figure 4.15 to Figure 4.20, different pattern of meshes (coarse, medium and fine) and effects in deformation for HS models of NATM and TBM construction methods are shown. Also, different patterns of meshes have been considered for MC and MCC models like this. And the element number, node number, and maximum settlement values for different mesh patterns are shown in Table 4.6 and Figure 4.21 with proper description.

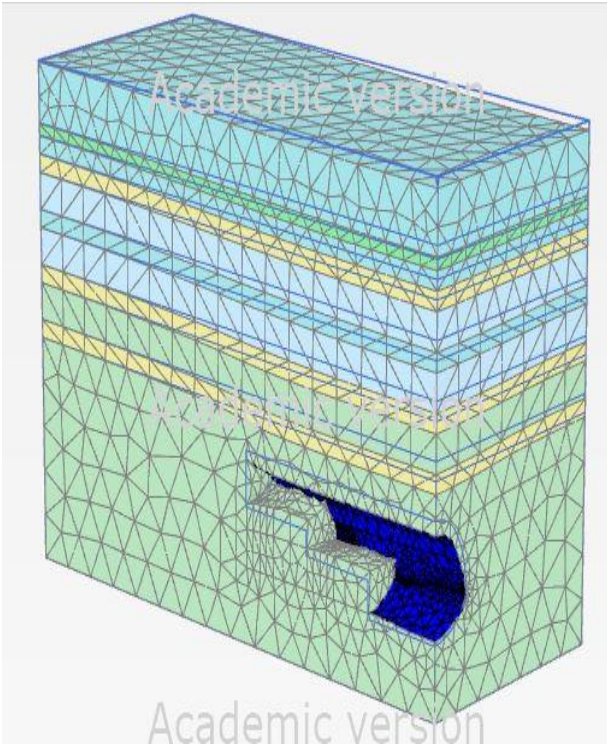

Figure 4.15: NATM method (HS Model): coarse mesh

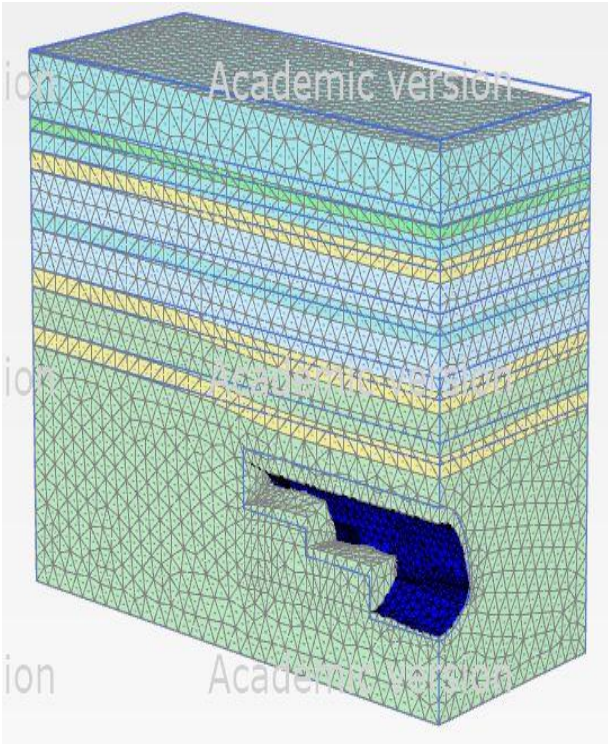

Figure 4.16: NATM method (HS Model): medium mesh

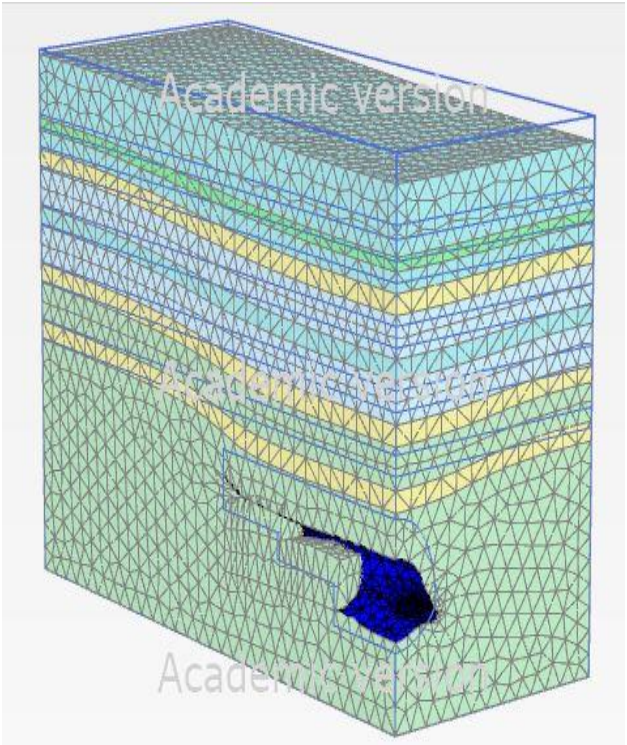

Figure 4.17: NATM method (HS Model): fine mesh

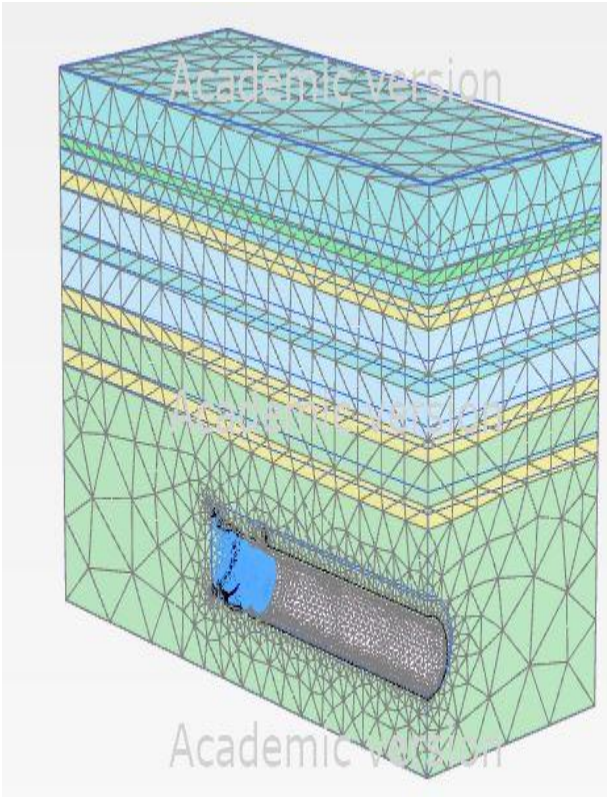

Figure 4.18: TBM method (HS Model): coarse mesh

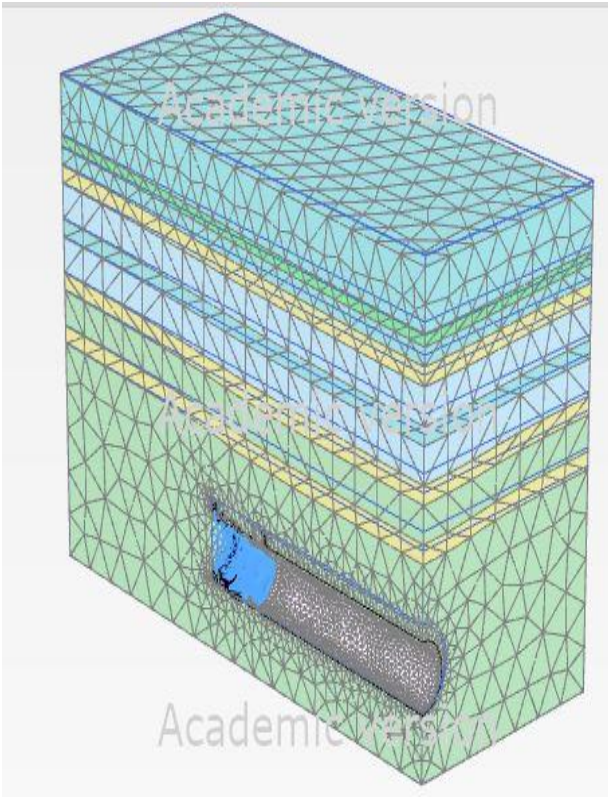

Figure 4.19: TBM method (HS Model): medium mesh

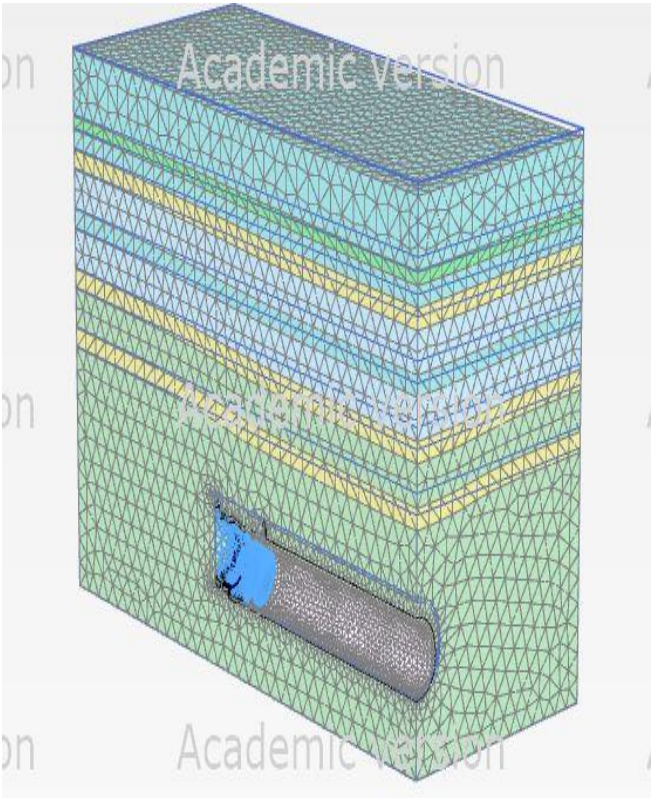

Figure 4.20: TBM method (HS Model): fine mesh

Table 4.6: Comparison of Settlement Values for Different Types of Mesh Sizes in NATM and TBM Methods

Method Type	Model Name	Meshing Type	Element No	Node No	Maximum Settlement (mm)
NATM	HS	Coarse	16987	24881	-23.72
		Medium	19246	28495	-20.98
		Fine	60145	87801	-19.22
	MCC	Coarse	16987	24881	-26.52
		Medium	19246	28495	-22.51
		Fine	60145	87801	-20.75
	MC	Coarse	16987	24881	-27.56
		Medium	19246	28495	-26.42
		Fine	60145	87801	-23.42
TBM	HS	Coarse	32439	51593	-19.53
		Medium	34047	54177	-18.54
		Fine	72882	110410	-18.46
	MCC	Coarse	32439	51593	-17.98
		Medium	34047	54177	-17.47
		Fine	72882	110410	-16.66
	MC	Coarse	32439	51593	-19.01
		Medium	34047	54177	-18.11
		Fine	72882	110410	-18.03

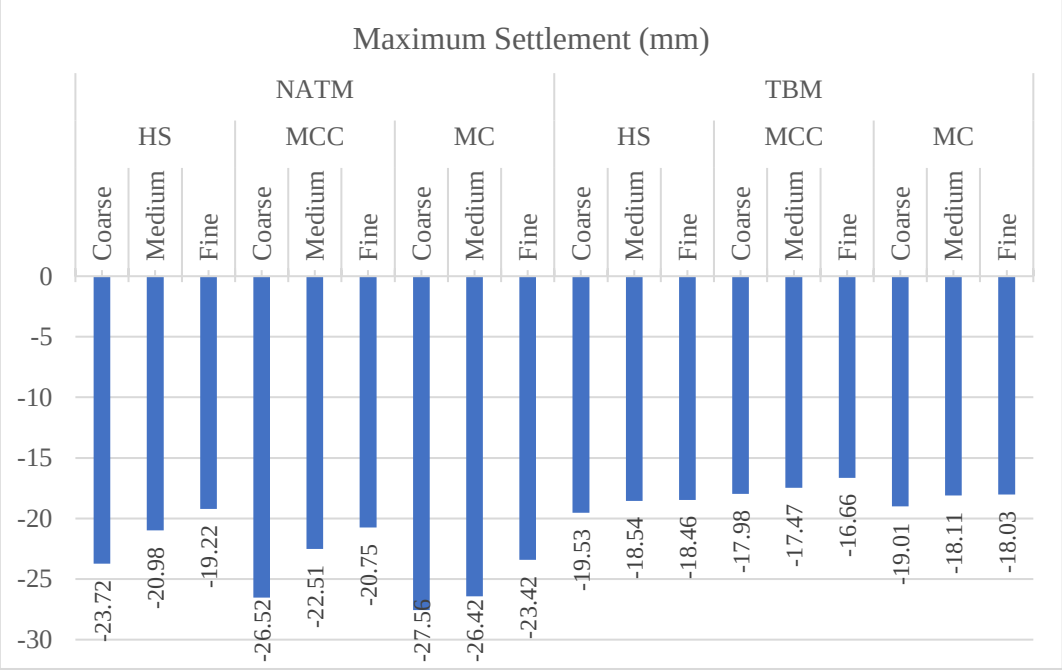

Figure 4.21: Effect on Maximum Settlement due to Refinements of Meshing for Different Models

It can be said from the above results that for the finer meshes, the settlement values are lower than the coarse and medium ones. It can be shown that the variation is more fluctuated for NATM models than TBM ones. For NATM models, the variation from medium mesh to coarse or fine mesh is about 10% whereas for TBM models, the variation value is almost 4% only. As the variation is considerable, medium mesh can be considered for models to save the running time.

3.7 Validation with Empirical Formulas for Inflexion Points and Maximum Settlement

Peck (1969) showed that a Gaussian distribution curve provided a reasonable fit to tunnel induced surface settlements. The value of inflexion point, i, is generally expressed as:

$$i = kZ_0 \tag{4.2}$$

Where Z_0 is the tunnel axis depth and K is a dimensionless empirical constant referred to as the trough width parameter. Values of K for Gaussian curves fitted to surface settlement data have been found to be close to 0.5 for tunnels in undrained clay, and typically range between 0.25 and 0.45 for tunnels in sands and gravels. Mair (1993) showed that subsurface settlement troughs in undrained clays can also be fitted well with a Gaussian curve, and that the value of i decreases approximately linearly with depth at a slope of -0.325.

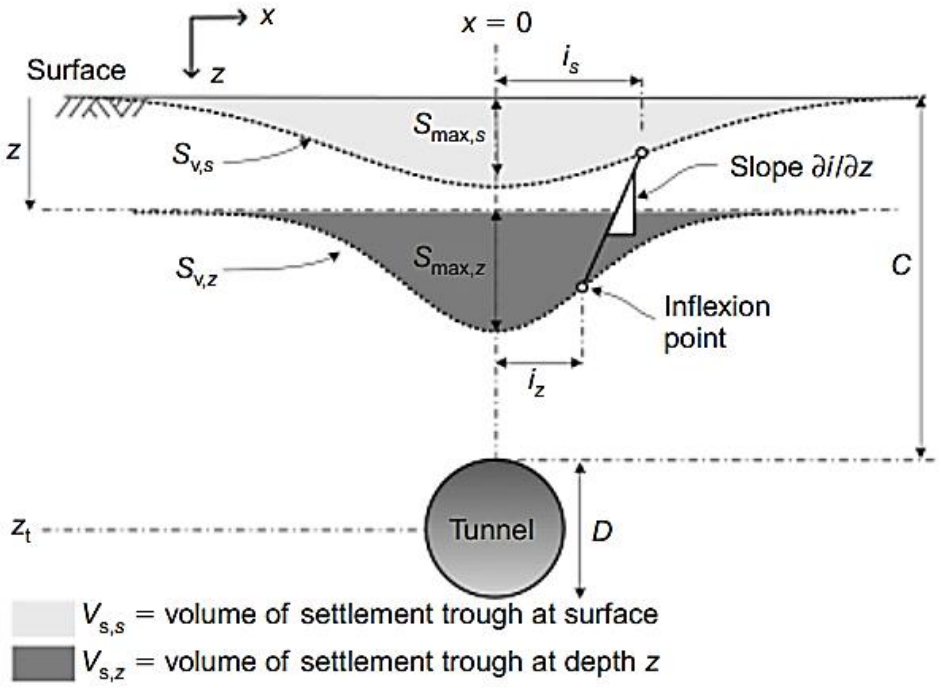

Figure 4.22: Greenfield Settlement Trough (Peck, 1969)

The tunnel excavation methods simulated in PLAXIS 3D and the settlement values from the analyses are validated with empirical formulas explained in different researches. These empirical formulas are applicable for TBM methods only. In numerical analyses, depth variations (30m, 32m and 35m) and diameter variations (5.0m, 6.0m, 7.0m) have been considered for TBM method to validate the analysis.

The empirical formula considered for validation are:

SL. No.	Researchers	Empirical Relations
1	Peck, 1969	$\frac{i}{R} = (\frac{Z_0}{2R})^n \ (n = 0.8 - 1)$
2	Clough & Schmidt, 1981	$\frac{i}{R} = (\frac{Z_0}{2R})^n \ (n = 0.8)$
3	Atkinson & Potts, 1977	$i = 0.25 \ (1.5Z_0 + 0.5R)$
4	O'Reily & New, 1982	$i = 0.43Z_0 + 1.1$
5	Mair & Taylor, 1999	$i = (0.4 - 0.5)Z_0 + 1.1$

Following the empirical formulas, distance of inflexion point from center for different models at different diameters and depths are calculated and compared with PLAXIS value in Table 4.7. Also, maximum settlement values and settlement values at inflexion point are determined from PLAXIS models. From Figure 4.23 and Figure 4.25, comparison of distance of point of inflexions from centers calculated from different empirical formulas for different depths and diameters are emphasized in three graphs for MC, MCC, and HS models respectively. Transverse settlement trough pattern for the half tunnel segment for three types of models with variation of depths and radiuses are shown in Figure 4.26 and Figure 4.27 respectively. The pattern is then compared with the empirical standard Gaussian curve to validate the shape of the curve. Effect on maximum settlement at varying depths and radius are emphasized clearly in Figure 4.28 and Figure 4.29 respectively. Also, effect on distance of inflexion point from center at varying depths and radius are shown effectively by graphical representation in Figure 4.30 and Figure 4.31 respectively.

According to the empirical formula of different researchers, O'Reily & New relationship has the best behavior of surface settlement in transverse section which follows the Gaussian distribution. Based on this assumption, Gaussian curve is fitted to the data monitoring outputs.

As a result, the average deviated values between the numerical result for obtaining trough width parameter, i, and the empirical result of O'Reily & New are obtained as 5.38%, 3.84% and 6.39% for MC, MCC and HS models respectively. These deviations are very less than other empirical relations described in researches. This difference is due to the fact that other researchers used the probability function in the estimation of inflexion point location which may not necessarily fit with the present results.

The transverse profile of the surface settlement of numerical results obtained from the MC, MCC and HS models are compared with the empirical relationship's graphs. It can be clearly seen that results of the MCC model have the best fit to the data points. The MCC model is considered to be suitable for this type of clay-based soils. To predict the surface settlement, the MCC model is proposed in soft clay with a low over consolidation ratio or normal consolidation similar to the soil in this site. In other words, where the shear modulus is independent of the shear strain, the surface settlement has a wide and shallow profile. Since the over consolidation clay exhibits non-linear stress strain behavior at the small strain prior to crossing the plastic yielding, it is very important to consider the behavior of these kinds of soils under small strain condition. Nevertheless, the shear modulus in the MC model is constant and the shear strain doesn't change with shear stress; this is probably the main reason for the difference between the results. The semi empirical method does not yield a precise prediction of ground settlement and this approach must be used only to give a general overview to designers. The implementation of MCC model is suggested in clayey soils as it has a relatively precise prediction of the surface displacement in clayey soil (normally consolidated or low OCR value). At depth, or as volume loss is increased, the fit of the Gaussian curve becomes less good.

Tunnel diameter has significant effect on the magnitude of the ground settlement, as a smaller tunnel tends to cause lesser ground settlements than larger tunnel. Distance of inflexion point from center tends to be smaller for increasing tunnel diameter. The stress redistribution from overburden soil must be the reason for the possibility of influencing zone below the tunnel especially of smaller diameter. This effect reduces when the tunnel diameter increases. The self-weight of the tunnel and grains redistribution may increase the settlement in loose sand below the bottom of the tunnel when the tunnel diameter increases.

And for larger depth, maximum settlement decreases than smaller depth as well as distance of inflexion point from center decreases for increasing tunnel diameter. This variation in

settlement due to the depth variation is because in elastic homogeneous medium, the upward movement of the soil is due to relief effect of the excavated soil above the tunnel but this movement decreases as depth increases. As the soil is remote from concentration of loading, the settlement value is larger in lesser depth and smaller in greater depth.

It can be concluded after analyzing the results that the total settlement decreases with an increase in depth of the tunnel (almost 11% decrement for every 5m increment of depth) and increases with an increase in diameter (almost 20% increment for every 1m increment of diameter). Increasing the TBM depth results to increase around 4% in distance of inflexion point from center whereas increasing in radius results to decrease around 5% in inflexion point distance from center of the tunnel.

Table 4.7: Calculation of distance of Inflexion Point from center and Settlement values (maximum and at inflexion point) for different models, diameters and depths

	Empirical Formula Researchers	Depth, Z_0 (m)	Radius, R (m)	Distance of Inflexion Point (m)	Distance of Inflexion Point from PLAXIS (m)	Deviated value (%)	Maximum Settlement (mm)	Settlement at Inflexion Point (mm)
MC Model	Depth considered as 30.0m, Radius considered as 3.50m							
	Peck, 1969	30	3.50	8.73	16.57	70.44	-20.85	-6.00
	Clough & Schmidt, 1981	30	3.50	8.73	16.57	39.81	-20.85	-6.00
	Atkinson & Potts, 1977	30	3.50	11.69	16.57	19.40	-20.85	-6.00
	O'Reilly & New, 1982	30	3.50	14.00	16.57	3.45	-20.85	-6.00
	Mair & Taylor, 1999	30	3.50	12.00	16.57	17.24	-20.85	-6.00
	Depth considered as 32.0m, Radius considered as 3.50m							
	Peck, 1969	32	3.50	9.19	15.85	71.16	-19.53	-6.00
	Clough & Schmidt, 1981	32	3.50	9.19	15.85	42.02	-19.53	-6.00
	Atkinson & Potts, 1977	32	3.50	12.44	15.85	21.53	-19.53	-6.00
	O'Reilly & New, 1982	32	3.50	14.86	15.85	6.25	-19.53	-6.00
	Mair & Taylor, 1999	32	3.50	12.80	15.85	19.24	-19.53	-6.00
	Depth considered as 35.0m, Radius considered as 3.50m							
	Peck, 1969	35	3.50	9.87	14.50	69.82	-18.11	-6.00
	Clough & Schmidt, 1981	35	3.50	9.87	14.50	40.42	-18.11	-6.00
	Atkinson & Potts, 1977	35	3.50	13.56	14.50	18.15	-18.11	-6.00
	O'Reilly & New, 1982	35	3.50	16.15	14.50	2.53	-18.11	-6.00
	Mair & Taylor, 1999	35	3.50	14.00	14.50	15.51	-18.11	-6.00
	Depth considered as 35.0m, Radius considered as 3.00m							

	Empirical Formula Researchers	Depth, Z_0 (m)	Radius, R (m)	Distance of Inflexion Point (m)	Distance of Inflexion Point from PLAXIS (m)	Deviated value (%)	Maximum Settlement (mm)	Settlement at Inflexion Point (mm)
	Peck, 1969	35	3.00	9.87	16.99	65.67	-16.7	-5.00
	Clough & Schmidt, 1981	35	3.00	9.87	16.99	41.89	-16.7	-5.00
	Atkinson & Potts, 1977	35	3.00	13.50	16.99	20.54	-16.7	-5.00
	O'Reilly & New, 1982	35	3.00	16.15	16.99	4.94	-16.7	-5.00
	Mair & Taylor, 1999	35	3.00	14.00	16.99	17.60	-16.7	-5.00
	Depth considered as 35.0m, Radius considered as 2.50m							
	Peck, 1969	35	2.50	9.87	17.89	60.87	-14.27	-4.00
	Clough & Schmidt, 1981	35	2.50	9.87	17.89	44.82	-14.27	-4.00
	Atkinson & Potts, 1977	35	2.50	13.44	17.89	24.89	-14.27	-4.00
	O'Reilly & New, 1982	35	2.50	16.15	17.89	9.73	-14.27	-4.00
	Mair & Taylor, 1999	35	2.50	14.00	17.89	21.74	-14.27	-4.00
	Depth considered as 30.0m, Radius considered as 3.50m							
MCC Model	Peck, 1969	30	3.50	8.73	16.27	70.00	-19.66	-9.00
	Clough & Schmidt, 1981	30	3.50	8.73	16.27	38.90	-19.66	-9.00
	Atkinson & Potts, 1977	30	3.50	11.69	16.27	18.18	-19.66	-9.00
	O'Reilly & New, 1982	30	3.50	14.00	16.27	1.99	-19.66	-9.00
	Mair & Taylor, 1999	30	3.50	12.00	16.27	15.99	-19.66	-9.00
	Depth considered as 32.0m, Radius considered as 3.50m							
	Peck, 1969	32	3.50	9.19	15.19	69.91	-18.93	-8.00
	Clough & Schmidt, 1981	32	3.50	9.19	15.19	39.51	-18.93	-8.00
	Atkinson & Potts, 1977	32	3.50	12.44	15.19	18.13	-18.93	-8.00
	O'Reilly & New, 1982	32	3.50	14.86	15.19	2.18	-18.93	-8.00
	Mair & Taylor, 1999	32	3.50	12.80	15.19	15.74	-18.93	-8.00
	Depth considered as 35.0m, Radius considered as 3.50m							
	Peck, 1969	35	3.50	9.87	14.28	69.27	-17.47	-8.00
	Clough & Schmidt, 1981	35	3.50	9.87	14.28	39.32	-17.47	-8.00
	Atkinson & Potts, 1977	35	3.50	13.56	14.28	16.64	-17.47	-8.00
	O'Reilly & New, 1982	35	3.50	16.15	14.28	0.74	-17.47	-8.00
	Mair & Taylor, 1999	35	3.50	14.00	14.28	13.95	-17.47	-8.00
	Depth considered as 35.0m, Radius considered as 3.00m							
	Peck, 1969	35	3.00	9.87	17.01	65.71	-16.25	-7.00

	Empirical Formula Researchers	Depth, Z_0 (m)	Radius, R (m)	Distance of Inflexion Point (m)	Distance of Inflexion Point from PLAXIS (m)	Deviated value (%)	Maximum Settlement (mm)	Settlement at Inflexion Point (mm)
	Clough & Schmidt, 1981	35	3.00	9.87	17.01	41.96	-16.25	-7.00
	Atkinson & Potts, 1977	35	3.00	13.50	17.01	20.63	-16.25	-7.00
	O'Reilly & New, 1982	35	3.00	16.15	17.01	5.06	-16.25	-7.00
	Mair & Taylor, 1999	35	3.00	14.00	17.01	17.70	-16.25	-7.00
	Depth considered as 35.0m, Radius considered as 2.50m							
	Peck, 1969	35	2.50	9.87	17.79	60.65	-13.95	-6.00
	Clough & Schmidt, 1981	35	2.50	9.87	17.79	44.50	-13.95	-6.00
	Atkinson & Potts, 1977	35	2.50	13.44	17.79	24.47	-13.95	-6.00
	O'Reilly & New, 1982	35	2.50	16.15	17.79	9.22	-13.95	-6.00
	Mair & Taylor, 1999	35	2.50	14.00	17.79	21.30	-13.95	-6.00
HS Model	Depth considered as 30.0m, Radius considered as 3.50m							
	Peck, 1969	30	3.50	8.73	16.92	70.67	-19.57	-9.00
	Clough & Schmidt, 1981	30	3.50	8.73	16.92	40.27	-19.57	-9.00
	Atkinson & Potts, 1977	30	3.50	11.69	16.92	20.00	-19.57	-9.00
	O'Reilly & New, 1982	30	3.50	14.00	16.92	4.18	-19.57	-9.00
	Mair & Taylor, 1999	30	3.50	12.00	16.92	17.86	-19.57	-9.00
	Depth considered as 32.0m, Radius considered as 3.50m							
	Peck, 1969	32	3.50	9.19	15.61	70.72	-18.77	-9.00
	Clough & Schmidt, 1981	32	3.50	9.19	15.61	41.14	-18.77	-9.00
	Atkinson & Potts, 1977	32	3.50	12.44	15.61	20.34	-18.77	-9.00
	O'Reilly & New, 1982	32	3.50	14.86	15.61	4.82	-18.77	-9.00
	Mair & Taylor, 1999	32	3.50	12.80	15.61	18.02	-18.77	-9.00
	Depth considered as 35.0m, Radius considered as 3.50m							
	Peck, 1969	35	3.50	9.87	14.61	70.45	-18.54	-9.00
	Clough & Schmidt, 1981	35	3.50	9.87	14.61	41.65	-18.54	-9.00
	Atkinson & Potts, 1977	35	3.50	13.56	14.61	19.84	-18.54	-9.00
	O'Reilly & New, 1982	35	3.50	16.15	14.61	4.55	-18.54	-9.00
	Mair & Taylor, 1999	35	3.50	14.00	14.61	17.25	-18.54	-9.00
	Depth considered as 35.0m, Radius considered as 3.00m							
	Peck, 1969	35	3.00	9.87	17.44	66.55	-17.04	-10.00
	Clough & Schmidt, 1981	35	3.00	9.87	17.44	43.39	-17.04	-10.00

	Empirical Formula Researchers	Depth, Z_0 (m)	Radius, R (m)	Distance of Inflexion Point (m)	Distance of Inflexion Point from PLAXIS (m)	Deviated value (%)	Maximum Settlement (mm)	Settlement at Inflexion Point (mm)
	Atkinson & Potts, 1977	35	3.00	13.50	17.44	22.59	-17.04	-10.00
	O'Reilly & New, 1982	35	3.00	16.15	17.44	7.40	-17.04	-10.00
	Mair & Taylor, 1999	35	3.00	14.00	17.44	19.72	-17.04	-10.00
	Depth considered as 35.0m, Radius considered as 2.50m							
	Peck, 1969	35	2.50	9.87	18.15	61.44	-14.48	-7.00
	Clough & Schmidt, 1981	35	2.50	9.87	18.15	45.61	-14.48	-7.00
	Atkinson & Potts, 1977	35	2.50	13.44	18.15	25.98	-14.48	-7.00
	O'Reilly & New, 1982	35	2.50	16.15	18.15	11.03	-14.48	-7.00
	Mair & Taylor, 1999	35	2.50	14.00	18.15	22.88	-14.48	-7.00

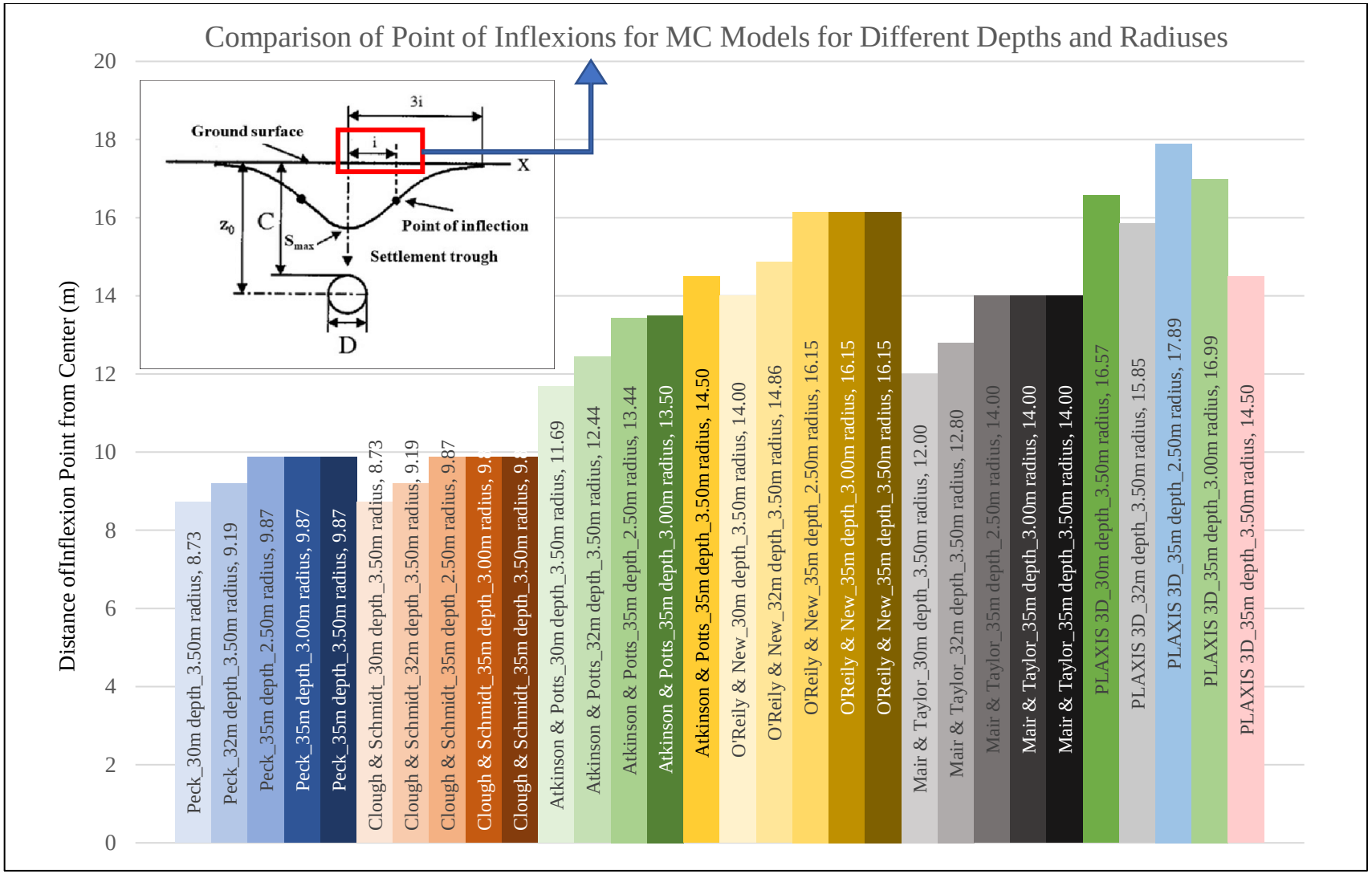

Figure 4.23: Comparison of Distance of Inflexion Points for MC Models for Different Depths (30m, 32m, 35m) and Different Radiuses (2.5m, 3m, 3.5m)

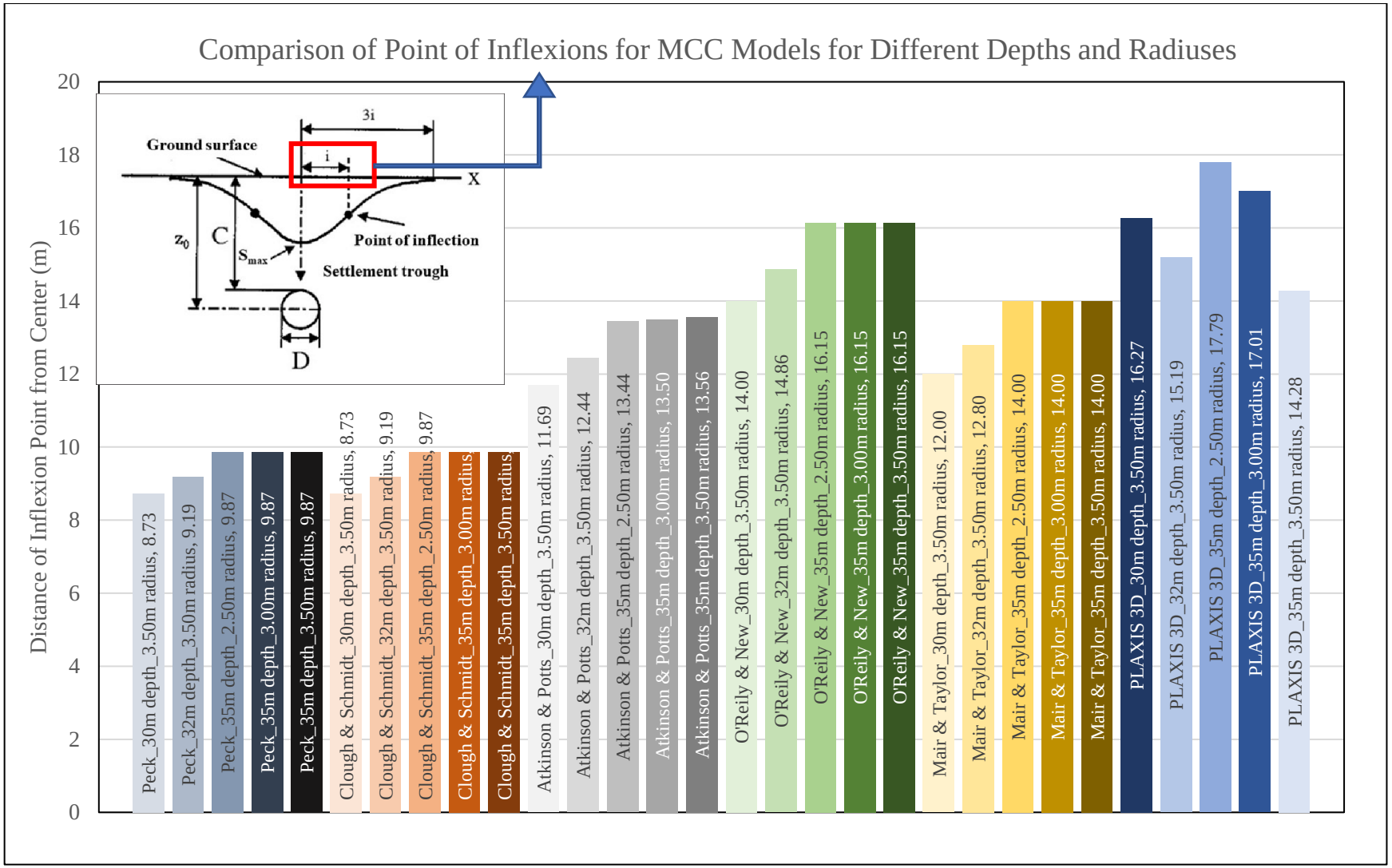

Figure 4.24: Comparison of Distance of Inflexion Points for MCC Models for Different Depths (30m, 32m, 35m) and Different Radiuses (2.5m, 3m, 3.5m)

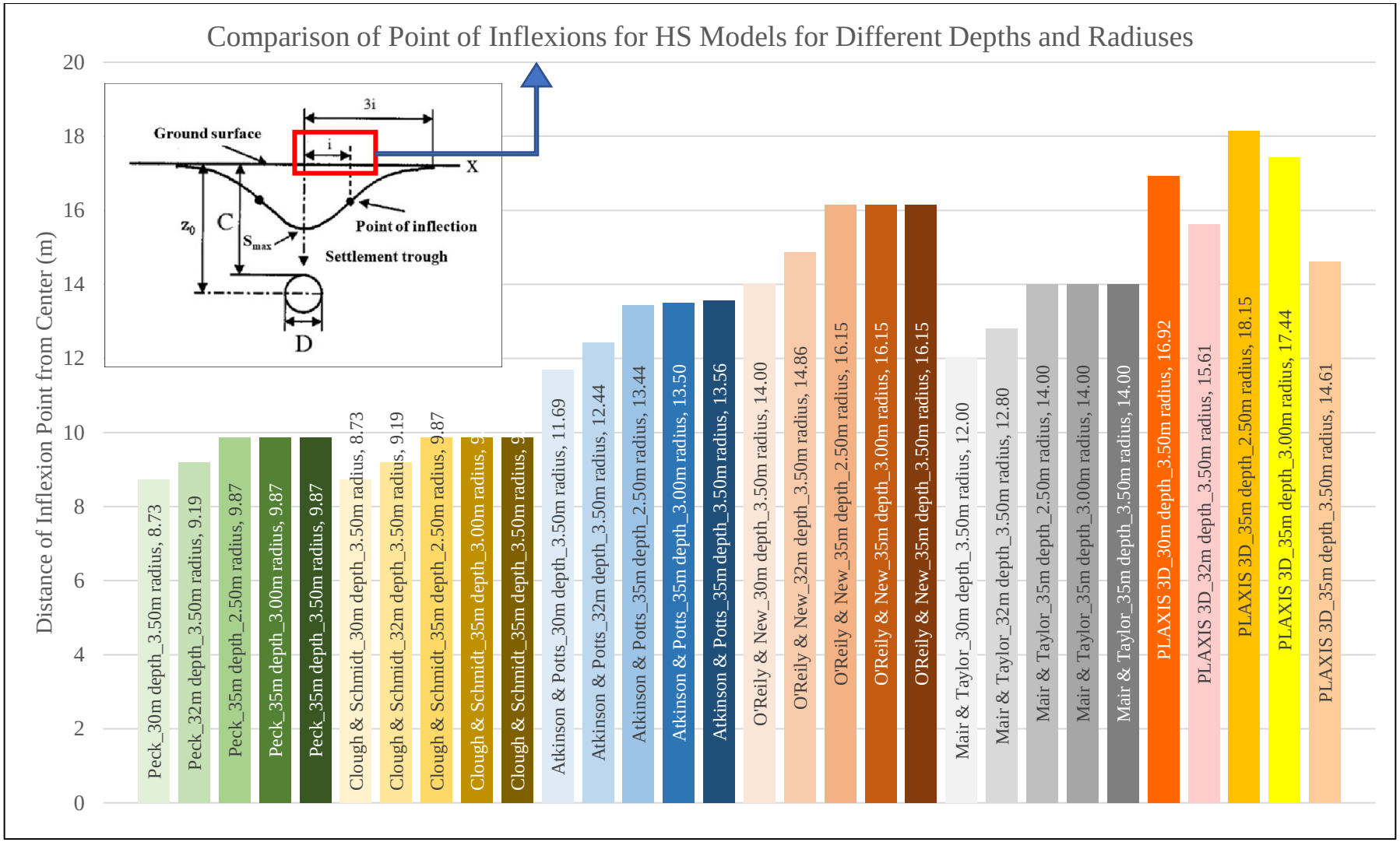

Figure 4.25: Comparison of Distance of Inflexion Points for HS Models for Different Depths (30m, 32m, 35m) and Different Radiuses (2.5m, 3m, 3.5m)

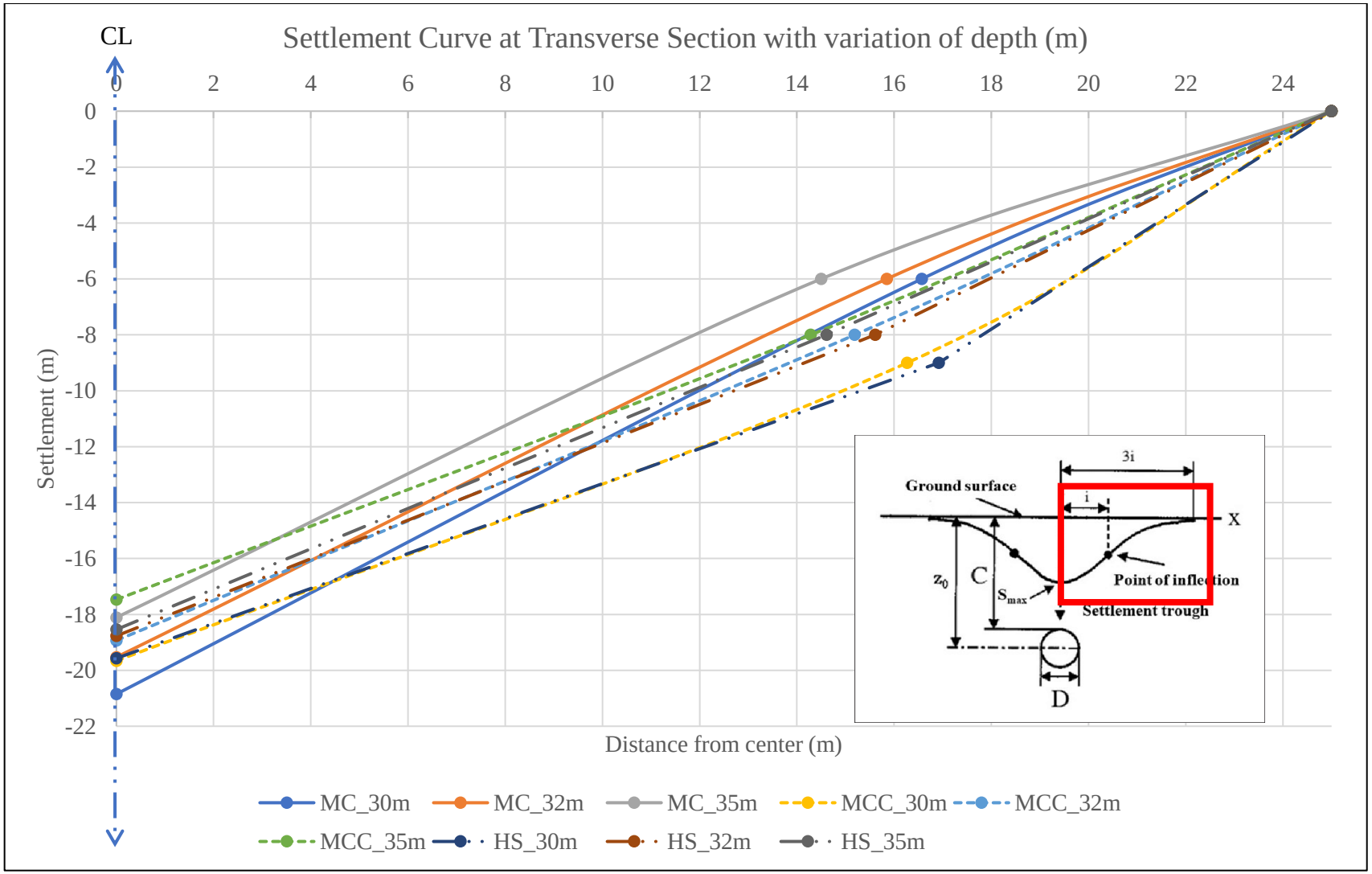

Figure 4.26: Transverse Settlement Trough Pattern with variation of depth (30m, 32m, 35m) for MC, MCC and HS Models

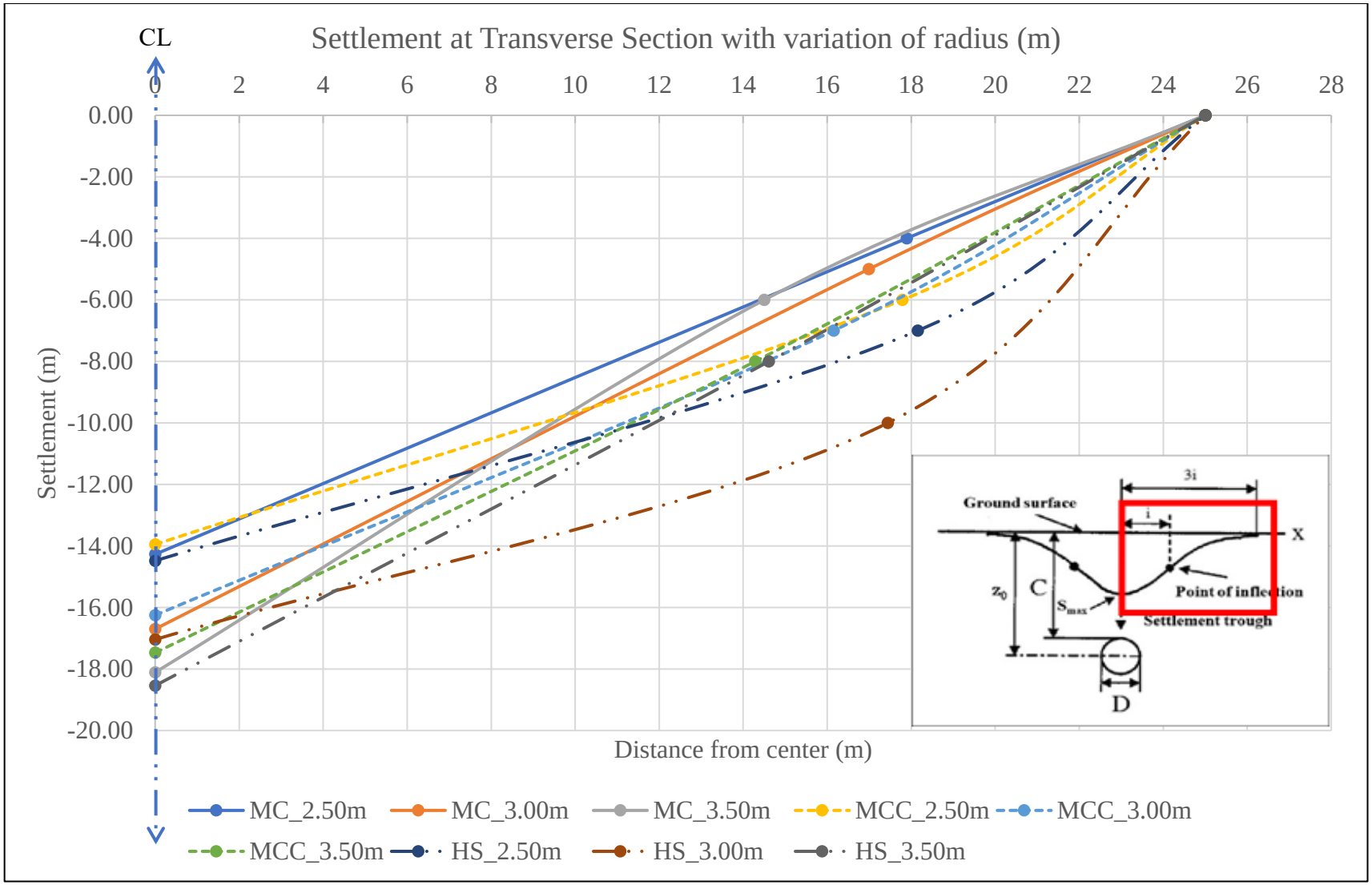

Figure 4.27: Transverse Settlement Trough Pattern with variation of radius (2.50m, 3.0m, 3.50m) for MC, MCC and HS Models

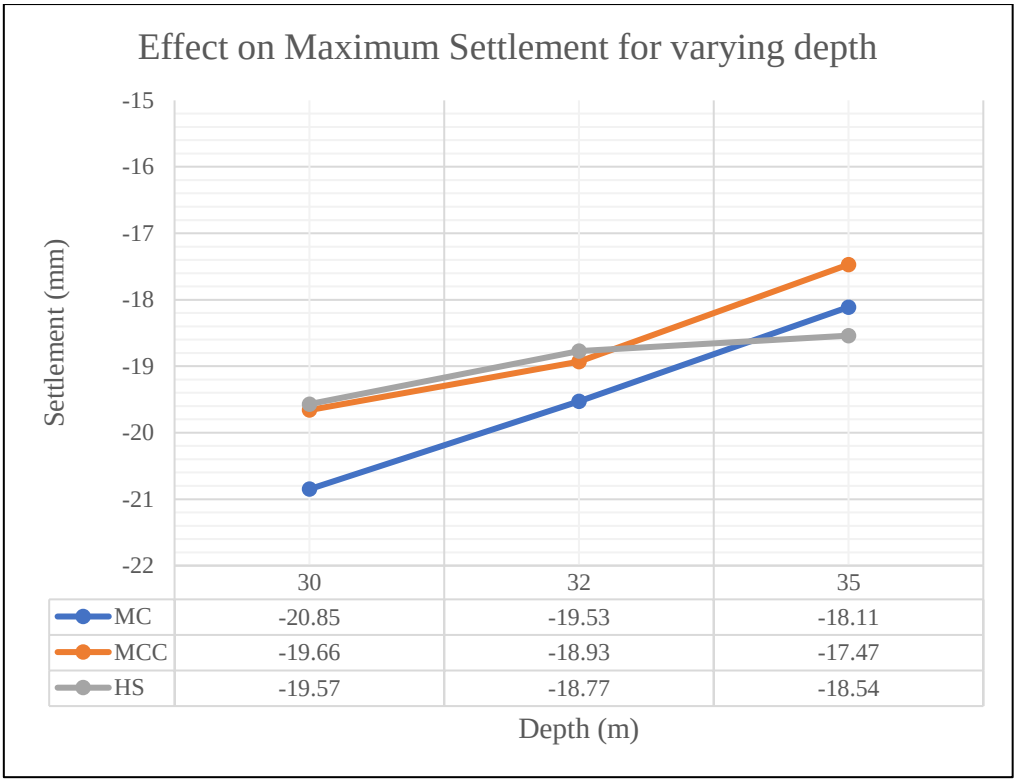

Figure 4.28: Effect on Maximum Settlement for increasing of depth (30m, 32m and 35m)

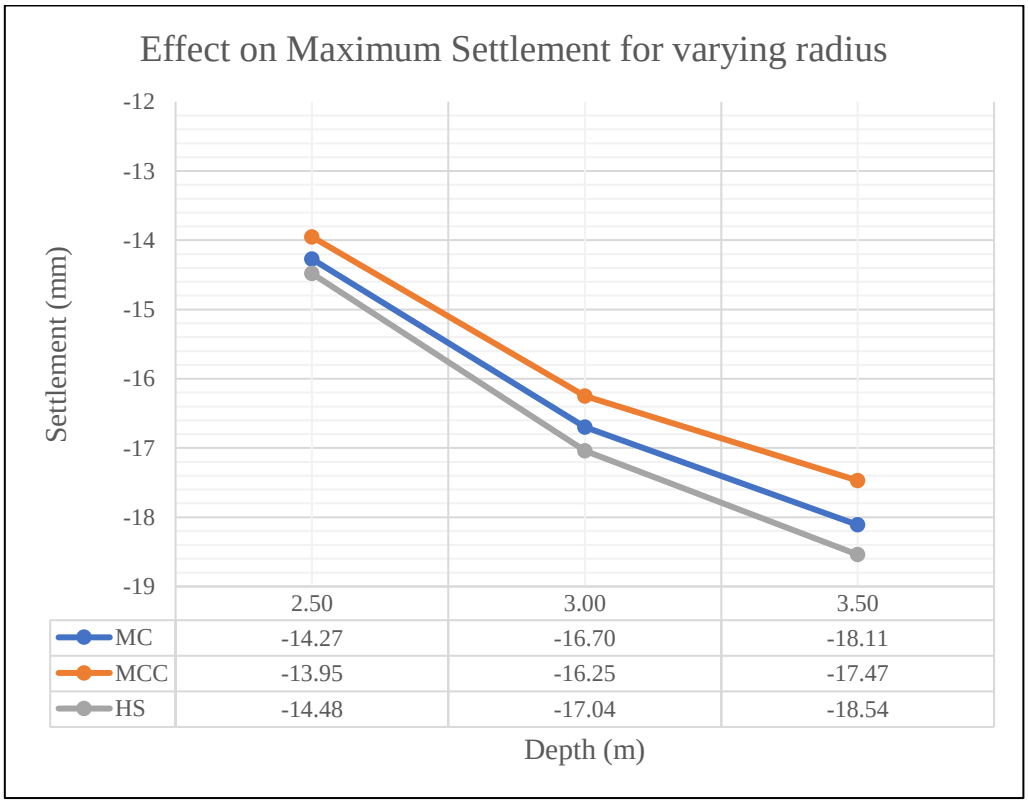

Figure 4.29: Effect on Maximum Settlement for increasing of radius (2.50m, 3.00m and 3.50m)

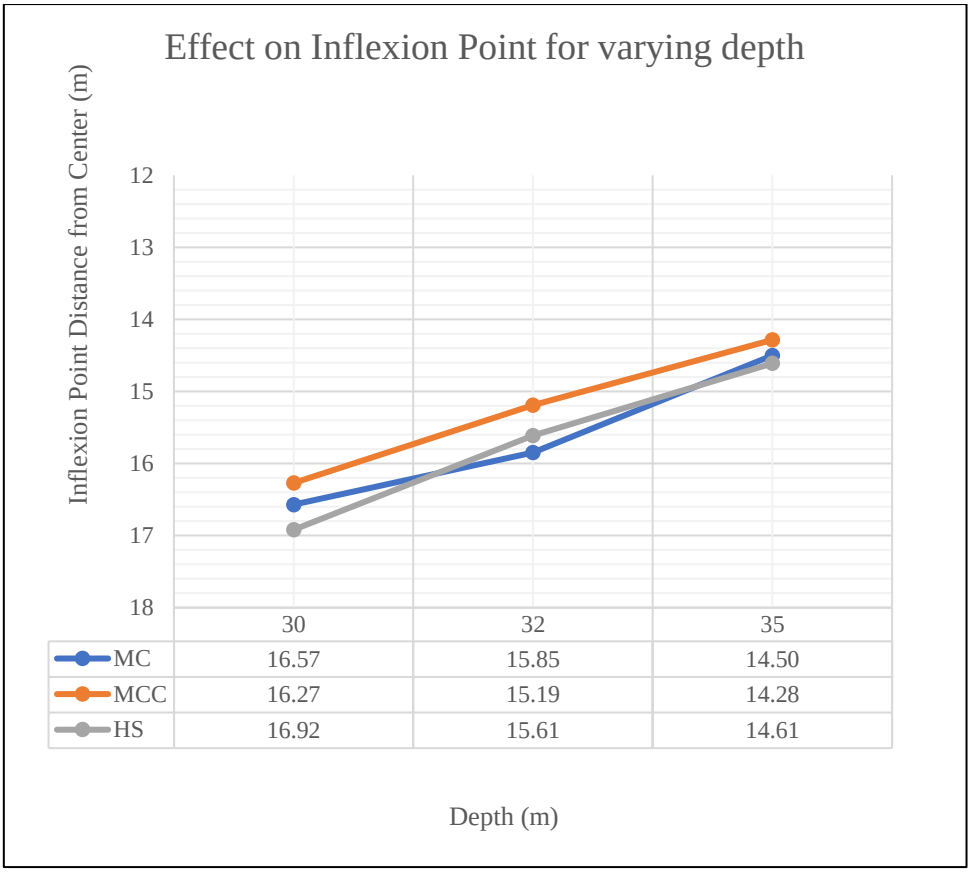

Figure 4.30: Effect on Inflexion Point for increasing of depth (30m, 32m and 35m)

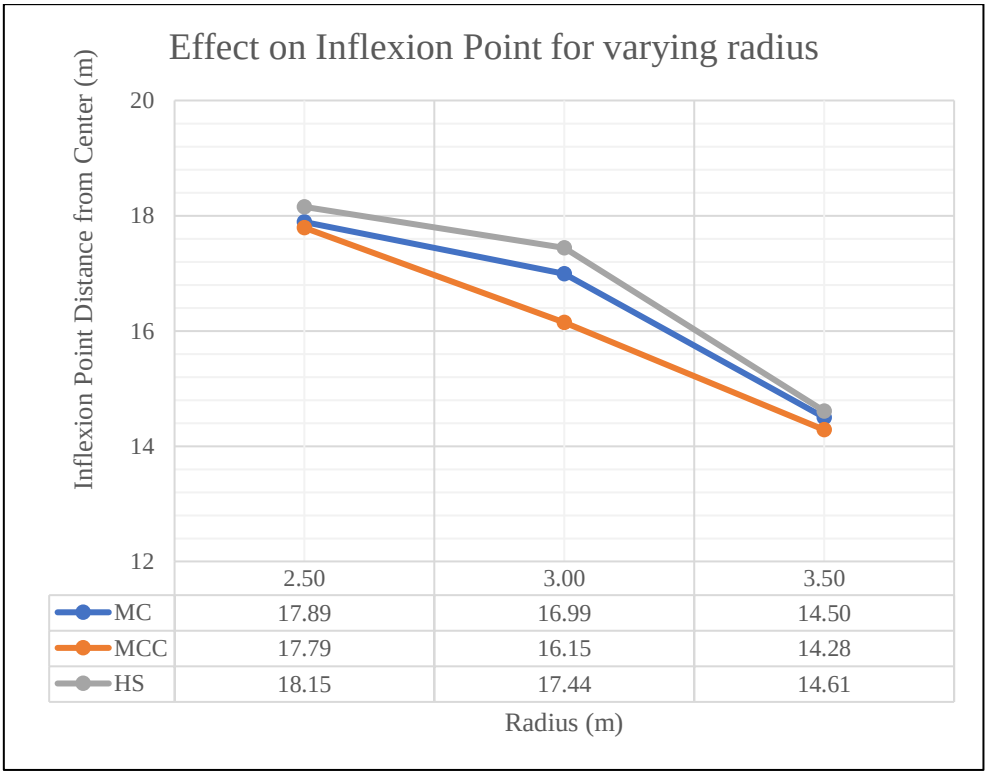

Figure 4.31: Effect on Inflexion Point for increasing of radius (2.50m, 3.00m and 3.50m)

3.8 Validation with Empirical Formulas for Vertical Settlement

For drained soils, such as sands and gravels, the volume of the soil is not constrained, and shearing causes contraction and dilation to occur. This causes the volume of the settlement trough, Vs, to vary with depth ($V_{s,s} \neq V_{s,z}$), and means that an assessment of volume loss based on surface measurements will not provide an entirely accurate measurement of subsurface volume loss. In order to analyze trends in settlement trough shape, a curve must be fitted to settlement data. The use of a curve that gives a good fit to settlement data is important in order to perform an effective analysis of trough shape, and when evaluating the effect of tunnelling on nearby infrastructure or buildings. It has been reported that the Gaussian curve does not always provide a good fit to settlement trough data. Jacobsz (2004) used a slightly different version of the Gaussian curve that, like the Gaussian curve, has two degrees of freedom, represented by S_{max} and i. Celestino and Vorster used curves with one additional degree of freedom compared with the Gaussian curve, thus giving more flexibility to the shape of the curve.

Vertical settlement values derived from PLAXIS 3D and different empirical formula and also the deviation percentages for both NATM and TBM methods are shown in Table 4.8. In Figure 4.32, these values are depicted in graphical representation. Maximum settlements for NATM and TBM methods from PLAXIS 3D for different types of models are compared in Figure 4.33. Transverse settlement trough curves for both methods considering 35m depth and 7m diameter derived from PLAXIS 3D are shown in Figure 4.34. Longitudinal settlements and lateral settlements for both methods from PLAXIS 3D are emphasized in Figure 4.35 and Figure 4.36.

It can be evaluated from the result that the deviation percentages of vertical settlement from PLAXIS with Peck, Peck & Schmidt and Jacobsz formula are almost 10% and 34% for TBM and NATM respectively. Chow's formula shows much less values than other empirical formulas (Peck, Peck & Schmidt, and Jacobsz), which can indicate that this formula is not appropriate for clayey soil. Also, the Jacobsz formula (2004) shows a good agreement and approximately close value compared to the settlement values obtained from PLAXIS 3D (for NATM, the variation is about 2 ~ 16% and for TBM 3 ~ 10%.

From comparison of longitudinal and lateral settlement, it can be shown that NATM method shows more settlement (10 to 30% more) than TBM method as it includes blast technique which induce more ground surface variation than TBM machine advancement, especially in

soft soil. In settlement at transverse sections for both NATM and TBM, MCC model shows the best fit curve in Gaussian distribution.

Table 4.8: Comparison of Settlements of PLAXIS with Empirical Formulas (for Depth 35m and Diameter 7m)

Method Type	Model Type	Maximum Settlement, Smax (mm)	Lateral Settlement, Ux (mm)	Longitudinal Settlement, Ux (mm)	Vertical Settlement, Uz (mm)	Inflexion Point from PLAXIS (m)	Uz according to Peck & Schmidt formula (mm)	Uz according to Peck formula (mm)	Uz according to Jacobsz formula (mm)	Uz according to Chow formula (mm)	U at Inflexion Point (mm)	Deviation of Uz value from Empirical formula to PLAXIS (%)
NATM	MC	-26.42	-5.818	-13.11	-12.31	9.85	-9.35	-16.01	-18.68	-1.94	-8.00	24.069
	HS	-20.98	-2.754	-11.24	-15.12	16.58	-12.50	-12.71	-14.83	-1.71	-9.00	17.343
	MCC	-22.51	-7.36	-10.34	-16.61	13.16	-10.58	-13.64	-15.91	-1.83	-11.00	36.280
TBM	MC	-18.11	-0.35	-8.67	-14.07	15.19	-12.49	-10.97	-12.80	-2.09	-6.00	11.218
	HS	-18.54	-0.85	-9.53	-13.53	16.92	-12.73	-11.24	-13.11	-2.09	-9.00	5.896
	MCC	-17.47	-0.62	-7.98	-13.99	18.15	-12.29	-10.59	-12.35	-2.09	-8.00	12.135

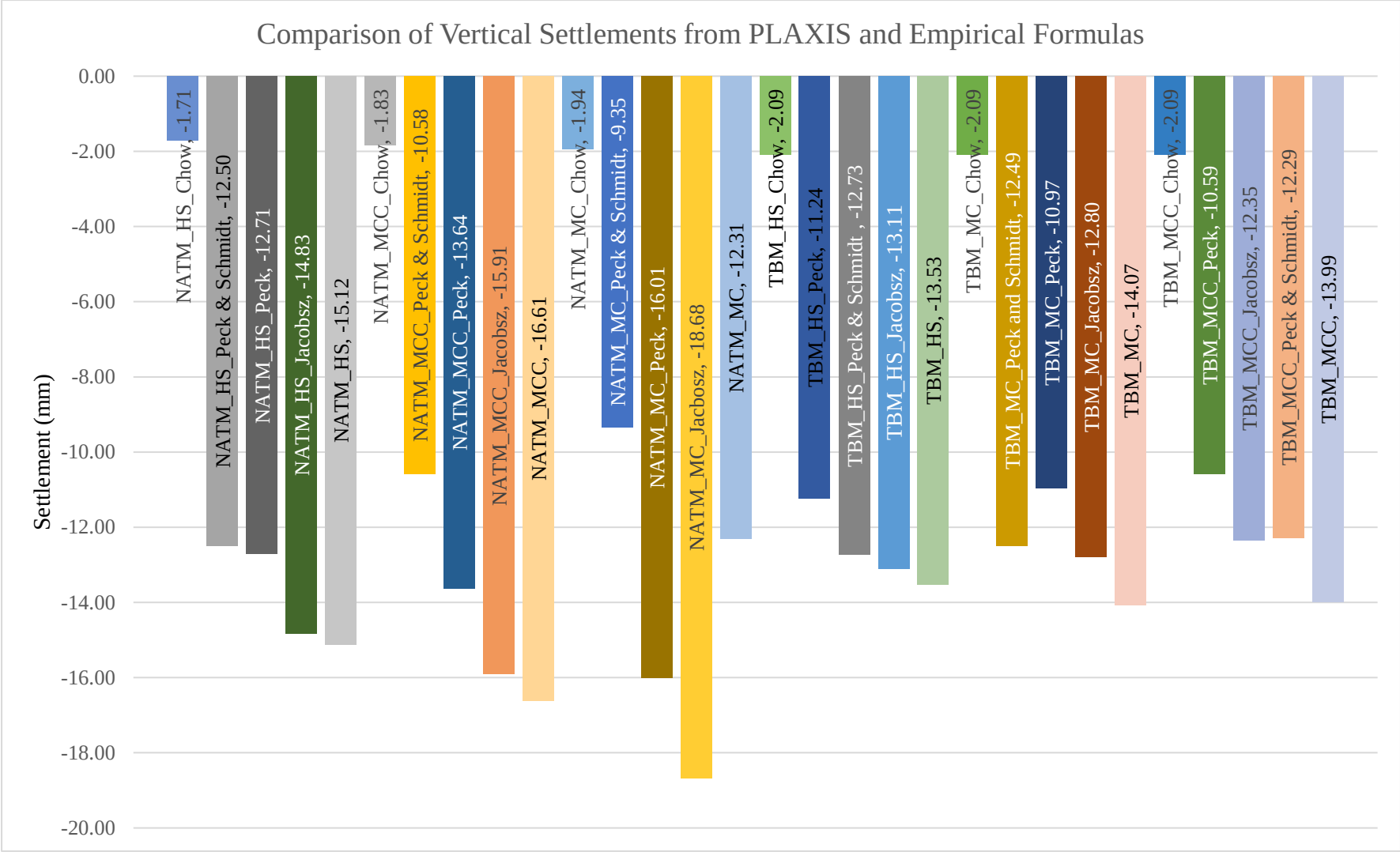

Figure 4.32: Comparison of Vertical Settlements of Different Empirical Formulas for both NATM and TBM methods (for different models)

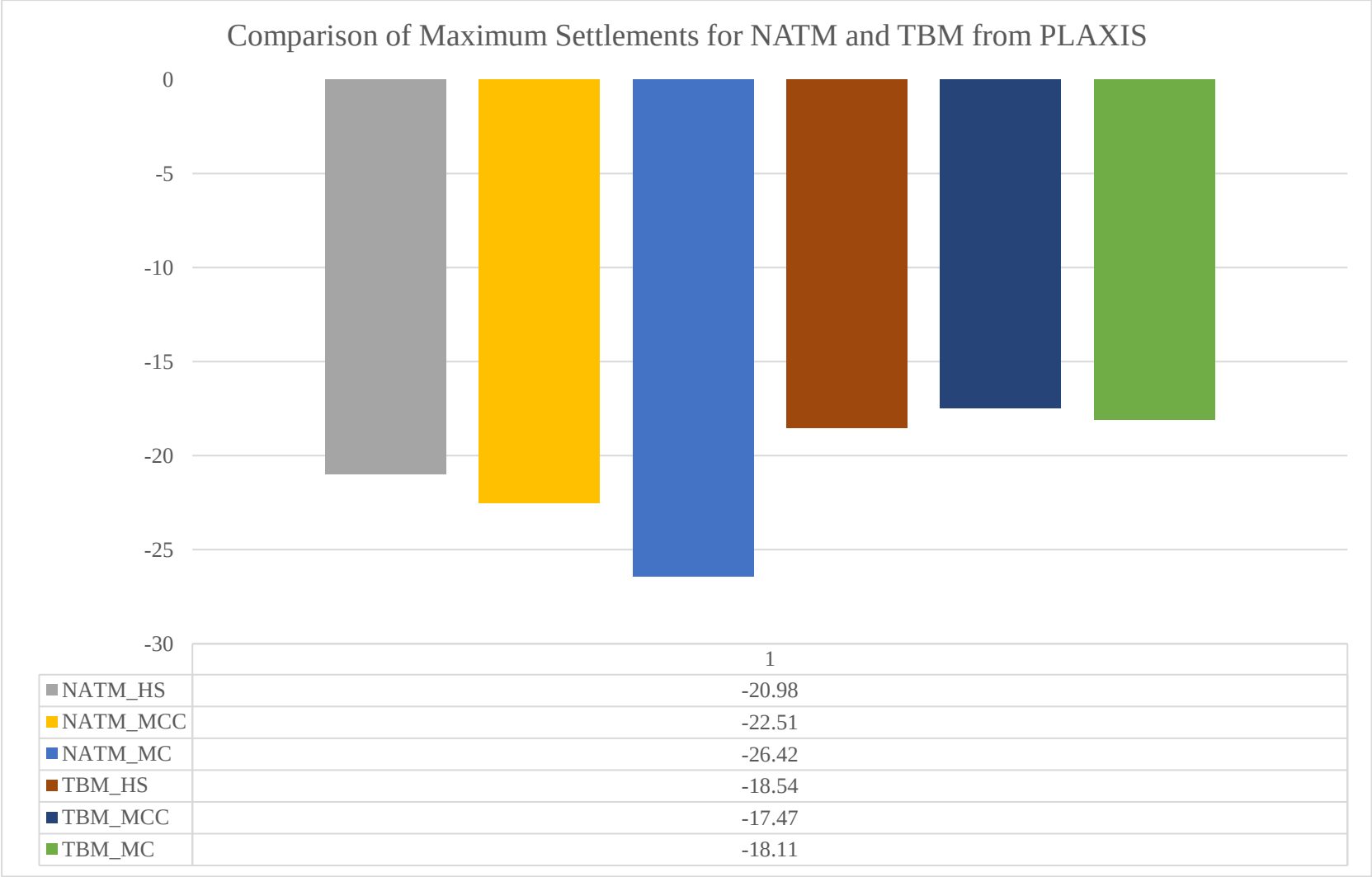

	1
NATM_HS	-20.98
NATM_MCC	-22.51
NATM_MC	-26.42
TBM_HS	-18.54
TBM_MCC	-17.47
TBM_MC	-18.11

Figure 4.33: Comparison of Maximum Settlement for NATM and TBM Methods from PLAXIS (for different types of models)

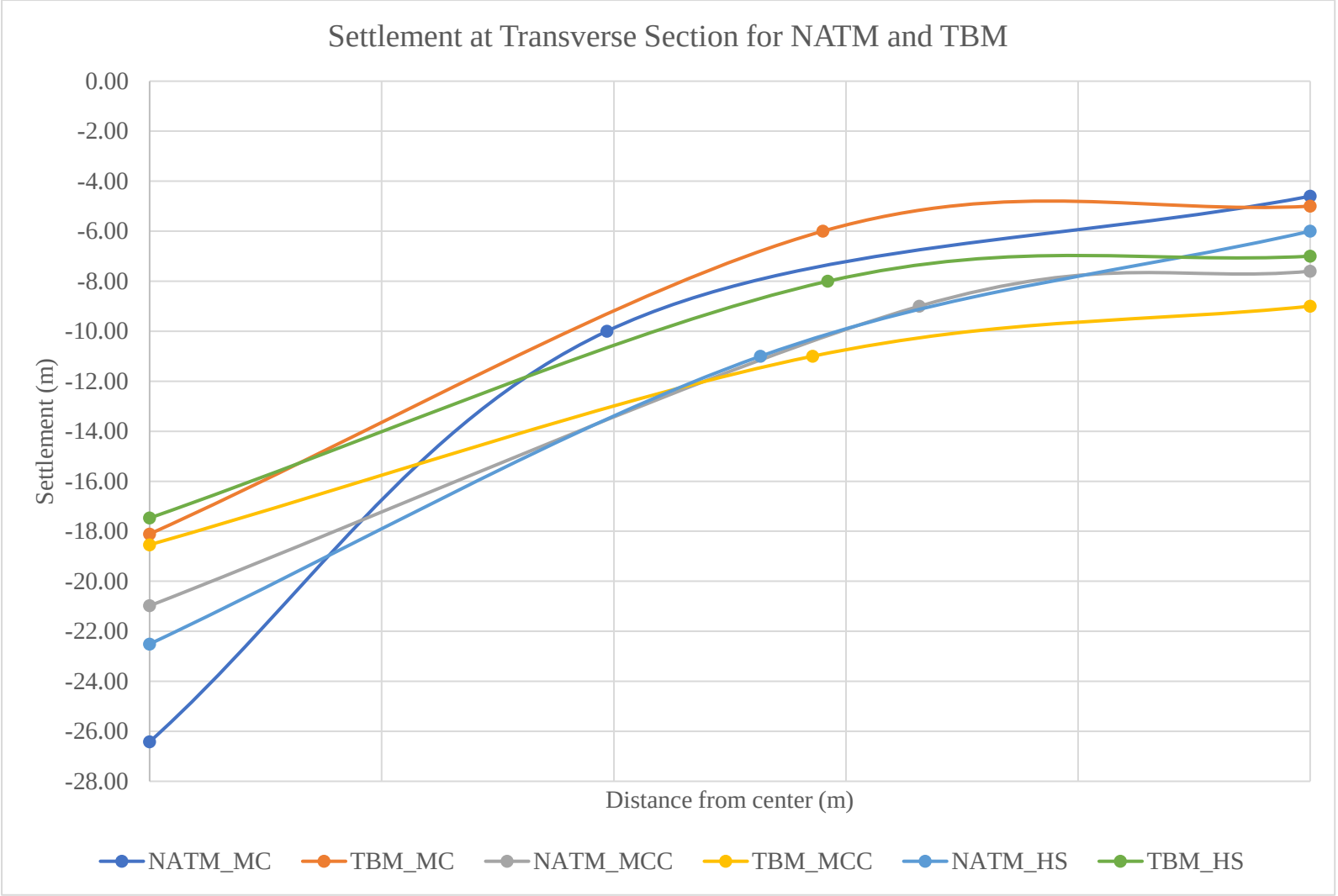

Figure 4.34: Settlement at Transverse Section for both NATM and TBM methods considering 35m depth and 3.50m radius (from PLAXIS)

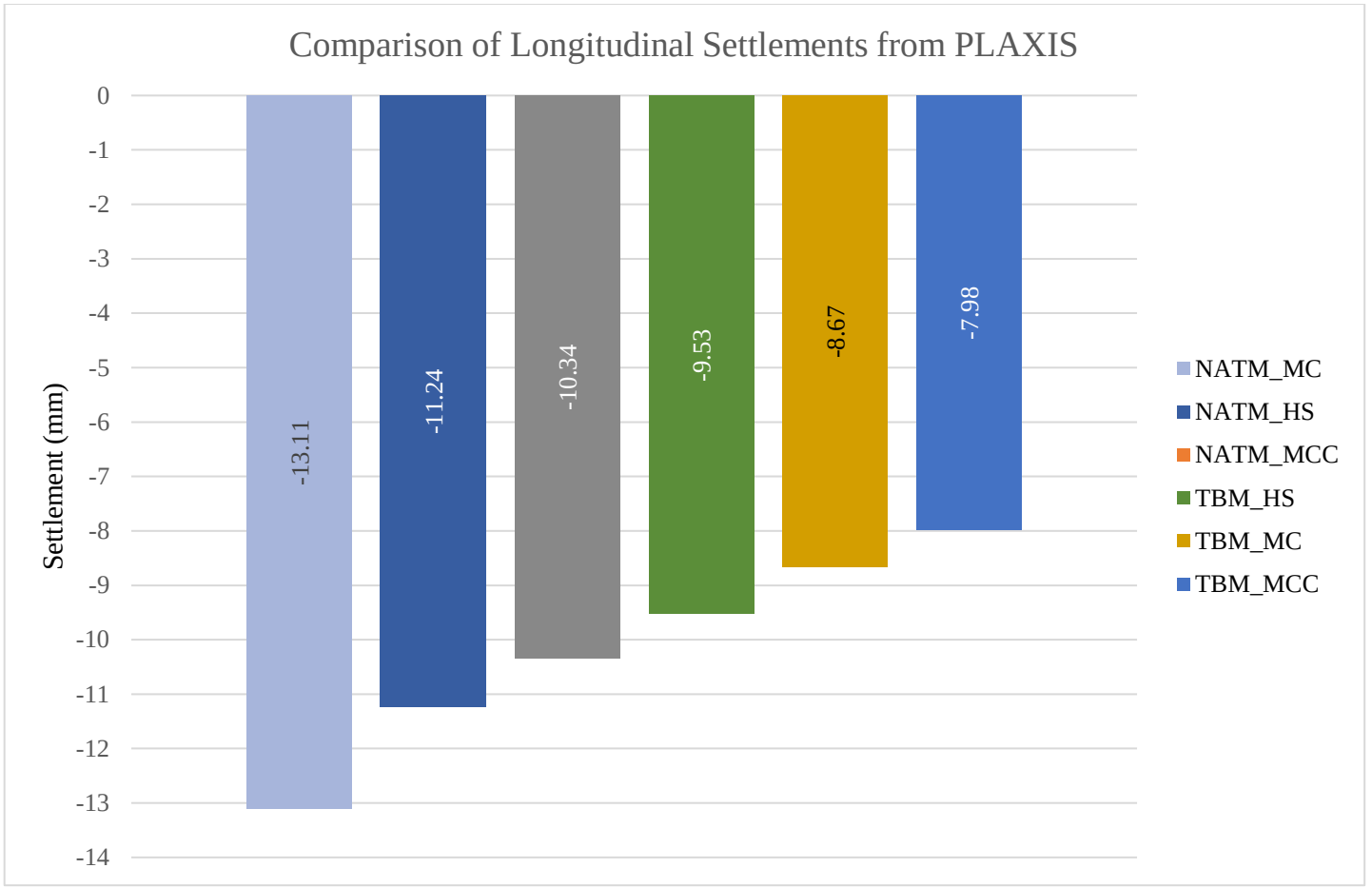

Figure 4.35: Longitudinal Settlements for both NATM and TBM methods considering 35m depth and 3.50m radius (from PLAXIS)

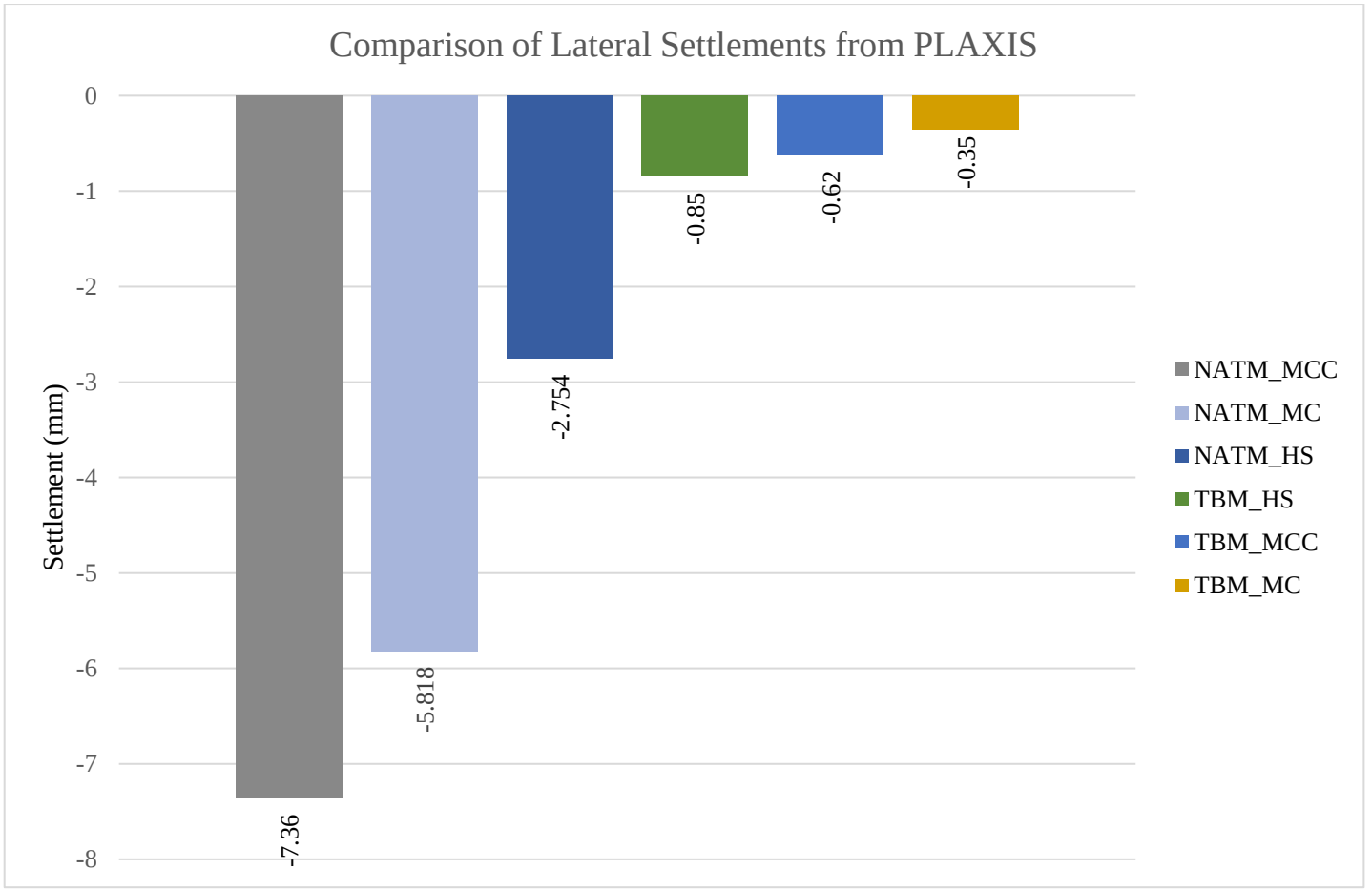

Figure 4.36: Lateral Settlements for both NATM and TBM methods considering 35m depth and 3.50m radius (from PLAXIS)

3.9 Summary

i. The mass rapid transit Line -1 is going to be established in underground and elevated portions. In this report, only underground section is focused whose length is approximately 14.8 km. The site area is basically from Pleistocene Madhupur clay and Holocene sediments with intermediate to high plastic clay and overlain by medium to coarse sand. The study area is in seismic zone II and it is mostly consisted of clayey soil than sandy soils. The borehole location is under Kuril flyover and all of the field investigation and laboratory tests collected from secondary sources. From the test results, subsoil stratifications are prepared.

ii. Numerical models are prepared in PLAXIS 3D for NATM and TBM methods for three different types of models (MC, MCC, and HS), where NATM models are done for depth 35m and 7m diameter, but TBM models are done for depth 30m, 32m, and 35m and for diameter of 5m, 6m, and 7m. Construction sequences for both methods are included in modelling.

iii. For practical application and model validation, realistic soil constitutive models need to be chosen which can simulate the nonlinear and stress dependent characteristics of soil. For FEM model, MC, MCC and HS model are chosen for simulating soil behavior with real time field and laboratory test data. The input parameters are determined from laboratory test results and empirical correlations. The empirical and analytical results are validated with the FEM model using the soil and structural parameters in PLAXIS 3D for MRT Line-1 tunnel alignment. Specific borehole data (BH-24, under the Kuril flyover) is chosen to simulate the soil structure interaction.

iv. The effect in maximum total displacements is computed for different types of mesh for different conditions of both NATM and TBM methods and for different models before starting the comparative analysis. For NATM models, the variation from medium mesh to coarse or fine mesh is about 10% whereas for TBM models, the variation value is almost 4% only. As the variation is considerable, medium mesh can be considered for models to save the running time.

v. From the comparison between the results of PLAXIS 3D and empirical formulas derived from different researchers for MRT Line 1, it can be said that the average deviated values between the numerical result for obtaining trough width parameter, i, and the empirical result of O'Reily & New are obtained as 5.38%, 3.84% and 6.39%

for MC, MCC and HS models respectively. These deviations are very less than other empirical relations described in researches.

vi. The transverse profile of the surface settlement of numerical results obtained from the MC, MCC and HS models are compared with the empirical relationship's graphs. It can be clearly seen that results of the MCC model have the best fit to the data points.

vii. After analyzing the relationship between settlement and depth or radius and also, between the location of inflexion point and depth or radius, it can be concluded to state that the total settlement decreases with an increase in depth of the tunnel (almost 11% decrement for every 5m increment of depth) and increases with an increase in diameter (almost 20% increment for every 1m increment of diameter). Increasing the TBM depth results to increase around 4% in distance of inflexion point from center whereas increasing in radius results to decrease around 5% in inflexion point distance from center of the tunnel.

viii. Comparing the vertical settlement found from PLAXIS 3D and various empirical formula given by different researchers, it can be said that the deviation percentages of vertical settlement from PLAXIS with Peck, Peck & Schmidt and Jacobsz formula are almost 10% and 34% for TBM and NATM respectively.

ix. The Jacobsz formula (2004) shows a good agreement and approximately close value compared to the settlement values obtained from PLAXIS 3D (for NATM, the variation is about 2 ~ 16% and for TBM 3 ~ 10%).

x. From comparison of longitudinal and lateral settlement found from PLAXIS 3D, it can be shown that NATM method shows more settlement (10 to 30% more) than TBM method. As the NATM method includes blast technique, it may induce more vibrating effect than TBM method which indicates this variation in settlement calculation.

xi. For Dhaka city, NKDOS consortium proposed TBM-EPB machine for MRT Line 1 tunnel construction. It can be said from this study that, for our city TBM should perform better than NATM method considering the settlement parameter and average soil condition.

Chapter 5

CONCLUSIONS AND RECOMMENDATIONS

5.1 Conclusions

In tunneling projects, it is essential to control and predict the ground surface settlements observed during and after the excavation process that may cause damage to the structures present on the earth surface. The prediction of surface settlements ought to be done independent to the tunnel excavation method, and safety measures against any damage to existing structures should be taken before the construction. Otherwise, project time and tunneling cost significantly increase due to damage to structures caused by the surface settlement that occurs above the bearable limits. PLAXIS 3D is a suitable software for engineers to evaluate interactions between soil and structural elements with accuracy.

This paper tries to estimate the surface settlement due to tunneling using both empirical and numerical methods for both NATM and TBM construction processes for different types of models, Mohr-Coulomb, Modified Cam-Clay and Hardening Soil. These parameters included over excavation, shield and lining element, tail void grouting, and face pressure. The conclusions drawn from this analysis are as follows:

i. Numerical analysis is an effective way to determine the performance of tunnel structures considering soil-structure interaction. The finite element model in PLAXIS 3D is validated with the empirical formulas using three types of constitutive models for representing the is-situ soil characteristics. The load-settlement curve acquired from the Gaussian and PLAXIS 3D showed good agreement and this model is used for further analysis. The standard procedure of finite element analysis of tunnels in soil element is described in chapter 4, which includes modeling (i) the soil and structural components (both geometry and material properties), (ii) the soil-structure interface behavior, (iii) boundary conditions, and (iv) the construction sequence.

ii. Two popular tunnels, Delhi Metro Phase 3 and Mashhad Metro Line 2, were used as validation analysis in the FEM model. For Mashhad Metro analysis, it was found that maximum settlement values for PLAXIS 3D is closer to empirical formula than FLAC3D values. Also, for Delhi Metro Phase 3, it was found that vertical surface

settlement values for PLAXIS 3D is closer to empirical formula than OptumG2 results.

iii. From the analysis of Mashhad Metro Line 2, it can be stated that, the deviated value of O'Reily and New empirical relation from monitored output value is 3.91%, whereas for PLAXIS 3D and FLAC 3D both these deviated values are almost 1.66% and 4.81% for MC and MCC models respectively. Comparing with Peck's formula with numerical analyses, it can be said that the deviation percentages for FLAC 3D are 9.6% and 41% for MC and MCC models respectively, whereas, these percentages for PLAXIS 3D are 11.11% and 44.4% respectively. Therefore, the deviation in result for PLAXIS 3D and FLAC 3D are considerable (1% to 3%), which does not imply different conclusions.

iv. From the analysis of Delhi Metro Phase 3, India, it can be stated that, the variation percentage between Optum G2 and Peck's formula found in literature was approximately 13% whereas in our computation between PLAXIS 3D and Peck's formula, this deviation becomes 15%. Therefore, the variation between PLAXIS 3D and Optum G2 is almost 2% which can be implied considerable.

v. From the collected soil parameters, the numerical analysis in PLAXIS 3D was done for Metro Rail Line 1 of Dhaka city by varying model types, depths and diameters for NATM and TBM method to determine the applicability of both methods. The effects of meshing, maximum settlements, transverse settlements, longitudinal settlements, and lateral settlements are compared to reach the concluding remarks.

vi. From the analysis of meshing effects for both NATM and TBM method, it can be stated that for NATM models, the variation from medium mesh to coarse or fine mesh is about 10% whereas for TBM models, the variation value is almost 4% only. As the variation is considerable, medium mesh can be considered for models to save the running time.

vii. From the comparison between the results of PLAXIS 3D and empirical formulas derived from different researchers for MRT Line 1, it can be said that the average deviated values between the numerical result for obtaining trough width parameter, i, and the empirical result of O'Reily & New are obtained as 5.38%, 3.84% and 6.39% for MC, MCC and HS models respectively. These deviations are very less than other empirical relations described in researches.

viii. The transverse profile of the surface settlement of numerical results obtained from the MC, MCC and HS models are compared with the empirical relationship's graphs. It can be clearly seen that results of the MCC model have the best fit to the data points. The implementation of the MCC in the soft clay with low consolidation is suggested. The shear modulus in this model is dependent on the shear strain, while, in the MC model, the shear modulus is independent of the shear strain. In other words, the MCC model has a high capability to consider the small strain in the elastic domain, especially in tunnel simulation where the maximum shear strain occurs in a small strain.

ix. After analyzing the relationship between settlement and depth or radius and also, between the location of inflexion point and depth or radius, it can be concluded to state that the total settlement decreases with an increase in depth of the tunnel (almost 11% decrement for every 5m increment of depth) and increases with an increase in diameter (almost 20% increment for every 1m increment of diameter). The stability of soil around the tunnel increases with an increase in depth of the tunnel. The maximum vertical displacement in the soil is not affected by tunnel depth. The maximum total settlement decreases with an increase in depth of the tunnel and increases with an increase in diameter. Therefore, the maximum total settlement in the soil is affected by both tunnel depth and diameter.

x. Increasing the TBM depth results to increase around 4% in distance of inflexion point from center whereas increasing in radius results to decrease around 5% in inflexion point distance from center of the tunnel. In TBM method numerical analysis, it can be shown that the curve diverges in the region far away from the center of the tunnel as the diameter is reduced. And for increasing depth, the curve converges closer to the center of the tunnel. Therefore, it can be said that the value of i decreases with the increase of both depth and diameter. Thus, the higher the depth and the larger the diameter, the smaller the impact on the tunnel structure.

xi. From the graphs derived from PLAXIS 3D, for every model it can be shown that crown is the most critical point in the tunnel periphery and has the maximum displacement in comparison with other locations around the tunnel periphery. Therefore, for the serviceability check of shallow tunnels, readings at the tunnel crown may only be used for the conservative design of the tunnel lining.

xii. Comparing the vertical settlement found from PLAXIS 3D and various empirical formula given by different researchers, it can be said that the deviation percentages of vertical settlement from PLAXIS with Peck, Peck & Schmidt and Jacobsz formula are almost 10% and 34% for TBM and NATM respectively. Also, it can be said that Chow's method underpredicted the vertical settlements than other empirical methods.

xiii. The Jacobsz formula (2004) shows a good agreement and approximately close value compared to the settlement values obtained from PLAXIS 3D (for NATM, the variation is about 2 ~ 16% and for TBM 3 ~ 10%).

xiv. From comparison of longitudinal and lateral settlement found from PLAXIS 3D, it can be shown that NATM method shows more settlement (10 to 30% more) than TBM method. As the NATM method includes blast technique, it may induce more vibrating effect than TBM method which indicates this variation in settlement calculation.

xv. For Dhaka city, NKDOS consortium proposed TBM-EPB machine for MRT Line 1 tunnel construction. It can be said from this study that, for our city TBM should perform better than NATM method considering the settlement parameter and average soil condition. Therefore, choosing TBM over NATM for the Dhaka MRT Line-1 is the right choice.

5.2 Recommendation for Future

With the development of researches and complex problem, it is become a necessary to conduct numerical analysis to confirm critical issues in routine design process. Advance constitutive models like MCC and HS model are very popular to tunnel design rather than MC model as MC model is a simplified model type. Following aspects should be taken into account for future research works:

i. For determining input parameters, soil samples should be collected from each layer of soil profile. Despite of being costly it is recommended to conduct such tests and validate the finite model with the field test data.

ii. MCC model can predict better response in tunnel settlement. However, HS model shows closer data also in the numerical analysis. Therefore, HS can be used for tunnel analysis in PLAXIS for accurate simulation but it requires field verification.

iii. This research includes excavation procedures for both NATM and TBM model and no static or dynamic motion is included. Therefore, the effect of loadings can be verified in PLAXIS with real time conditions.

iv. The groundwater level is not considered for omitting the flow condition effect, however, for extreme flood condition, i.e., for highest flood level (GL+1m), the effect of submerged tunnel should be verified before the tunnel construction.

v. The tunnels for both NATM and TBM have been considered in deep sections of soil to reduce the effect of other structures' foundations, but in real time condition the effect of piles of high-rise structures may conflict the tunnel behavior. Therefore, the effect of foundations should be verified with PLAXIS by considering real time conditions.

vi. The length of the tunnel has been considered $1/1000^{th}$ of the real tunnel length to minimize the computation time and complexity. For real project, the tunnel length should be considered the total length with varying soil profile.

REFERENCES

Abdallah, M. and Marzouk, M. 2013. Planning Of Tunneling Projects Using Computer Simulation And Fuzzy Decision Making. *Journal Of Civil Engineering And Management,* 19**,** 591.

Atkinson, J. H. and Potts, D. M. 1977. Stability Of A Shallow Circular Tunnel In Cohesionless Soil. 27**,** 203-215.

Attewell, P. B. 1986. *Soil Movements Induced By Tunnelling And Their Effects On Pipelines And Structures,* Glasgow : New York, Blackie

Attewell, P. B. and Farmer, I. W. 1974. Ground Deformations Resulting From Shield Tunnelling In London Clay. 11**,** 380-395.

Barbosa, A. R. J. 2016. Three-Dimensional Modelling And Assessment Of The Effects Of New Developments In Existing Tunnels.

Bentley 2018. Plaxis 3d Tutorial 06: Phased Excavation Of A Shield Tunnel. *Plaxis 3d Tutorial.*

C. Jeremy Hung, J. M., Nasri Munfah, and John Wisniewski 2009. Technical Manual For Design And Construction Of Road Tunnels — Civil Elements National Highway Institute, U.S. Department Of Transportation.

Chapman, D., Metje, N., and Stärk, A. 2017. *Introduction To Tunnel Construction: Second Edition*.

Chappell, M., and Parkin, D. 2004. Tunnel Construction.

Chen 1975. Three-Dimensional Numerical Parametric Study Of The Influence Of Basement Excavation On Existing Tunnel.

Cheng, C. Y., Dasari, G. R., Leung, C. F., Chow, Y. K., and Rosser, H. B. 3d Numerical Study Of Tunnel-Soil-Pile Interaction. 2004.

Chow, L., and Chow, L. 2016. *The Prediction Of Surface Settlements Due To Tunnelling In Soft Ground.* University Of Oxford.

Clough, G. W., and Schmidt, B. 1981. Chapter 8 - Design And Performance Of Excavations And Tunnels In Soft Clay. *Developments In Geotechnical Engineering.* Elsevier.

Daraei, A., and Zare, S. 2019. Modified Criterion For Prediction Of Tunnel Deformation In Non-Squeezing Ground Conditions. *Journal Of Modern Transportation,* 27**,** 11-24.

Eslami, B., Golshani, A., and Arefizadeh, S. Evaluation Of Constitutive Models In Prediction Of Surface Settlements In Cohesive Soils@ A Case Study: Mashhad Metro Line 2. 2020.

Esward T J, A. W. L. 2003. Guide To The Use Of Finite Element And Finite Difference Software. *In:* Computing, C. F. M. A. S. (Ed.). Teddington.

Fargnoli, V., Boldini, D., and Amorosi, A. 2013. Tbm Tunnelling-Induced Settlements In Coarse-Grained Soils: The Case Of The New Milan Underground Line 5. *Tunnelling And Underground Space Technology,* 38**,** 336-347.

Fattah, M., Shlash, K., and Salim, N. 2011. Settlement Trough Due To Tunneling In Cohesive Ground. *Indian Geotechnical Journal,* 41**,** 64-75.

Franca, P. T. 2006. Study Of Components Of Tunnels: Three Dimensional Numerical Analysis For Elasto-Plastic Models. Sao Paulo.

Franzius, J. N. 2003. *Behaviour Of Buildings Due To Tunnel Induced Subsidence.* Doctor Of Philosophy And For The Diploma, Imperial College Of Science, Technology And Medicine.

Galavi, V., Petalas, A., and Brinkgreve, R. 2013. Finite Element Modelling Of Seismic Liquefaction In Soils. *Geotechnical Engineering,* 44**,** 55-64.

Galler, R., Schneider, E., Bonapace, P., Moritz, B., and Eder, M. 2009. The New Guideline Natm - The Austrian Practice Of Conventional Tunnelling. *Berg- Und Hüttenmännische Monatshefte : Bhm***,** 441-449.

Galli, G., Grimaldi, A., and Leonardi, A. 2004. Three-Dimensional Modelling Of Tunnel Excavation And Lining. *Computers And Geotechnics,* 31**,** 171-183.

Garry, D. 2012. *Handbook Of Tunnel Engineering: Design , Construction & Risk Assessment,* Auris Reference.

Girmscheid, G., and Schexnayder, C. 2002. Drill And Blast Tunneling Practices. 7**,** 125-133.

Gnilsen, R. 1989. Underground Structures Design And Instrumentation (Ed. Sinha R.S.). *Elsevier***,** 84-128.

Golpasand, M. R. B., Nikudel, M. R., and Uromeihy, A. 2016. Specifying The Real Value Of Volume Loss (Vl) And Its Effect On Ground Settlement Due To Excavation Of Abuzar Tunnel, Tehran. *Bulletin Of Engineering Geology And The Environment,* 75**,** 485-501.

Guo, H. 2019. A Review Of Metro Tunnel Construction Methods. *Iop Conference Series: Earth And Environmental Science,* 218**,** 012110.

Harer, G., Mussger, K., Hochgatterer, B., and Bopp, R. 2008. Considerations For Development Of The Typical Cross Section For The Koralm Tunnel. *Geomechanics And Tunnelling,* 1**,** 257-263.

Hellmich, C., Ulm, F.-J., and Mang, H. A. 1999. Numerical Studies On Natm Tunneling. 125**,** 702-713.

Ice 1996. *Channel Tunnel Transport System,* Scotland, Thomas Telford Ltd.

Ieronymaki, E., Whitttle, A., and Einstein, H. 2018. Comparative Study Of The Effects Of Three Tunneling Methods On Ground Movements In Stiff Clay. *Tunnelling And Underground Space Technology,* 74**,** 167-177.

Japan Society of Civil, E. 2007. *Standard Specifications For Tunneling, 2006,* Tokyo, Tunnel Engineering Committee.

Kaçar, O. 2007. *3d Finite Element Modelling Of Surface Excavation And Loading Over Existing Tunnels.* Master Of Science In Civil Engineering Department, Middle East Technical University

Karakus, M., and Fowell, R. 2004. *An Insight Into The New Austrian Tunnelling Method (NATM).*

Khan, A. A., Rini 2016. A Review On Selection Of Tunneling Method And Parameters Effecting Ground Settlements. 21**,** 4459-4475.

Kuesel, T. R., King, E. H., and Bickel, J. O. 2012. *Tunnel Engineering Handbook,* Springer US.

Lambrughi, A., Medina Rodríguez, L., and Castellanza, R. 2012. Development And Validation Of A 3d Numerical Model For TBM–EPB Mechanised Excavations. *Computers And Geotechnics,* 40**,** 97-113.

Le, B. T., and Taylor, R. N. 2018. Response Of Clay Soil To Three-Dimensional Tunnelling Simulation In Centrifuge Models. *Soils And Foundations,* 58**,** 808-818.

Leca, E., and Clough, G. W. 1992. Preliminary Design For Natm Tunnel Support In Soil. 118**,** 558-575.

Loganathan, N., and Poulos, H. 1998. Analytical Prediction For Tunneling-Induced Ground Movements In Clays. *Journal Of Geotechnical And Geoenvironmental Engineering - J Geotech Geoenviron Eng,* 124.

Lu, H., Shi, J., Wang, Y., and Wang, R. 2019. Centrifuge Modeling Of Tunneling-Induced Ground Surface Settlement In Sand. *Underground Space,* 4**,** 302-309.

Luo, Y., Chen, J., Chen, Y., Diao, P., and Qiao, X. 2018. Longitudinal Deformation Profile Of A Tunnel In Weak Rock Mass By Using The Back Analysis Method. *Tunnelling And Underground Space Technology,* 71**,** 478-493.

Mair, R. J., and Taylor, R. N. J. Bored Tunnelling In The Urban Environments. 1999.
Marshall, A., Farrell, R., Klar, A., and Mair, R. 2012. Tunnels In Sands: The Effect Of Size, Depth And Volume Loss On Greenfield Displacements. *Geotechnique,* 62**,** 385-399.
Mašín, D., and Herle, I. 2015. *Numerical Analyses Of A Tunnel In London Clay Using Different Constitutive Models*.
Naqvi, M. W., Akhtar, M. F., Zaid, M., and Sadique, R. 2021. Effect Of Superstructure On The Stability Of Underground Tunnels. *Transportation Infrastructure Geotechnology,* 8.
Ng, C. W. W. A. S., Noel A Menzies, Bruce. *A Short Course In Soil–Structure Engineering Of Deep Foundations, Excavations And Tunnels*.
O'reilly, M. P., and New, B. M. Settlements Above Tunnels In The United Kingdom - Their Magnitude And Prediction. 1982.
Peck, R. B. Deep Excavations And Tunnelling In Soft Ground. 1969.
Phadke, V. A. T., Nikhil 2017. Construction Of Tunnels, By New Austrian Tunneling Method (Natm) And By Tunnel Boring Machine (Tbm). *International Journal Of Civil Engineering (Ijce).*
Potts, D. M. 2001. *Finite Element Analysis In Geotechnical Engineering*.
Proposal, N. C. 2019. Technical Proposal For Consultancy Services For Detailed Design And Tender Assistance For Dhaka Mass Rapid Transit Development Project (Line-1). *In:* Consortium., N. (Ed.). Dhaka: Nkdos Consortium.
Schanz, T., Vermeer, P., and Bonnier, P. G. 2019. The Hardening Soil Model: Formulation And Verification. *Beyond 2000 In Computational Geotechnics.* Routledge.
Schubert, W., and Riedmüller, G. 2001. Project And Rock Mass Specific Investigation For Tunnels In P Särkkä (Ed.), Rock Mechanics - A Challenge For Society. *Isrm Regional Symposium Eurock - Rock Mechanics: A Challenge For Society***,** 369-376.
Shi, J., Ng, C. W. W., and Chen, Y. 2015. Three-Dimensional Numerical Parametric Study Of The Influence Of Basement Excavation On Existing Tunnel. *Computers And Geotechnics,* 63**,** 146-158.
Sinha, R. S. 1989. Underground Structures : Design And Instrumentation.
Survey, P. G. 2019. Geotechnical Survey For The Feasibility Study Of Dhaka Mrt Line 1 Project. Dhaka: Prosoil Foundation Consultant.
Tamagnini, C., Miriano, C., Sellari, E. Cipollone, N. 2022. Two-Dimensional Fe Analysis Of Ground Movements Induced By Shield Tunnelling: The Role Of Tunnel Ovalization.
Tan, W. L., and P.G, R. 2003. Parameters And Considerations In Soft Ground Tunneling. *Electronic Journal Of Geotechnical Engineering,* 8.
Tatiya, R. 2005. *Civil Excavations And Tunnelling: A Practical Guide*.
Üçer, S. 2006. *Comparison Of 2d And 3d Finite Element Models Of Tunnel Advance In Soft Ground: A Case Study On Bolu Tunnels.* Master Of Science, Middle East Technical University.
Urschitz, G., Gildner, J. 2004. Sem/Natm Design And Contracting Strategies *North American Tunneling Conference.* Atlanta, GA, US.
Wang, X., Tan, W., Ni, P., Chen, Z. & Hu, S. 2020. Propagation Of Settlement In Soft Soils Induced By Tunneling. *Tunnelling And Underground Space Technology,* 99**,** 103378.
Wood 1990. *Soil Behavior And Critical State Soil Mechanics,* Cambridge University.
Wood, D. M. 1991. *Soil Behaviour And Critical State Soil Mechanics,* Cambridge, Cambridge University Press.
Yu, C.-W., and Chern, J. 2007. Expert System For D&B Tunnel Construction. 1.
Yun, B. 2019. Chapter 5 - Project Management. *In:* Yun, B. (Ed.) *Underground Engineering.* Academic Press.

Zhao, J., Gong, Q. M., and Eisensten, Z. 2007. Tunnelling Through A Frequently Changing And Mixed Ground: A Case History In Singapore. *Tunnelling And Underground Space Technology,* 22**,** 388-400.

APPENDIX – A

LL= Liquid limit
PL= Plastic limit
PI = Plasticity index
γ_{WT}= Wet (kN/m^3)
γ_d= Dry (kN/m^3)
G_s= Specific gravity
σ'_{pc}= Preconsolidation pressure (kPa)
c_u= Undrained shear strength (kPa)
C_{uu}= Undrained Cohesion (kPa)
ϕ^o= Angle of internal friction (deg)
e_i= Initial void ratio
C_c= Compression index

BORE HOLE NO	SAMPLE		ATTERBERG LIMIT			BULK DENSITY		GRAIN SIZE (%)				NATURAL MOISTURE CONTENT	SPECIFIC GRAVITY	UNCONFINED COMPRESSION TEST	CONSOLIDATION TEST			TRIAXIAL TEST (UU)	
	Sample	Depth	LL	PL	PI	γ_{WT}	γ_d	GRAVEL	SAND	SILT	CLAY	% (wt)	G_s	c_u	σ'_{pc}	e_i	C_c	C_{uu}	ϕ^o
BH 24	UD-1	5.0-6.0	57.92	25.48	32.44	20.45	15.94		3.80	55.03	41.17	23.71	2.727	53.00				48.0	5.1
	D-1	1.5																	
	D-2	3																	
	D-3	4.5	35.41	21.83	13.58				6.81	63.67	29.52		2.724						
	D-4	6	35.80	21.18	14.62				9.63	59.49	30.89	20.51	2.726						
	D-5	7.5							43.18	42.13	14.69	21.13	2.678						
	D-6	9	32.75	25.50	7.25				12.58	64.68	22.73	21.42	2.682						
	D-7	10.5	30.78	25.41	5.37				10.65	68.08	21.27								
	D-8	12	35.85	19.94	15.90				5.03	65.46	29.51	17.04	2.721						
	D-9	13.5							10.69	65.84	23.47	16.75	2.673						
	D-10	15							7.66	68.13	24.21	16.11	2.686						
	D-11	16.5							46.28	38.87	14.85	15.56							
	D-12	18							56.37	29.84	13.80	14.19	2.658						
	D-13	19.5							58.92	30.98	10.09	14.10	2.656						
	D-14	21							39.26	51.70	9.05		2.690						
	D-15	22.5							73.74	16.44	9.82	13.41							
	D-16	24							61.83	27.41	10.76	14.07	2.659						
	D-17	25.5							78.20	21.80	0.00	14.16	2.657						
	D-18	27							76.52	23.48	0.00								
	D-19	28.5							80.29	19.71	0.00	14.13							
	D-20	30							73.93	26.07	0.00	13.94	2.659						
	D-21	31.5							72.01	27.99	0.00	13.79	2.660						
	D-22	33							73.61	26.39	0.00	12.94	2.653						
	D-23	34.5							84.20	15.80	0.00		2.664						
	D-24	36							78.79	21.21	0.00	12.73	2.663						
	D-25	37.5							81.00	19.00	0.00	12.63	2.661						
	D-26	39							80.58	19.42	0.00	12.51	2.657						
	D-27	40.5							83.78	16.22	0.00	12.47	2.659						

Figure A-1 Summary of All Test Results (Atterberg Limit, Density, Grain Size Analysis, Moisture Content, Specific Gravity, Unconfined Compression, Triaxial Test)